The Effect of Development and Ecology on the Evolution of Ovary Size in Drosophila

The effect of development and ecology on the evolution of ovary size in *Drosophila*

A dissertation presented

by

Didem Pelin Sarikaya

to

The Organismic and Evolutionary Biology Department

in partial fulfillment of the requirements

for the degree of

Doctor of Philosophy

in the subject of

Biology

Harvard University

Cambridge, Massachusetts

December, 2014

Dissertation Adviser: Professor Cassandra Extavour

Didem Pelin Sarikaya

The effect of development and ecology on the evolution of ovary size in *Drosophila*

Abstract

How the size of an organ is established and altered during evolution is poorly understood. The ovary of fruit flies of the genus *Drosophila* serves as an interesting model for understanding organ size evolution, as the number of egg-producing structures called ovarioles determines the ovary's functional 'size'. Species with more ovarioles can lay more eggs, and ovariole number can evolve rapidly between closely related species. However, the developmental and genetic mechanisms that determine and alter ovariole number were poorly characterized at the beginning of this thesis. I first analyzed the developmental basis of plasticity and species-specific ovariole number changes in *D. melanogaster* and closely related species. This analysis revealed distinct developmental mechanisms that alter ovariole number via changes in one cell type (terminal filament cells) in the developing ovary. To characterize the genetic mechanisms underlying proliferation patterns and potential cell-type interactions within the ovary, I then studied the role of the Hippo pathway in the somatic and germ cells of *D. melanogaster*. I uncovered a complex interaction between somatic cells and germ line cells, where proportional growth of these cell types is maintained by the Hippo pathway via interactions with the EGFR and JAK/STAT pathways. Finally, I expanded this work to investigate the physical, ecological, and developmental parameters that influence ovariole number evolution in Hawaiian Drosophila, where previous studies suggested that ovariole number correlated with larval food substrate. I describe my ongoing efforts to test correlations of ecology and ovariole number in a

phylogenetic context in Hawaiian Drosophila. Primary differences in ovariole number between species occur through changes in cell number.

Table of Contents

Title Page i

Copyright Page ii

Abstract iii

Table of Contents v

Acknowledgements xii

Chapter I: Introduction 1

References 18

Chapter II: The role of cell size and cell number in determining ovariole number in *Drosophila*

2. 1 Abstract 24

2.2 Introduction 25

2.3 Material and Methods 29

2.4 Results 37

2. 5 Discussion 52

2.7 References 59

Chapter III: The Hippo pathway regulates the homeostatic growth of stem cell niche precursors in the *Drosophila* ovary

3.1 Abstract 64

3.2 Introduction 65

3.3 Results 72

3.4 Discussion 92

3.5 Material and Methods 101

3.6 Acknowledgements 106

3.7 References 107

Chapter IV: The role of ecology and development in ovariole number evolution in Hawaiian Drosophila

4.1 Abstract 117

4.2 Introduction 118

4.3 Material and Methods 124

4.4 Results 129

4.5 Discussion 140

4.6 Acknowledgements 143

4.7 References 144

Chapter V: Discussion 146

References 155

Appendix A: Supplemental materials for Chapter II 159

Appendix B: Comparative developmental analysis of additional *melanogaster* subgroup species

B.1 Introduction 166

B.2 Material and Methods 169

B.3 Results 170

B.4 Discussion 172

B. 5 References 175

Appendix C: Supplemental materials for Chapter III 177

Appendix D: A protocol for FACS sorting of larval ovarian cells

D.1 Introduction 194

D.2 Materials and Methods 195

D.3 Results and Discussion 198

D.5 Acknowledgement 202

D.6 References 203

List of Figures

1.1	Huxley's deer	2
1.2	Schematic of Drosophila adult ovary and ovariole structure	7
1.3	Diagram of larval ovarian development in Drosophila	14
2.1	Terminal filament cell (TFC) specification, and TF morphogenesis during larval development in *D. melanogaster*	26
2.2	Methodology for measuring TFC parameter in late larval ovaries	36
2.3	Expression of constitutively active S6K alleles in TFCs increases ovariole number	38
2.4	Expression of constitutively active S6K alleles in TFCs increases TFC cell size and cell number.	41
2.5	Decreasing Hippo pathway activity in TFCs increases ovariole number	43
2.6	Decreasing Hippo pathway activity in TFCs increases total TFC number, without affecting cell size or sorting.	45
2.7	TF number, TFC number and TF morphogenesis in *D. yakuba*.	47
2.8	The effects of temperature and nutrition on ovariole number	51
2.9	Models for developmental parameters that determine ovariole number	55
3.1	Hippo pathway activity is cell-type specific in the larval ovary	70
3.2	Hippo pathway influences proliferation of TFCs, thereby influencing ovariole number	76
3.3	Altering Hippo pathway activity in somatic cells changes IC and GC number	79
3.4	Yorkie activity regulates GC number	82
3.5	The Hippo pathway interacts with the EGFR pathway to regulate IC and GC growth	88
3.6	Hippo pathway interacts with JAK/STAT pathway to regulate TFC and IC proliferation, and non-autonomous regulation of GC number	91

3.7	The Hippo pathway regulates coordinated growth of the soma and germ line	99
4.1	Simplified phylogeny of Hawaiian *Drosophila* and egg laying substrates	119
4.2	Images of egg laying substrates and *Drosophila* larvae in the field	131
4.3	BLASTn hit of mitochondrial DNA sequences from field specimens	133
4.4	Ovariole number variation in Hawaiian *Drosophila*	135
4.5	Plot of thorax length (mm) and ovariole number of Hawaiian Drosophila	136
4.6	Developmental mechanisms underlying ovariole number changes in Hawaiian Drosophila	138
4.7	Correlation of total TFC number and TFC number per TF with TF number	139
A.1	Experimental design	160
A.2	Constitutively active *S6K* alleles increase wing cell size but do not affect cell number.	161
A.3	*bab:GAL4* is expressed in TFCs throughout larval development	162
A.4	Number of cells per TF is not correlated with TFC size	163
A.5	Effects of temperature and nutrition on wing cell size, wing size, and wing cell number	164
B.1	Phylogenetic relationship of *melanogaster* subgroup species and their average ovariole number per female	168
B.2	LP stage morphology of larval ovary in *melanogaster* subgroup species	170
B.3	TFC number and sorting differences between *melanogaster* subgroup species	171
C.1	Hippo pathway core components are expressed in the larval ovary	178
C.2	Expression pattern of Hippo pathway activity reporter lines in larval ovarian cell types	179
C.3	GFP expression driven by *traffic-jam* and *nanos* GAL4 during larval ovarian development	181

C.4	Homozygous mutants of Hippo pathway components significantly influence TFC, IC, and GC number	182
C.5	RNAi against Hippo pathway members driven by *ptc:*GAL4 or *hh:*GAL4 drivers does not significantly influence proliferation of larval ovarian cell types non-autonomously	183
C.6	Spectrosome morphology does not change when *yki* activity is altered in GC	184
C.7	ICs and GCs generally maintain homeostatic growth when Hippo pathway activity is reduced in the soma	185
C.8	RNAi against EGFR and JAK/STAT pathway components reduce respective pathway activity in the larval ovary	186
D.1	FACS sorting results	201

List of Tables

4.1	Comparison of TF number per ovary to ovariole number per ovary	142
C1	Summary of mean TFC and TF number in LP stage ovaries of genotypes used in RNAi analysis	187
C2	Summary of mean ovariole, TFC, IC, and GC number in ovaries of genotypes used in mutant analysis	188
C3	Summary of mean IC and GC number in LP stage ovaries of genotypes used in RNAi analysis	189
C4	Summary of mean TFC, IC, and GC number in LP stage ovaries of genotypes used in double RNAi analysis	190
C5	Summary of TFC and IC number in *ptc:GAL4* and *hh:GAL4* analysis	191
C6	Summary of GC-IC proportion for single and double RNAi experiments influencing IC and/or GC number	192
D1	Summary of FACS sort trials	201

Acknowledgements

I am extremely grateful to my PhD adviser extraordinaire, Cassandra Extavour, for all the support and mentoring she has provided over the years. She untangled many of my thoughts, provided feedback that helped me develop better writing and speaking habits, and generously accommodated my horribly last minute requests for pending funding applications. She taught me to expect more from myself, and I was able to do the kind of science I never thought I would. I only hope I will be able to pass on the learning experience to others.

I am also grateful for the advising and guidance that was provided by my thesis committee members Arkhat Abzhanov, David Haig, Elena Kramer, and Norbert Perrimon. Our discussions were extremely helpful in developing the content of this thesis.

The Extavour lab has always been a place full of intelligent, kind, giving and thoughtful scientists. I would like to thank the support and friendship of the fellow graduate students Ben Ewen-Campen, John Srouji, Seth Donoghe and Tamsin Jones. Postdocs Tripti Gupta and Abha Ahuja provided much insight into my projects through our discussions. My work was greatly influenced by and inspired by my partner-in-crime Delbert Andre Green who spear-headed the ovariole project together with thoroughness and generosity. Our countless hours of discussion and troubleshooting taught me the spirit of scientific collaboration.

The field component of my research for Chapter IV would not have been possible without the generous help of Drs. Patrick O'Grady and Brian Ort for applying for collection permits, Drs. Ken Kaneshiro, Durrell Kapan, and Don Price for taking me to

the field and introducing me to two excellent entomologists Drs. Karl Magnacca and Steve Montgomery. I have learned a tremendous amount of technical and practical knowledge of fieldwork through Karl and Steve, and am indebted for their sharing of their dedication to the native habitat of Hawaiian forests. My fieldwork would not have been as fruitful or exciting without the help of Inanna Carter. Whether it was to ease me into Hawaiian names of plants or animals, or to drive a truck that was out of gas by the sheer use of momentum, it was all a very exciting ride.

Diane Duplissa of the Drosophila facilities in the Biological Laboratories kept the facility running and was always ready to help when we needed her. Renate Hellmiss of mcographics taught me the value of Adobe Illustrator and how to construct more visually pleasing figures/posters. The staff of the Harvard Biological Imaging Center run a fantastic imaging facility with beautiful confocal microscopes, which was critical for the success of my project.

I was supported by the National Science and Engineering Research Council of Canada's post-graduate fellowship between 2011-2013, Quebec's Fondes de la recherché de Sante du Quebec between 2013-2014, and Harvard's Merit fellowship for the fall semester of 2014. My research for Chapter IV was supported by the National Science Foundation's Doctoral Dissertation Improvement Grant.

A doctoral thesis can be an all-encompassing endeavor and I am grateful to the companionship of my family and friends who have supported by over the years. My cohort of OEB students inspired me to think outside of my usual developmental biology box, and inspired me to become a better academic. My classmates Laura Lagomarsino, Dipti Nayak, Elizabeth Sefton and Heather Olins have been great sports and provided a

much needed support-network of friends. Laura was also instrumental in improving the experimental design of Chapter IV, and generously spent time discussing the basics of field biology studies with me.

Arwa Aulaqi never fails to ask me the most important questions in life (is there anything pizza can't solve?), Fatima Kamenge can pinpoint my thoughts with a soft nudge, Shinichiro Waki manages to get me food poisoning even though he says he didn't intend to (yes I'm still holding it against you), and Aisha Sheikh makes me dance to the latest moves if I'm forgetting to have fun. Elif Genc, Nafisa Jadavji, Wells Cushnie, and Natasha Sidhu traveled with me, laughed with me, and shared their valuable friendship with me.

My mother Nursen, father Behcet, and brother Deniz Sarikaya make up the most supportive and encouraging family anyone can ask for, and continue to teach me the most important virtues in life: hard-work, integrity, and compassion. My work is inspired by the endless curiosity for nature and its creatures displayed by my undergraduate research adviser Dr. Ellen Larsen and my grandfather Ali Ihsan Arikan. Everyone listed in this section has continued to inspire me to live by the rules of the Notorious: "*If the game breaks me or shakes me/ I hope it makes me a better man/ Take a better stand/ (…) Stay far from timid/ Only make moves when you're hearts in it/ And live the phrase sky's the limit… See you chumps on top*" (Notorious B.I.G., Bad Boy Records 1997).

Chapter I:

Introduction

1.1 Introduction

Understanding how organs grow and attain their final size is a fundamental question in biology. It is a field that combines interests of genetics, development, and evolution as organ size is regulated genetically and established in the developing animal, and is frequently altered during evolution. Early studies of organ growth relied on measuring adults of various animals to derive patterns. Pioneering work by D'Arcy Thompson described changes in animal morphology as primarily changes in scale and shear of body shapes (Thompson, 1917). Thompson's work on scaling of animals was further refined by Julian Huxley's categorization of animal growth at two levels: change in overall size of the animal, and changes in relative size of its body parts (Huxley, 1932).

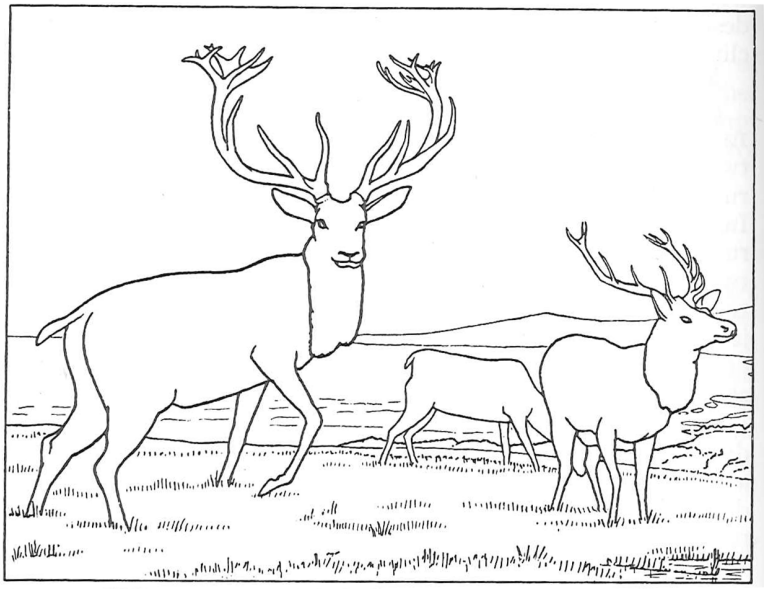

Figure 1.1 Huxley's deer. Illustration representing prehistoric (left) and modern (right) Scottish red deer. Figure adapted from Huxley (1932), Figure 90.

The above figure (Figure 1.1) visually demonstrates the difference between these two modes of growth. The drawing depicts prehistoric (left) and modern (right) Scottish red deer next to each other. The prehistoric deer is much larger in overall body size compared

to the modern deer. Another noticeable feature is the difference in the size of antlers. Deer antlers are shed every winter, and grow back in the spring. For young males, this is an important occurrence as the new antlers grow in proportion to body size. If the male has grown over the previous year, its antlers will be larger than the previous year. The antler's size relative to the deer's body size, however, is different between the two depicted deer. The prehistoric deer is larger but also has relatively larger antlers. Using the deer as an example, Huxley draws our attention to two major concepts in understanding animal growth: the regulation of the size as a whole, and the regulation of the size of its parts.

Huxley's pioneering work on describing the mathematical formulae of relative growth has received much attention, but a less discussed part of his thesis on relative growth of animals sheds an enlightening view on how he perceived the underlying causes of differential growth. He recognized that changes must occur through differences during development, and categorized developmental stages of animals into two phases: (1) histodifferentiation, or when different cell types are emerging, and (2) the growth phase where the cell types that emerged earlier in development proliferate to create increased mass. He predicts that majority of the changes that explain size differences would be the latter, changes in proliferation rate. While his prediction was based on histological work, the hypothesis holds true even in today's literature as reviewed by Stern and Emlen (1999).

Studies of developmental biology from recent decades have shed much light on the genes and processes that regulate both differentiation and proliferation across many different animals. Differentiation of cell types are is achieved by combinations of

different transcription factors, often referred to as developmental tool kit genes (Kauffman, 1987; Rokas, 2008). The expression patterns of these conserved transcription factors are strikingly conserved in similar cell types of animals from sponges to humans (Finnerty et al., 2004a; Hejnol and Martindale, 2009; Ryan et al., 2013). Similarly, the genes that regulate proliferation at the tissue level or body level are also highly conserved across metazoans (Bossuyt et al., 2013; Nichols and Smith, 2011). The genes that regulate terminal differentiation are often involved in cell cycle exit (Reviewed in Buttitta and Edgar, 2007; Miller et al., 2007), which can complicate the distinction between differentiation and proliferation, as both may be tied closely together through genetic programming. As in most situations in biological studies, there are also cases where genes that generally only regulate proliferation can also regulate differentiation in special cases (Nishioka et al., 2009).

Thus we have moved forward in the last century from primarily having tools to observe and record differences in overall sizes of animals, to having access to the precise tools (genes) that regulate the formation of these animals. The power of Huxley's thesis comes from his interdisciplinary approach and interest in many different types of biological information to find patterns that can explain how sizes of animals or organs change during evolution. Incorporating modern developmental genetics into the study of how cell types evolve and emerge during evolution has successfully identified previously uncharacterized cell types in animals that were once considered 'simple' (lacking complex cell types) (Finnerty et al., 2004b; Hejnol and Martindale, 2009; Ryan et al., 2013). However, unlike cell types, which can be defined by the presence or absence of gene expression, changes in proliferation rate likely result from changes in modulation of

growth-regulating genes. This is considerably more difficult to study, as modulation of growth-regulating genes remains poorly understood even in model organisms.

One well-studied example is that of beak size and shape in Darwin's finches. Two separate developmental pathways, BMP and Calmodulin, regulate the length and depth of the break, thereby altering the size of the break (Abzhanov et al., 2004, 2006). The patterning and proliferation level of the growth zone that gives rise to the beak explain beak size/morphology differences in song birds (Fritz et al., 2014). However, the genetic mechanisms that dictate these differences are poorly understood, partly made difficult by the fact that these birds cannot be bred in the lab.

Perhaps the best-studied model to investigate change in size comes from wings of *Drosophila melanogaster*. Populations of *D. melanogaster* with divergent wing sizes have differences in the number and/ size of cells that make up the wing (James et al., 1995; Partridge et al., 1999; Zwaan et al., 2000). However, identifying the genes that regulate size differences have been complicated by the interaction between genes that can regulate growth of the animal at different levels. For example, the wing size of *D. melanogaster* can be modified by differences in proliferation rate or length of development time (Edgar, 2006). Multiple genes have been implicated in population-level differences in *D. melanogaster* body size (Calboli et al., 2003; Kennington and Hoffmann, 2010; Lee et al., 2011) and one gene that has been functionally characterized affects growth in seemingly conflicting ways by positively regulating development time while negatively regulating growth rate (Lee et al., 2013). Therefore the genetics of regulating growth are likely to be pleiotropic and important to analyze in systems where background genetics can be carefully controlled.

Given that the genetic architecture controlling size appears to be complex with multiple genes of small effect, it may make characterization of how organ size evolves more difficult compared to phenotypes regulated by one or two large effect loci of evolution. Nonetheless, I believe we now have many of the tools needed to combine developmental and evolutionary studies to meaningfully push forward our understanding of animal growth. Most studies investigating this question have focused on external morphological traits, likely because they were better characterized and easier to study in a quantitative manner. Internal organs have received less attention, as they are more difficult to obtain quantitatively rigorous measurements for. In this thesis, I present the *Drosophila* ovary as a model to investigate the cellular mechanisms that underlie organ size evolution.

The evolution of ovariole number in Drosophila

Insect ovaries are composed of egg-producing structures called ovarioles, which serve as assembly lines of developing eggs (King, 1970) (Figure 1.2A). The germarium, which harbors the germ line stem cells (GSCs) that give rise to the developing oocyte, is located at the anterior of the ovariole (Figure 1.2 B) (Xie and Spradling, 2000); progressively maturing oocytes are found toward the posterior. While the total volume of the ovary can dramatically vary depending on environmental factors such as nutrition (Schmidt et al., 2005), the functional output of the ovary, measured by number of eggs laid by the female per unit time, is strongly influenced by the number of ovarioles the females has (David, 1970; Klepsatel et al., 2014; R'kha et al., 1997).

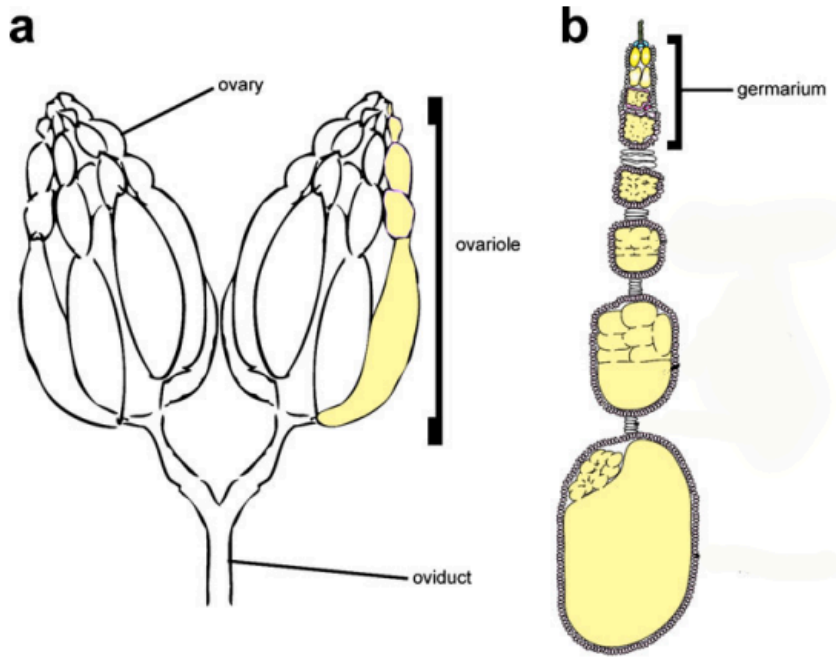

Figure 1.2. Schematic of adult *Drosophila* ovarian structure. (A) Adult ovary composed of multiple strands of ovarioles, one of which is highlighted in yellow. (B) A single ovariole with the germarium, which contains the germ line stem cells, at the anterior, and maturing oocytes towards the posterior. Figure adopted from Green *et al.* (2012).

Species-specific variation in ovariole number of Drosophilids is best described in the African *melanogaster* subgroup and Hawaiian *Drosophila* species. In the African *melanogaster* subgroup, ovariole number ranges from average of 43 to 18 per female depending on the species (Markow and O'Grady, 2007; R' kha et al., 1997). The highest variability exists between *D. melanogaster* and its sister species *D. simulans, D. mauritiana,* and *D. sechellia* which diverged around 2-5 million years ago (Tamura et al., 2004). *D. melanogaster* and *D. simulans* are generalist cosmopolitan species, and have the highest ovariole number, average of 43 and 40 respectively, within the group. *D mauritiana* is an island endemic generalist on the Mauritius islands with an average of 26 ovarioles per female, and *D. sechellia* is a specialist on the toxic noni fruit on the Seychelles islands, and has evolved the lowest ovariole number of the group, with an average of 18 ovarioles per female. *D. sechellia* has the lowest fecundity amongst these species, partly due to reduced ovariole number and partly due to reduced oocyte production rate (R kha et al., 1997). It is hypothesized that *D. sechellia* evolved lower fecundity in response to adapting to a toxic and limited larval food source (R kha et al., 1997; R'Kha et al., 1991)

The effect of egg-laying substrate appears to be particularly important in evolution of ovariole number in Hawaiian Drosophila. Hawaiian Drosophila species are specialists on decaying bark, sap fluxes, fungi, flowers or leaves of endemic plants (Magnacca et al., 2008). One or two colonization events have given rise to close to 1000 species that are endemic on the Hawaiian islands (O'Grady et al., 2011; Tamura et al., 2004). Ovariole number ranges between two to 101 per female in Hawaiian Drosophila, and it has been suggested that ovariole number of the species correlates with the

substrates the species lays eggs on (Kambysellis and Heed, 1971). Species that lay eggs on more ephemeral food sources, such as flowers or decaying leaves, have low ovariole numbers (two to 18), compared to species that lay eggs on less ephemeral food sources, such as bark, which have average of 32 to 101 ovarioles depending on the species.

Intra-species differences in ovariole number are best documented in *D. melanogaster* in different populations. *D. melanogaster* populations evolving at higher latitudes and altitudes have genetically fixed differences that correlate with larger body size and higher ovariole numbers compared to lower latitude and altitude populations (Gibert et al., 2004; Klepsatel et al., 2014). Similar clinal variation in ovariole number has also been observed in *D. simulans* and *D. kikkawai* populations (Gibert et al., 2004; Parkash et al., 1998). In addition to fixed genetic differences between populations, ovariole number also shows developmental plasticity in response to lower developmental temperature or reduced nutritional conditions, both of which result in lower ovariole number (Hodin and Riddiford, 2000).

Thus ovariole number serves as the functional 'size' of the adult Drosophila ovary that is variable, and is a quantitative trait that potentially confers a strong fitness effect by influencing egg-laying capacity. Characterization of inter-species and intra-species variation in ovariole number suggests that it is a frequent target of evolutionary change.

Genes that regulate ovariole number

The genes that regulate ovariole number have been investigated through Quantitative trait loci (QTL) studies within *D. melanogaster* (Telonis-Scott et al., 2005; Wayne and Mackay, 1998; Wayne and McIntyre, 2002; Wayne et al., 2001) and a

between-species comparison of *D. simulans* and *D. sechellia* (Orgogozo et al., 2006a). QTL studies for both inter- and intra-species differences in ovariole number do not show any significant peaks for genes on the X chromosome. Ovariole number differences within *D. melanogaster* strains mapped strongly to the third chromosome, and were further narrowed down by using microarrays to identify differentially expressed genes that fell within the peaks (Wayne and McIntyre, 2002; Wayne et al., 2001). This analysis revealed mostly genes of unidentified function, and a suppressor of a Hedgehog pathway member.

QTL analysis between *D. simulans* and *D. sechellia* also resulted in coarse peaks that were difficult to interpret by QTL results alone (Orgogozo et al., 2006b). The second and third chromosomes had large peaks encompassing many genes, including Insulin and Hippo pathway members. It should be noted that one of the primary difficulties in conducting QTL studies on ovariole number results from the fact that the phenotype cannot be measured without killing the female. This makes it impossible to conduct backcrosses while selecting for the trait, which are often done on QTLs for external morphological features. However, while narrowing down of regions is difficult due to these obstacles, the QTL results strongly suggest that ovariole number is polygenic (Orgogozo et al., 2006a; Wayne and McIntyre, 2002).

While QTL studies have added great insight into the genes that regulate morphological and adaptive evolution for a number of traits, the polygenic nature of ovariole number combined with the difficulty in conducting backcrosses suggests that we must take an alternative approach to understand the evolution of this particular trait. To better understand how ovariole number can be altered during evolution, I turned to

development to identify developmental and cellular mechanisms that alter ovariole number.

Ovariole morphogenesis during development of the Drosophila ovary

The three major cell types of the larval ovary are terminal filament cells (TFCs), interstitial cells (ICs) and germ cells (GCs). TFCs form stacks cells called terminal filaments (TFs), which serve as beginning points for ovariole formation. GCs give rise to the early differentiating oocytes and the GSCs of the adult ovary. ICs support GC proliferation and differentiation during larval development and give rise to somatic stem cells that support oogenesis in the adult ovary.

Different stages of larval ovarian development are depicted in Figure 1.3. At the first larval instar (L1) stage, the ovary consists of GCs and somatic cells surrounding GCs. At the second larval instar (L2) some somatic cells closely associate with GCs and become ICs (Li et al., 2003). At early third larval instar (L3), TFCs begin to differentiate from the medial side of the ovary, as a group of cells on the lateral begin to migrate toward the posterior (Sahut-Barnola et al., 1995). The migrating cells are called swarm cells. Throughout early to late L3, TFCs emerge and intercalate into TFs. Swarm cells complete their migration to the posterior of the ovary, and will give rise to the structural cells of the adult ovary. Apical cells surrounding the TFCs migrate between TFs, separating each TF to begin ovariole morphogenesis (Cohen et al., 2002). By the larval-pupal transition (LP) stage, the ovary consists of fully formed TFs separated by apical cells. Ovariole formation continues during pupal development where the structure of the germarium and ovarian stalk cells are established (King, 1970).

In this paragraph, I will discuss TF formation in detail. TFCs first intercalate and form stacks of 4-6 cells held together by a focus of actin filaments to the neighboring TF (Godt and Laski, 1995). The foci are separated by the migration of apical cells between TFs (Figure 1.3, white cells between the TFs), which begins the formation of ovarioles. The TFs then recruit 1-4 more TFCs from the posterior cells, and give rise to a TF that contains 6-8 cells per TF in *D. melanogaster*. A cofilin protein called *twinstar* that regulates actin depolymerization is required for TF morphogenesis (Chen et al., 2001). *twinstar* mutants form abnormally shaped TFs with fewer TFCs per TF. In addition, the swarm cells do not appear to migrate to the posterior. The sorting of TFCs into TFs is regulated by the BTB-PAZ domain transcription factors *bric-a-brac 1 and bric-a-brac 2* (*bab1, bab2*) (Bartoletti et al., 2012; Godt and Laski, 1995). *bab* mutants have defective TF formation and swarm cell migration. These studies suggest that the cellular dynamics and movement of TFCs and surrounding somatic cells is a critical part of TF morphogenesis.

TFs serve as the beginning point of ovariole formation, and TF number at the late larval stage corresponds to adult ovariole number in *D. melanogaster* (Hodin and Riddiford, 2000). This is in contrast to honeybees, where ovarioles can be destroyed through cell death during pupal development (Capella and Hartfelder, 1998; Reginato and Da Cruz-Landim, 2002). Ovarioles form in ovaries lacking GCs, suggesting that TF morphogenesis does not depend on GCs during larval development (Barnes et al., 2006).

ICs are intermingled with the GCs, and remain closely associated throughout L2-L3 development. IC differentiation is regulated in part by the expression of the transcription factor *traffic Jam* (*tj*) (Li et al., 2003). In *tj* mutant ovaries, GCs cluster

tightly together and have defects in proliferation and differentiation. ICs give rise to somatic stem cell populations in the adult ovary (Decotto and Spradling, 2005), and may give rise to the cap cells of the adult germ line niche that support the GSCs. GCs close to TFs will remain undifferentiated, and GCs away from TFs will begin differentiating into early oocytes starting mid to late L3 development (Gancz and Gilboa, 2013; Gancz et al., 2011).

In summary, larval ovarian development in Drosophila is a dynamic process involving multiple differentiation events and cell migration.

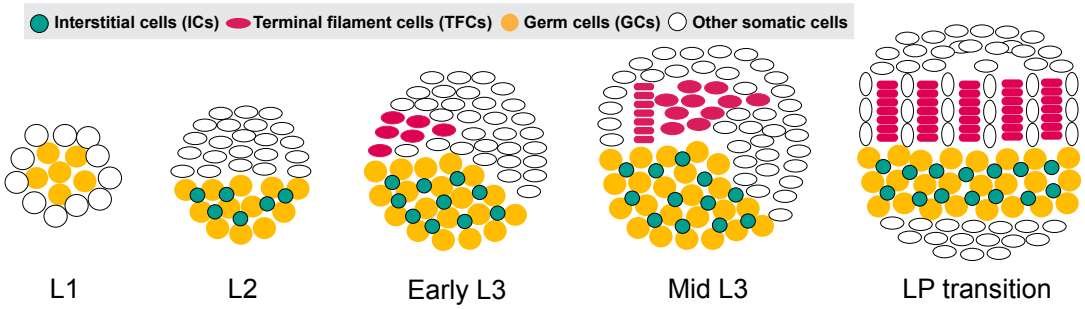

Figure 1.3. Schematic of larval ovarian development. The schematics are drawn with the anterior of the ovary towards the top and posterior toward the bottom of the page. Yellow circles denote germ cells (GCs), green circles denote interstitial cells (ICs), red circles denote terminal filament cells (TFCs), and white circles with black outline denote other somatic cells. Figure adopted from Sarikaya and Extavour (2015).

Genes regulating cell proliferation and interaction

The proliferation of TFCs and TFC precursors occurs through L1 to early L3 development. TFCs appear to exit the cell cycle as they enter a TF, and are not clonally related to other TFCs within a TF (Godt and Laski, 1995; Sahut-Barnola et al., 1995, 1996). The timing of TF formation is regulated by Ecdysone signaling via Broad-Z1 (Gancz et al., 2011). Ovaries with defective Ecdysone signaling in the somatic cells form excess TFs with defective positioning of TFs or failure of apical cell migration between TFs. The authors of this study did not investigate whether this was because a higher proportion of anterior cells were recruited to become TFCs, or because TFC precursors proliferated more than controls. In addition, Insulin signaling also regulates the proliferation of TFCs, and may also be involved in proper differentiation of TFCs into TFs (Gancz and Gilboa, 2013; Green and Extavour, 2012).

IC and GCs influence each others' proliferation and differentiation. GC differentiation is suppressed during larval development until mid to late L3, where GCs that are not close to the TFs begin to express *bag of marbles*, an early differentiation marker for oocytes (Gancz and Gilboa, 2013; Gancz et al., 2011). The differentiation program is controlled by both Ecdysone and Insulin signaling activity in the ICs. Activation of Ecdysone signaling in the soma during L1-L2 development represses GC differentiation, while Ecdysone signaling in the soma during L3 development promotes GC differentiation (Gancz et al., 2011). Activation of Insulin signaling in the soma also promotes GC differentiation, though this requires Ecdysone activity (Gancz and Gilboa, 2013). IC number is regulated by activation of Insulin signaling and receiving EGFR ligands from GCs (Gilboa and Lehmann, 2006). Interestingly, when IC number is

decreased by expressing a constitutively active version of *egfr*, GC number increases as a result, suggesting that ICs may be secreting a growth-suppressing factor that is detected by GCs.

In summary, the ovary has very interesting morphogenetic processes and cell-cell interactions that are critical in establishing the adult ovary. The IC-GC interactions that regulate each other's number provides an interesting example of relative growth within an organ, a paradigm that might extend Huxley's work to not only parts of animals, but parts of organs as well.

Thesis outline and summary

In this thesis, I investigate the developmental and environmental factors that influence the evolution of the functional size of the Drosophila ovary, as measured by ovariole number. My research goals were informed by the development of the larval ovary and the studies of ecology and genetics of ovariole number. Because TFs serve as the beginning point for ovariole morphogenesis, in Chapter II I start by addressing whether changes in TFC size or number influence TF number, thereby changing ovariole number. I identified two distinct developmental mechanisms that alter ovariole number by using both genetic manipulation and a study of plasticity response to temperature or nutrition in *D. melanogaster*. I also determined that one of these developmental mechanisms, changes in total TFC number, also underlies species-specific differences between two Drosophila species. In Appendix B, I extend this analysis to include two more species, which reveals that the second mechanism, change in TFC sorting, can also underlie species-specific differences. Given that one of the strongest predictors of

ovariole number was TFC number, in Chapter III, I set out to understand the genes that regulate cell proliferation in the larval ovary and how these genes influenced the relative growth of different cell types of the ovary. I implicate the Hippo pathway in regulating somatic cell number in the larval ovary, and also uncover a novel non-canonical role for this pathway in GCs. In Chapter IV, I investigate ovariole number differences in Hawaiian Drosophila, to understand how ecology and shifts in body size affect ovariole number evolution in this group of species that have undergone rapid island radiation.

1.2 References

Abzhanov, A., Protas, M., Grant, B.R., Grant, P.R., and Tabin, C.J. (2004). Bmp4 and morphological variation of beaks in Darwin's finches. Science (80-.). *305*, 1462–1465.

Abzhanov, A., Kuo, W.P., Hartmann, C., Grant, B.R., Grant, P.R., and Tabin, C.J. (2006). The calmodulin pathway and evolution of elongated beak morphology in Darwin's finches. Nature *442*, 563–567.

Barnes, A.I., Boone, J.M., Jacobson, J., Partridge, L., and Chapman, T. (2006). No extension of lifespan by ablation of germ line in Drosophila. Proc Biol Sci *273*, 939–947.

Bartoletti, M., Rubin, T., Chalvet, F., Netter, S., Dos Santos, N., Poisot, E., Paces-Fessy, M., Cumenal, D., Peronnet, F., Pret, A.-M., et al. (2012). Genetic basis for developmental homeostasis of germline stem cell niche number: a network of Tramtrack-Group nuclear BTB factors. PLoS One *7*, e49958.

Bossuyt, W., Chen, C.-L., Chen, Q., Sudol, M., McNeill, H., Pan, D., Kopp, A., and Halder, G. (2013). An evolutionary shift in the regulation of the Hippo pathway between mice and flies. Oncogene.

Buttitta, L.A., and Edgar, B.A. (2007). Mechanisms controlling cell cycle exit upon terminal differentiation. Curr. Opin. Cell Biol. *19*, 697–704.

Calboli, F.C.F., Kennington, W.J., and Partridge, L. (2003). QTL mapping reveals a striking coincidence in the positions of genomic regions associated with adaptive variation in body size in parallel clines of Drosophila melanogaster on different continents. Evolution (N. Y). *57*, 2653–2658.

Capella, I.C.S., and Hartfelder, K. (1998). Juvenile hormone effect on DNA synthesis and apoptosis in caste-specific differentiation of the larval honey bee (Apis mellifera L.) ovary. J. Insect Physiol. *44*, 385–391.

Chen, J., Godt, D., Gunsalus, K., Kiss, I., Goldberg, M., and Laski, F.A. (2001). Cofilin/ADF is required for cell motility during Drosophila ovary development and oogenesis. Nat. Cell Biol. *3*, 204–209.

Cohen, E.D., Mariol, M.-C., Wallace, R.M.H., Weyers, J., Kamberov, Y.G., Pradel, J., and Wilder, E.L. (2002). DWnt4 regulates cell movement and focal adhesion kinase during Drosophila ovarian morphogenesis. Dev. Cell *2*, 437–448.

David, J.R. (1970). Le nombre d'ovarioles chez Drosophila melanogaster: relatiion avec la fécondité et valeur adaptive. Arch. Zool. Exp. Gen. *111*, 357–370.

Decotto, E., and Spradling, A.C. (2005). The Drosophila ovarian and testis stem cell niches: similar somatic stem cells and signals. Dev. Cell *9*, 501–510.

Edgar, B.A. (2006). How flies get their size: genetics meets physiology. Nat. Rev. Genet. *7*, 907–916.

Finnerty, J.R., Pang, K., Burton, P., Paulson, D., and Martindale, M.Q. (2004a). Origins of bilateral symmetry: Hox and dpp expression in a sea anemone. Science (80-.). *304*, 1335–1337.

Finnerty, J.R., Pang, K., Burton, P., Paulson, D., and Martindale, M.Q. (2004b). Origins of bilateral symmetry: Hox and dpp expression in a sea anemone. Science *304*, 1335–1337.

Fritz, J. a, Brancale, J., Tokita, M., Burns, K.J., Hawkins, M.B., Abzhanov, A., and Brenner, M.P. (2014). Shared developmental programme strongly constrains beak shape diversity in songbirds. Nat. Commun. *5*, 3700.

Gancz, D., and Gilboa, L. (2013). Insulin and Target of rapamycin signaling orchestrate the development of ovarian niche-stem cell units in Drosophila. Development *140*, 4145–4154.

Gancz, D., Lengil, T., and Gilboa, L. (2011). Coordinated regulation of niche and stem cell precursors by hormonal signaling. PLoS Biol. *9*, e1001202.

Gibert, P., Capy, P., Imasheva, A., Moreteau, B., Morin, J.P., Pétavy, G., and David, J.R. (2004). Comparative analysis of morphological traits among Drosophila melanogaster and D. simulans: genetic variability, clines and phenotypic plasticity. Genetica *120*, 165–179.

Gilboa, L., and Lehmann, R. (2006). Soma-germline interactions coordinate homeostasis and growth in the Drosophila gonad. Nature *443*, 97–100.

Godt, D., and Laski, F.A. (1995). Mechanisms of cell rearrangement and cell recruitment in Drosophila ovary morphogenesis and the requirement of bric à brac. Development *121*, 173–187.

Green, D.A., and Extavour, C.G. (2012). Convergent evolution of a reproductive trait through distinct developmental mechanisms in Drosophila. Dev. Biol. *372*, 120–130.

Hejnol, A., and Martindale, M.Q. (2009). Coordinated spatial and temporal expression of Hox genes during embryogenesis in the acoel Convolutriloba longifissura. BMC Biol. *7*, 65.

Hodin, J., and Riddiford, L.M. (2000). Different mechanisms underlie phenotypic plasticity and interspecific variation for a reproductive character in drosophilids (Insecta: Diptera). Evolution (N. Y). *54*, 1638–1653.

Huxley, J.S. (1932). Problems of Relative Growth (Dover Publications).

James, A.C., Azevedo, R.B., and Partridge, L. (1995). Cellular basis and developmental timing in a size cline of Drosophila melanogaster. Genetics *140*, 659–666.

Kambysellis, M.P., and Heed, W.B. (1971). Studies of oogenesis in natural populations of Drosophilidae. I. Relation of Ovarian development and ecological habitats of the Hawaiian species. Am. Soc. Nat. *105*, 31–49.

Kauffman, S.A. (1987). Developmental logic and its evolution. Bioessays *6*, 82–87.

Kennington, W.J., and Hoffmann, A.A. (2010). The Genetic Architecture of Wing Size Divergence at Varying Spatial Scales Along a Body Size Cline in Drosophila Melanogaster. Evolution (N. Y). *64*, 1935–1943.

King, R.C. (1970). Ovarian development in Drosophila melanogaster. Acad. Press.

Klepsatel, P., Gáliková, M., Huber, C.D., and Flatt, T. (2014). SIMILARITIES AND DIFFERENCES IN ALTITUDINAL VERSUS LATITUDINAL VARIATION FOR MORPHOLOGICAL TRAITS IN DROSOPHILA MELANOGASTER. Evolution (N. Y).

Lee, S.F., Rako, L., and Hoffmann, A.A. (2011). Genetic mapping of adaptive wing size variation in Drosophila simulans. Heredity (Edinb). *107*, 22–29.

Lee, S.F., Eyre-Walker, Y.C., Rane, R. V, Reuter, C., Vinti, G., Rako, L., Partridge, L., and Hoffmann, A.A. (2013). Polymorphism in the neurofibromin gene, Nf1, is associated with antagonistic selection on wing size and development time in Drosophila melanogaster. Mol. Ecol. *22*, 2716–2725.

Li, M.A., Alls, J.D., Avancini, R.M., Koo, K., and Godt, D. (2003). The large Maf factor Traffic Jam controls gonad morphogenesis in Drosophila. Nat Cell Biol *5*, 994–1000.

Magnacca, K.N., Foote, D., and O'Grady, P.M. (2008). A review of the endemic Hawaiian Drosophilidae and their host plants. Zootaxa *1728*, 1–58.

Markow, T.A., and O'Grady, P.M. (2007). Drosophila biology in the genomic age. Genetics *177*, 1269–1276.

Miller, J.P., Yeh, N., Vidal, A., and Koff, A. (2007). Interweaving the cell cycle machinery with cell differentiation. Cell Cycle *6*, 2932–2938.

Nichols, J., and Smith, A. (2011). The origin and identity of embryonic stem cells. Development *138*, 3–8.

Nishioka, N., Inoue, K., Adachi, K., Kiyonari, H., Ota, M., Ralston, A., Yabuta, N., Hirahara, S., Stephenson, R.O., Ogonuki, N., et al. (2009). The Hippo signaling pathway components Lats and Yap pattern Tead4 activity to distinguish mouse trophectoderm from inner cell mass. Dev. Cell *16*, 398–410.

O'Grady, P.M., Lapoint, R.T., Bonacum, J., Lasola, J., Owen, E., Wu, Y., and Desalle, R. (2011). Phylogenetic and ecological relationships of the Hawaiian Drosophila inferred by mitochondrial DNA analysis. Mol. Phylogenet. Evol. *58*, 244–256.

Orgogozo, V., Broman, K.W., and Stern, D.L. (2006a). High-resolution quantitative trait locus mapping reveals sign epistasis controlling ovariole number between two drosophila species. Genetics *173*, 197–205.

Orgogozo, V., Broman, K.W., and Stern, D.L. (2006b). High-resolution quantitative trait locus mapping reveals sign epistasis controlling ovariole number between two Drosophila species. Genetics *173*, 197–205.

Parkash, R., Karan, D., and Munjal, A.K. (1998). Geographical divergence for quantitative traits in colonising populations of Drosophila kikkawai from India. Hereditas *128*, 201–205.

Partridge, L., Langelan, R., Fowler, K., Zwaan, B., and French, V. (1999). Correlated responses to selection on body size in Drosophila melanogaster. Genet. Res. *74*, 43–54.

R kha, S., Moreteau, B., Coyne, J.A., and David, J.R. (1997). Evolution of a lesser fitness trait: egg production in the specialist Drosophila sechellia. Genet. Res. *69*, 17–23.

R' kha, S., Moreteau, B., Coyne, J.A., and David, J.R. (1997). Evolution of a lesser fitness trait: egg production in the specialist Drosophila sechellia. Genet Res *69*, 17–23.

R'Kha, S., Capy, P., and David, J.R. (1991). Host-plant specialization in the Drosophila melanogaster species complex: a physiological, behavioral, and genetical analysis. Proc Natl Acad Sci USA *88*, 1835–1839.

Reginato, R.D., and Da Cruz-Landim, C. (2002). Morphological characterization of cell death during the ovary differentiation in worker honey bee. Cell Biol. Int. *26*, 243–251.

Rokas, A. (2008). The origins of multicellularity and the early history of the genetic toolkit for animal development. Annu. Rev. Genet. *42*, 235–251.

Ryan, J.F., Pang, K., Schnitzler, C.E., Nguyen, A.-D., Moreland, R.T., Simmons, D.K., Koch, B.J., Francis, W.R., Havlak, P., Smith, S. a, et al. (2013). The genome of the

ctenophore Mnemiopsis leidyi and its implications for cell type evolution. Science *342*, 1242592.

Sahut-Barnola, I., Godt, D., Laski, F.A., and Couderc, J.L. (1995). Drosophila ovary morphogenesis: analysis of terminal filament formation and identification of a gene required for this process. Dev. Biol. *170*, 127–135.

Sahut-Barnola, I., Dastugue, B., and Couderc, J.-L. (1996). Terminal filament cell organization in the larval ovary of Drosophila melanogaster: ultrastructural observations and pattern of divisions. Roux's Arch Dev Biol *205*, 356–363.

Schmidt, P.S., Matzkin, L., Ippolito, M., and Eanes, W.F. (2005). Geographic variation in diapause incidence, life-history traits, and climatic adaptation in Drosophila melanogaster. Evolution (N. Y). *59*, 1721–1732.

Stern, D.L., and Emlen, D.J. (1999). The developmental basis for allometry in insects. Development *126*, 1091–1101.

Tamura, K., Subramanian, S., and Kumar, S. (2004). Temporal patterns of fruit fly (Drosophila) evolution revealed by mutation clocks. Mol. Biol. Evol. *21*, 36–44.

Telonis-Scott, M., McIntyre, L.M., and Wayne, M.L. (2005). Genetic architecture of two fitness-related traits in Drosophila melanogaster: ovariole number and thorax length. Genetica *125*, 211–222.

Thompson, D. (1917). On growth and form.

Wayne, M.L., and Mackay, T.F. (1998). Quantitative genetics of ovariole number in Drosophila melanogaster. II. Mutational variation and genotype-environment interaction. Genetics *148*, 201–210.

Wayne, M.L., and McIntyre, L.M. (2002). Combining mapping and arraying: An approach to candidate gene identification. Proc Natl Acad Sci USA *99*, 14903–14906.

Wayne, M.L., Hackett, J.B., Dilda, C.L., Nuzhdin, S. V, Pasyukova, E.G., and Mackay, T.F. (2001). Quantitative trait locus mapping of fitness-related traits in Drosophila melanogaster. Genet. Res. *77*, 107–116.

Xie, T., and Spradling, A.C. (2000). A niche maintaining germ line stem cells in the Drosophila ovary. Science *290*, 328–330.

Zwaan, B.J., Azevedo, R.B., James, A.C., Van 't Land, J., and Partridge, L. (2000). Cellular basis of wing size variation in Drosophila melanogaster: a comparison of latitudinal clines on two continents. Heredity (Edinb). *84 (Pt 3)*, 338–347.

Chapter II:

The roles of cell size and cell number in determining ovariole number in *Drosophila*

The contents of this chapter are reprinted from Sarikaya DP, Belay AA, Ahuja A, Dorta A, Green DA 2nd, Extavour CG. The roles of cell size and cell number in determining ovariole number in *Drosophila*. *Developmental Biology*. 363: 279-289.

2.1 Abstract

All insect ovaries are composed of functional units called ovarioles, which contain sequentially developing egg chambers. The number of ovarioles varies between and within species. Ovariole number is an important determinant of fecundity and thus affects individual fitness. Although Drosophila oogenesis has been intensively studied, the genetic and cellular basis for determination of ovariole number remains unknown. Ovariole formation begins during larval development with the morphogenesis of terminal filament cells (TFCs) into stacks called terminal filaments (TFs). We induced changes in ovariole number in *Drosophila melanogaster* by genetically altering cell size and cell number in the TFC population, and analyzed TF morphogenesis in these ovaries to understand the cellular basis for the changes in ovariole number. Increasing TFC size contributed to higher ovariole number by increasing TF number. Similarly, increasing total TFC number led to higher ovariole number via an increase in TF number. By analyzing ovarian morphogenesis in another Drosophila species we showed that TFC number regulation is a target of evolutionary change that affects ovariole number. In contrast, temperature-dependent plasticity in ovariole number was due to changes in cell-cell sorting during TF morphogenesis, rather than changes in cell size or cell number. We have thus identified two distinct developmental processes that regulate ovariole number: establishment of total TFC number, and TFC sorting during TF morphogenesis. Our data suggest that the genetic changes underlying species-specific ovariole number may alter the total number of TFCs available to contribute to TF formation. This work provides for the first time specific and quantitative developmental tools to investigate the evolution of a highly conserved reproductive structure.

2.2 Introduction

All insect ovaries are composed of highly conserved functional units called ovarioles (Büning, 1994). Ovariole number varies within and between species (Markow and O'Grady, 2007; Telonis-Scott et al., 2005). Because each ovariole produces eggs autonomously (R kha et al., 1997), the number of ovarioles is an important determinant of fecundity (Cohet and David, 1978; David, 1970; R kha et al., 1997), thereby influencing evolutionary fitness (Orr, 2009). It is therefore important to understand the developmental mechanisms that regulate ovariole number. This will inform our understanding of how evolutionary changes in these mechanisms might lead to ovariole number differences, and thus fitness differences, within and between species.

Ovariole development and function are best understood in *Drosophila melanogaster*. Each ovariole consists of an anterior germarium and maturing egg chambers, or follicles. The germarium houses germ line stem cells that divide to produce oocytes (Wieschaus and Szabad, 1979). As follicles leave the germarium, they move posteriorly and continue to develop to form mature oocytes. *D. melanogaster* ovaries consist of approximately 16 to 23 ovarioles (depending on the strain). Ovariole number is determined during larval development through the morphogenesis of somatic structures called terminal filaments (TFs), each of which is composed of a stack of seven to ten terminal filament cells (TFCs) (Godt and Laski, 1995). TFC specification begins at the second larval instar (L2; Figure 2.1A), and proceeds until the onset of the pupal stage (LP; Figure 2.1D) (Godt and Laski, 1995; Sahut-Barnola et al., 1995). TFs begin to form in the late third larval instar (L3; Figure 2.1B) by intercalation of TFCs in a medial to lateral progression across the ovary (Godt and Laski, 1995). As TF formation is completed, apical somatic cells

migrate posteriorly between the TFs, secreting a basement membrane that separates TFs from each other. The progressive posterior migration of these apical cells encapsulates two to three germ line stem cells, and several early oogonia, into each forming ovariole. Finally, a stack of basal stalk cells is incorporated into the posterior end of each ovariole. These stalk cells ultimately connect ovarioles to the oviduct, providing an outlet for the oocytes formed in each ovariole (King, 1970; King et al., 1968). Because TFs serve as beginning points for ovariole formation, elucidating how TF number is established is critical to understanding the developmental and evolutionary basis of ovariole number.

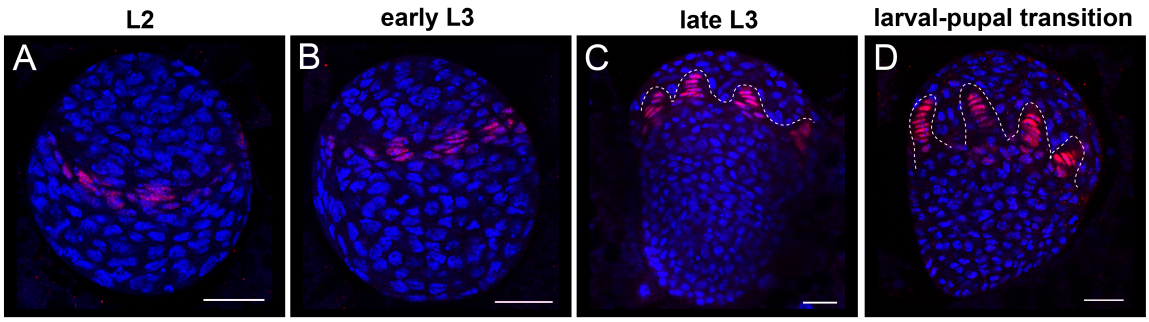

Figure 2.1. Terminal filament cell (TFC) specification, and TF morphogenesis during larval development in *D. melanogaster*. Progressive specification and intercalation of TFCs (red) begins in the second larval instar L2 (A) and progresses throughout the third larval instar L3 (B, C). Mature terminal filaments (TFs) are found at the larval–pupal stage (D). Dotted line in (C, D) outlines the forming TFs. Red: Engrailed; blue: Hoechst. Anterior is up. Scale bar = 20 μm.

Because TFs are neither created nor destroyed during normal pupal development (King, 1970), TF number at the larval-pupal transition determines adult ovariole number (Hodin and Riddiford, 2000). Ovarioles can form in the absence of germ cells (Aboïm, 1945; Engstrom et al., 1982), and changes in germ cell number do not induce changes in TF number (Barnes et al., 2006; Gilboa and Lehmann, 2006). The germ cell population thus does not have a major influence on ovariole number. This suggests that developmental processes that form and sort the somatic cells that create TFs, the TFCs, determine changes in ovariole number.

Although *D. melanogaster* oogenesis has been intensively studied, the formation of ovarioles during ovarian morphogenesis is still not well understood. Specifically, the genetic and cellular basis for determination of ovariole number remains unknown. Correct regulation of size and number in other organs, including wings in flies and somites in frogs (Cooke, 1975; Resino and Garcia-Bellido, 2004), relies on the coordination of cell number (proliferation), cell size (growth), and cell sorting behavior. Moreover, evolutionary change in body size is thought to be the result of changes in the numbers and sizes of cells (French et al., 1998; James et al., 1995; Partridge et al., 1999). We therefore hypothesized that the developmental parameters influencing ovariole number might include the numbers, sizes, and cell sorting behaviors of TFCs. In this context, we analyzed TFC number, size and morphogenesis in ovaries with genetically- or environmentally-induced differences in ovariole number. To assess the role of TFC size in determining ovariole number, we changed the activity of S6 kinase (S6K), which is a downstream regulator of Insulin/TOR signaling (reviewed by Fenton and Gout, 2011). Altering S6K activity changes cell size without affecting cell number in ectodermal

tissues (Montagne et al., 1999a). We also assessed the role of TFC number in regulating ovariole number, by manipulating the activity of the Hippo pathway. This recently described pathway plays a conserved role in controlling cell number in fruit flies and mammals, but does not alter cell size (Dong et al., 2007; Harvey et al., 2003; Wu et al., 2003). Based on the data from these manipulations, we propose a model for the major developmental processes that regulate changes in ovariole number.

We used this model to investigate the developmental basis of evolutionary change in this trait. Ovariole number is species-specific and largely genetically determined. Intra and inter-species genetic studies on ovariole number indicate that genetic variation in the trait is additive and polygenic (Coyne et al., 1991; Orgogozo et al., 2006; Telonis-Scott et al., 2005; Wayne and McIntyre, 2002; Wayne et al., 2001). To determine the roles of TFC size, number, and sorting behavior in evolutionary change in ovariole number, we compared TF morphogenesis in two Drosophila species with different ovariole numbers. Finally, we addressed the role of these cell biological parameters in phenotypic plasticity in ovariole number. Environmental inputs such as temperature and nutrition can also influence adult ovariole number (Bergland et al., 2008; Hodin and Riddiford, 2000). To assess the reasons for ovariole number changes induced by rearing environment, we compared (1) flies reared at two different temperatures, and (2) flies reared on standard or reduced nutrition, and analyzed TFC behavior. Our data suggest that genetic and environmental variation can affect ovariole number through different developmental processes.

2.3 Material and Methods

Fly strains

TRiP (Harvard Medical School) RNAi lines used to knock down Hippo pathway members were $y^1 v^1$; *P{TRiP*^{hpo}*}attP2* (Bloomington Drosophila stock center 33614; abbreviated to *UAS:RNAi*^{hpo}) and $y^1 v^1$; *P{TRiP*^{wts}*}attP2* (Bloomington Drosophila stock center 27662; abbreviated to *UAS:RNAi*^{wts}). These lines were selected as they have been reported to increase cell proliferation in the gut epithelium of flies (Karpowicz et al., 2010). Mutant S6K allele lines used were *w; P{w*$^{+mC}$*=UAS-S6k.TE}2* (Bloomington Drosophila Stock Center 6912) and *w; P{w*$^{+mC}$*=UAS-S6k.STDE}2 / CyO actinGFP*, (derived from Bloomington Drosophila Stock Center 6913 and 4533; abbreviated to *UAS:S6K*^{X}. These lines were selected as they have been reported to increase cell size (but not cell proliferation) in the wing (Barcelo and Stewart, 2002). The GAL4 driver lines used were *w; P{GawB}bab1*$^{Pgal4\text{-}2}$*/TM6, Tb*^{1} (Bloomington Drosophila Stock Center 6803) (Cabrera et al., 2002) and *nubbin:GAL4* (gift of Tassos Pavlopoulos), abbreviated to *bab:GAL4* and *nub:GAL4*, respectively. The *bab:GAL4* driver is expressed in somatic cells of the larval ovary, most strongly in the somatic cells anterior to the germ cells, which are largely destined to become TF cells (Cabrera et al., 2002). Additional somatic cell populations expressing this driver at lower levels are the intermingled cells in direct contact with germ cells, and at late L3 and prepupal stages, the somatic cells posterior to the germ cells; neither of these latter cell populations contributes to terminal filaments. The *bab:GAL4* driver is not expressed in germ cells. GAL4 line virgins were crossed to

UAS:RNAi^{hpo}, *UAS:RNAi*^{wts}, *UAS:dS6K*^{TE} and *UAS:dS6K*^{STDE} males. *D. yakuba* (UC San Diego Drosophila Stock Center 1402-0261.01 via Daniel Hartl's lab) was maintained at 25°C for all experiments.

Rearing conditions: variation of temperature and nutritional regimes

Temperature sensitive experiments were conducted with OregonR-C flies (Bloomington Drosophila Stock Center 5 via Daniel Hartl's lab). Flies were reared at 25°C or 18°C at 60% humidity on standard fly medium (0.8% agar, 2.75% yeast, 5.2% corn meal, 11% dextrose) for at least two generations before experiments were conducted (Figure A-1A). Because reduced nutritional intake of larvae resulting from crowded tubes can reduce adult ovariole number, adults were permitted to lay eggs in vials for two to six hours and then removed from the vial to prevent overcrowding of larvae. Only tubes containing fewer than 100 pupae were used for analysis of larval-pupal ovaries, and for counts of ovariole number in adults. Adults hatched from these tubes were used to create new parent cultures at the same temperature. For starvation experiments, flies were reared at 25°C on 1⁄4 standard fly medium ("quarter food") made by mixing one part standard fly medium with three parts 3% agar (VWR); overcrowding of larvae was prevented as described above.

Adult analysis: ovariole number

As described above, only tubes containing fewer than 100 larvae were used for all experiments. Adult female flies from non-crowded tubes were placed in 70% ethanol until sedated, and ovaries were dissected in 1X PBS/0.01% Triton X-100. Ovariole

number was counted in 1X PBS under a dissecting microscope using tungsten needles. At least 20 ovaries were analyzed for each strain. For temperature comparisons, a two-tailed t-test was conducted using Microsoft Excel. Ovariole number comparison for Hippo pathway and S6K experimental adults were conducted by one-way analysis of variance (ANOVA), followed by Tukey's Honestly Significant Difference (HSD) using JMP (SAS Institute Inc., Cary, NC). ANOVA is a standard statistical method based on Fisher's methodology (Fisher, 1918) for determining whether significant differences exist between means from multiple groups; the ANOVA F statistic is the ratio of the variance of the means of different groups, to the variance between samples comprising a group, and is reported in the relevant figure legends for all data. The HSD test is a method based on pairwise comparisons of means in order to determine which means are significantly different from each other.

Adult analysis: wing cell size and number

Rearing temperature was reported to affect wing cell size but not number (Azevedo et al., 2002). We confirmed these results in our experimental conditions by analyzing wing cell size and density in flies used in our experiments. Wings were removed from dissected adults and placed in 100% ethanol overnight. Wings were then washed in 70% ethanol, 1:1 ethanol : glycerol, and 50% glycerol in distilled water for 10 minutes, and mounted in 50% glycerol. Mounted wings were imaged using a Zeiss AxioImager Z1 and a Zeiss MRm AxioCam driven by AxioVision v4.6, and total surface area of the wing, cell number per area of interest, and cell size were measured using AxioVision v4.6 or Adobe Photoshop CS3. Total surface area was measured for the entire wing. Cell number per unit area was measured in the ventral region of compartment C of the wing (Baena-López

et al., 2005); the number of bristles was counted for the same surface area region of interest in different wings. Cell size was measured by selecting a single bristle, and connecting the surrounding six bristles to obtain the surface area. Alternatively, the distance between trichomes was measured and taken as the diameter of the cell to calculate cell area. Comparable cell size values were obtained with both methods. At least ten cells were measured per wing to obtain the individual's average wing cell size.

Immunohistochemistry

For larval analysis, the transition stage between the larval and pupal stages was used (referred to as "larval-pupal stage" throughout). Pupae with hardened, white pupal cases were collected from vials containing less than 100 pupae. This stage was chosen for analysis because TF formation, which is gradual throughout the third larval instar, ends at the larval-pupal stage, and so the TF number of these ovaries is the final TF number for that individual. Ovaries with incomplete TFs (still in the process of intercalating) were discarded from the dataset, and only ovaries where all TFs were separated by migrating anterior cells were used. Samples were dissected in 1X PBS, fixed in 4% paraformaldehyde/1X PBS for 25 minutes at room temperature, and blocked in 0.5% goat serum (Jackson ImmunoLabs) in 1X PBS/0.01% Triton-X for 30 minutes at room temperature. Primary antibody incubation in mouse anti-Engrailed (Developmental Studies Hybridoma Bank 4D9, 1:40) and/or anti-Traffic jam (gift of D. Godt, 1:4000) in blocking solution was conducted overnight at 4oC. Engrailed labels the TF population (Forbes et al., 1996), and Traffic jam (Tj) labels intermingled cells and cap cells (Li et al., 2003). Samples were washed in 1X PBS/0.01% Triton-X twice for 15 minutes at room temperature, and incubated with FITC-Phalloidin or A555-Phalloidin (Invitrogen, 1:120

of 200 U/ml stock solution), Hoechst 33342 (Sigma, 1:500 of 10 mg/ml stock solution), and goat anti-Mouse Alexa 568 (Invitrogen, 1:500) and/or goat anti-Guinea Pig Cy5 (Jackson ImmunoLabs, 1:500) overnight at 4oC. Samples were mounted in Vectashield mounting medium (Vector labs), and imaged using a Zeiss LSM 710 confocal microscope.

Larval analysis: TFC number per TF

Z-stack confocal images of stained ovaries were taken with a 40X objective and 1.2-1.6x zoom to capture the entire ovary at 1 mm intervals (Figure A.1B). Total TF number was counted and comparisons between samples were conducted using a two-tailed t-test. TFCs were identified by morphology and Engrailed expression. Engrailed-expressing cuboidal cells at the posterior of the TF were excluded from the TFC number count, as they were adjacent to germ cells and had characteristics of cap cells. Ten ovaries were analyzed per temperature for the environmental manipulations, and five individual ovaries for each genetic condition were analyzed for TFC number per TF. The dataset for each manipulation (temperature/genetic) contained measurements of several cells from each of for five or ten individuals, which were randomly selected. To account for potential individual variation affecting the dataset, we conducted a nested mixed model ANOVA (JMP, SAS Institute Inc., Cary, NC) with a fixed manipulation term (genetic or environmental) and a random-effects individual term nested within manipulation. Sample sizes reported reflect the individual ovary number, rather than the number of measurements made per individual, unless indicated otherwise.

Larval analysis: TFC size

Larval TFC size (= volume in mm^3) was obtained specifically in the third and fourth TFC of each TF, counting from the anterior tip of the TF in order to ensure the cells were comparable in size (Figure A.2A). Cell outlines were visualized by Phalloidin staining. For each individual ovary, four to ten cells (average 7.8 cells per sample) were analyzed by measuring the surface area of the cell through serial confocal image stacks for all stacks where the selected cell was visible (Figure A.2A). The sum of the surface areas was multiplied by the thickness of each individual stack to obtain the cell size. In the case of GAL4/UAS experiments, the maternal strain (w; babGAL4$^{P4.2}$/TM6b, Tb^1) and F1 siblings (w; UAS- S6K^X/+; TM6b/+) carry the TM6b balancer that contains a mutant allele of the gene Tubby. Flies carrying this Tubby allele are visibly shorter and stouter than wild type as adults and larvae (L. Lindsley and G. Zimm, 1992). The mechanistic causes for the phenotype are unknown, but they may affect cell size. Because cell size is one of the parameters under analysis, and the TM6b chromosome is not present in any experimental animals of interest, we excluded these genotypes from the analysis. Similar to TFC number per TF, a mixed model nested ANOVA (see above) was used to analyze the data by setting temperature/genetic treatment as a fixed effect, and the individual nested within temperature/genetic treatment as random effect using JMP (SAS Institute Inc., Cary, NC).

Larval analysis: total TFC number

Obtaining images of larval ovaries where all TFCs can be resolved at the late L3 and larval-pupal stage is inefficient. As an alternative, we estimated total TFC number by calculating an average TFC number per TF (by averaging measurements from more than eight TFs; Figure 2.2B), and multiplying by the TF number of that ovary (Figure 2.2C).

We tested the validity of this method by randomly choosing eight TFC number per TF measurements from ovaries where total TFC number had also been counted manually, and comparing the calculated and counted measurements. For all eight ovaries analyzed, our calculation method gave total TFC numbers that matched the counted number with an accuracy of ±4 (average TFC number was 134.5 for manual counts and 135.8 for proxy calculation; p=0.79, two-tailed t-test; Figure A.1D). Calculating total TFC number in this manner thus provides an accurate proxy for total TFC number.

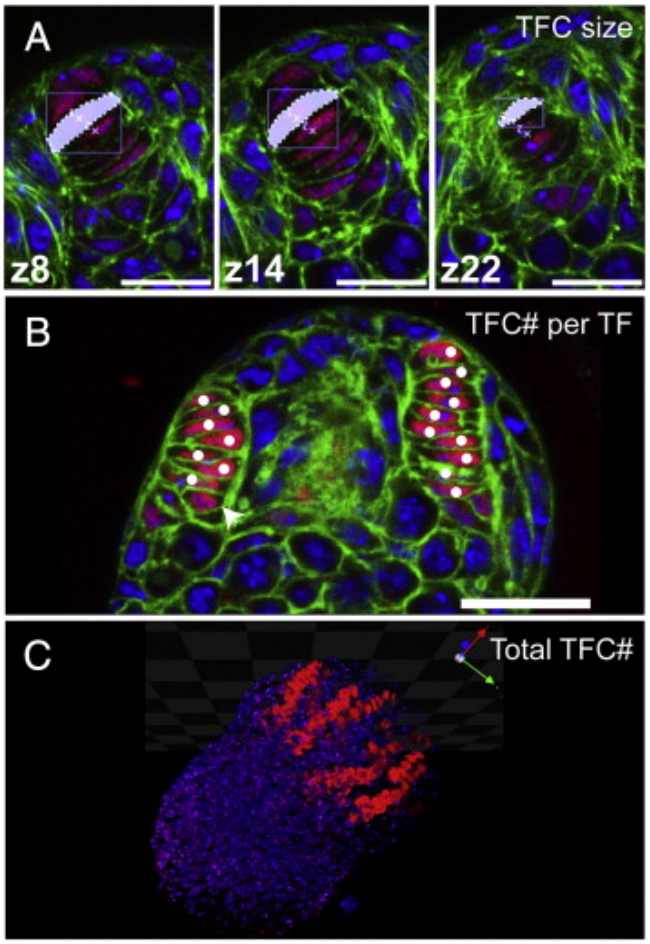

Figure 2.2. Methodology for measuring TFC parameters in late larval ovaries. (A) Examples of optical sections used to measure TFC size. Measurements of TFC sizes were per- formed on the third and fourth cell from the anterior of the TF. For a given TF cell (iden- tifiable by Engrailed-positive signal and flattened morphology), the surface area (visible with phalloidin-labeled cell outlines) is measured in every optical section where the cell is present, and cell size is obtained by multiplying the sum of the surface area measurements by the thickness of the optical sections. Examples of three Z-plane optical sections through a TF are shown. Optical section thickness is uniform for all im- ages of a given ovary. (B) Example of an optical section used to count TFC number per TF. TFCs are identified (white dots) as engrailed-positive cells (red) with flattened nu- clei in stacks. Cuboidal cells at the posterior of stacks with lower levels of Engrailed sig- nal (arrowhead) are not included in TFC number counts, as they are cap cell precursors. (C) Examples of optical section reconstructions used to count total TF number. Sections are taken through a larval–pupal stage ovary, and reconstructed in three dimensions in order to visualize TFs where all TFCs are visible; the average number of TFCs per TF is then multiplied by the total TF number for that ovary (see Materials and methods and Figure A1B). To count TF number manually (Figure A1B), all optical sections of an ovary were examined. Red: Engrailed; blue: Hoechst; green: phalloidin. Anterior is up and scale bar=6μm in A and B; in C anterior is to the top right and scale bar = 10 μm.

2.4 Results

Constitutively active S6K in TFCs results in increased adult ovariole number

We hypothesized that TF number would be affected by cellular behaviors during TF morphogenesis. Specifically, we examined TFC size, TFC number per TF, and total TFC number to gain insight into how the dynamics of TF morphogenesis could affect TF number, and therefore ovariole number. To test whether changes in TFC size could influence TF number, we used mutations in S6 Kinase (S6K) as a tool to change cell size. S6K phosphorylates the ribosomal subunit S6 and as a result, regulates translation downstream of the Insulin and TOR signaling pathways (Jefferies et al., 1997). Expression of constitutively active S6K alleles in the wing increases cell size, but does not alter cell number (Montagne et al., 1999) (Figure A.2). We took advantage of the GAL4/UAS system (Brand and Perrimon, 1993)to increase S6K activity in the TFC population (Figure A.3) with a bab:GAL4 driver line (Cabrera et al., 2002) (Figure 1.2A, B; see Methods).

Expression of two different constitutively active alleles of S6K ($S6K^{TE}$ and $S6K^{STDE}$; see Methods) in TFCs resulted in an increase in ovariole number of females from the experimental cross (Figure 2.3A, B). Ovariole number in the experimental F1 flies (*w; UAS-S6K^{X}/+; bab:GAL4$^{p4.2}$/+)* was compared to ovariole numbers in GAL4-only or UAS-only parental and sibling controls. We compared samples using a one-way ANOVA followed by Tukey's HSD, and found that in both cases, F1 adult females had significantly more ovarioles compared to parents and siblings ($S6K^{TE}$: $p<0.001$; $S6K^{STDE}$: $p<0.001$). This increase was also reflected in larval TF number ($S6K^{TE}$ $p<0.01$; $S6K^{STDE}$ $p<0.05$) (Figure 2.3C).

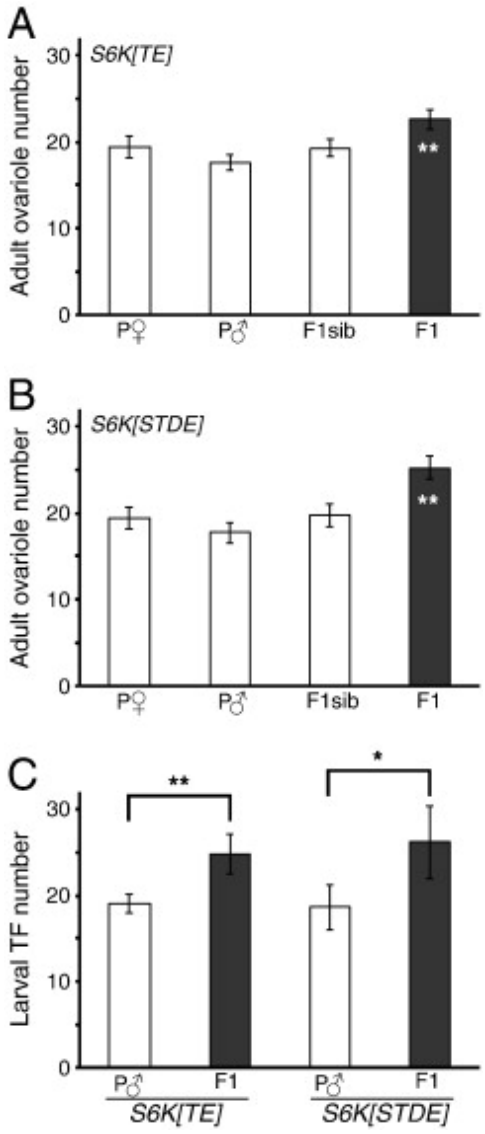

Figure 2.3. Expression of constitutively active S6K alleles in TFCs increases ovariole number. (A) Ovariole number in ovaries expressing$S6K^{TE}$ with the *bab:GAL4* driver (Fig. A3) (F1) is significantly higher than that of siblings (F1sib) and both parental strains (P♂, P♀) ($F_{(3,75)} = 26.14$, $p < 0.0001$), indicated by **. (B) Ovariole number in larval ovaries expressing *S6KSTDE* with the *bab:GAL4* driver (Fig. A3) (F1) is significantly higher ($p < 0.01$) than that of siblings (F1sib) and parental strains (P♂, P♀) ($F_{(3,76)} = 14.12$,$p < 0.0001$), indicated by **. (C) TF number in larval/pupal stage ovaries expressing the different *S6K* alleles (F1) with the*bab:GAL4* driver (Fig. S3) compared with the parental strains (P♂). $n = 20$ per genotype for adult ovariole number analysis, and$n = 5$ per genotype for larval analysis. In (C) * $p < 0.05$, ** $p < 0.01$. Error bars indicate 95% confidence interval.

Constitutively active S6K increases both size and number of TFCs

In Drosophila ectodermal tissues (wing, eye) and in mouse ectodermal tissues (adrenal gland) and embryonic fibroblasts, S6K activity is linked to control of cell size, but not of cell number (Lawlor et al., 2002; Montagne et al., 1999b). However, the function of S6K in mesodermal tissues in Drosophila has not yet been investigated. We therefore asked whether the effect on adult ovariole number caused by constitutive S6K activity was due to a size change in TFCs. Cell size measurements were taken manually at the larval-pupal transition stage (referred to as "larval-pupal stage" throughout; see Methods) using confocal z-stacks of TFs (Figure 2.2A) from four to ten cells per sample (average 7.8; see Methods). F1s (*w; UAS-S6K^{X}/+; babGAL4$^{p4.2}$/+*) and UAS-only controls were compared using a mixed-model nested ANOVA (see Methods). Average TFC size increased in both S6K alleles as compared to controls, although the increase was not statistically significant in the case of the STDE allele (S6K^{TE}: $p<0.05$; S6K^{STDE}: $p=0.52$; Figure 2.4A, B).

A model that could explain how larger TFCs would result in more terminal filaments, is one where developmental regulation controls total overall TF size. This model predicts that TFs made of larger cells would contain fewer TFCs per TF, in order to maintain constant TF size. To test this model we measured TFC number per TF, and found that it was significantly lower ($p<0.01$) for the S6K^{TE} allele and slightly lower ($p=0.075$) in the S6K^{STDE} allele (Figure 2.4C, D). However, TFC size was not correlated with the number of cells per TF (Figure A.4). This suggests that S6K may have a role in sorting TFCs that is independent of cell size.

The reductions in TFC number per TF were not steep enough to account for the

generation of all supernumerary TFs induced by S6K constitutive expression. We therefore analyzed the effect of constitutive S6K activity on total TFC number. Surprisingly, expression of both $S6K^{TE}$ and $S6K^{STDE}$ resulted in a significant increase in total TFC number in the experimental cross ($S6K^{TE}$: $p<0.01$; $S6K^{STDE}$: $p<0.05$) (Figure 2.4E, F), indicating that constitutively active S6K alleles alter cell number in the developing ovary. This contrasts with what has been observed in ectodermal tissues, where S6K only affects cell size (Lawlor et al., 2002; Montagne et al., 1999) (Figure A.2). In summary, the increase in ovariole number induced by overexpression of constitutively active S6K results from an increase both in TFC size and in cell number. This shows that S6K activity can have cell-type specific effects in *D. melanogaster*.

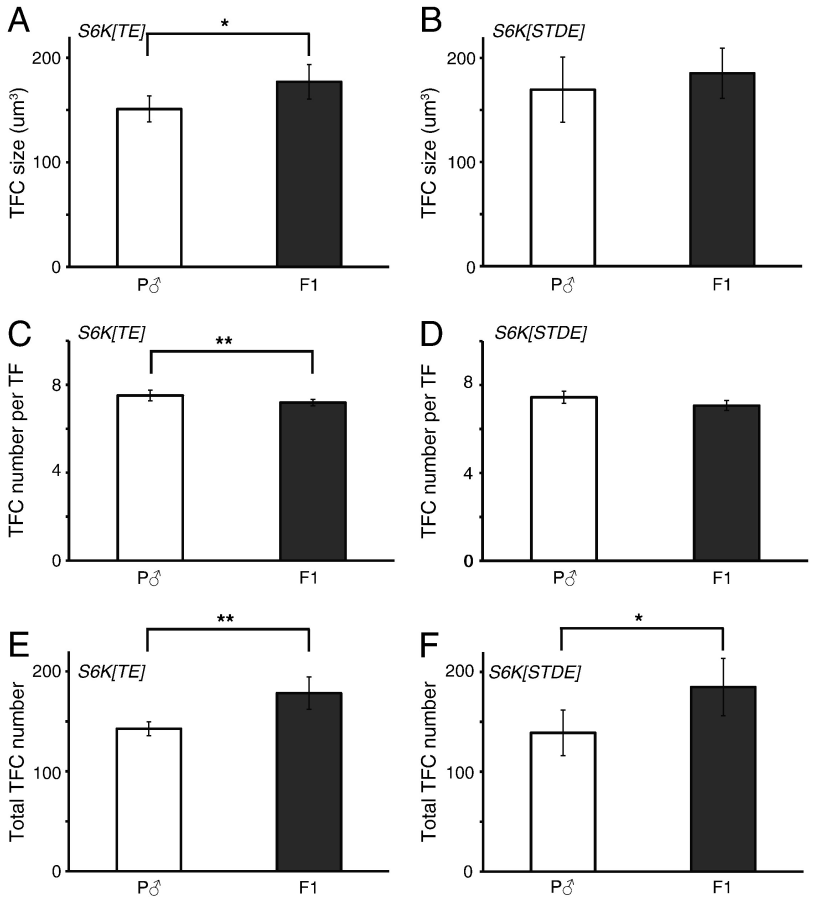

Figure 2.4 Expression of constitutively active S6K alleles in TFCs increases TFC cell size and cell number. TFC size in larval–pupal stage ovaries expressing $S6K^{TE}$ (A) and $S6K^{STDE}$ (B) with the *bab:GAL4* driver (Fig. A3) compared with the parental strains (P♂). Total TFC number in larval–pupal stage ovaries expressing $S6K^{TE}$ (C) and $S6K^{STDE}$ (D) compared with the parental strain (P♂). $n = 5$ per genotype for analysis. * $p < 0.05$, ** $p < 0.01$. Error bars indicate 95% confidence interval.

RNAi knockdown of Hippo pathway components in TFCs increases ovariole number

Previous studies had suggested that total ovarian cell number could contribute to ovariole number determination (Hodin and Riddiford, 2000), but did not distinguish between different ovarian cell types. Our cell size manipulation experiments unexpectedly resulted in changes in cell number as well, leading us to suspect that TFC number could be an important parameter in determining TF number. We therefore tested the hypothesis that changes specifically in total TFC number would affect TF number, and hence affect ovariole number. In order to change cell number without changing cell size, we disrupted the activity of the Hippo pathway, a conserved metazoan growth pathway (Dong et al., 2007; Huang et al., 2005; Wu et al., 2003). We used the *bab:GAL4* driver (Figure A3) and UAS-RNAi strains against two key Hippo pathway kinases, *hippo* (*hpo*) and *warts* (*wts*). RNAi knockdown of these two genes using the same strains from the Transgenic RNAi Project (TRiP) increases proliferation in the gut epithelium (Karpowicz et al., 2010). RNAi knockdown of hippo and warts in TFCs (Figure A2C, D) increased ovariole number of females from the experimental cross (*w; UAS:RNAi /+ ; bab:GAL4*$^{p4.2}$/+) compared with GAL4-only and UAS-only parental and sibling controls (Figure 1.5A, B). One-way ANOVA revealed a significant difference in ovariole number between these genotypes (*hpo*-RNAi: $p<0.0001$; *wts*-RNAi: $p<0.0001$), and comparisons using Tukey's HSD revealed that in both cases, F1 adult females had significantly more ovarioles compared to parents and siblings ($p<0.05$). This increase was reflected in larval TF number (*hpo*-RNAi: $p=0.028$; *wts*-RNAi: $p=0.037$; Figure 2.5C), suggesting that the cellular behaviors underlying the increase in ovariole number take place during larval stages.

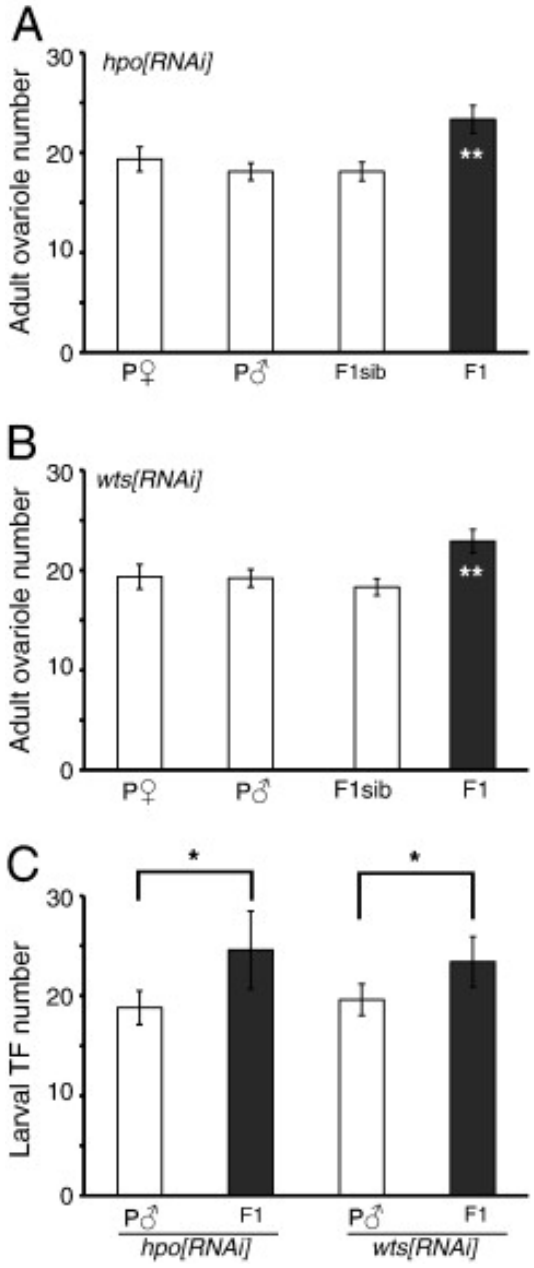

Figure 2.5. Decreasing Hippo pathway activity in TFCs increases ovariole number. (A–B) Ovariole number in ovaries expressing *hpo*-RNAi (A) or *wts*-RNAi (B) with the *bab:GAL4* driver (Fig. A3) during development (F1) is significantly higher than F1 siblings carrying only a balancer (F1sib) than both parental strains (P♂, P♀). *hpo*: $F_{(1,80)} = 18.16$, $p < 0.0001$; *wts*: $F_{(1,80)} = 16.29$, $p < 0.0001$. (C) TF number in ovaries at larval–pupal stage ovaries expressing the different Hippo pathway RNAi lines (F1) compared with the parental strain (P♂). $n = 20$ per genotype for adult ovariole number analysis, and $n = 5$ per genotype for larval analysis. * $p < 0.05$, ** $p < 0.01$. Error bars indicate 95% confidence interval.

Reduced Hippo pathway activity increases total TFC number

To investigate the developmental causes underlying the increase in ovariole number, we then analyzed larval-pupal TFCs with reduced *hpo* and *wts* activity. As expected, TFC cell size was unchanged from controls (*hpo*-RNAi: p=0.93; *wts*-RNAi: p=0.23; Figure 2.6A, B), and we did not observe a difference in TFC number per TF (*hpo*-RNAi: p=0.58; *wts*- RNAi: p=0.72; Figure 2.6C, D). However, there was a significant increase in total TFC number (*hpo*-RNAi: p<0.01; *wts*-RNAi: p=0.028; Figure 2.6E, F). This shows that TF number can be modified by direct changes in total TFC number, without affecting the stacking mechanism that creates TFs. In summary, downregulating the Hippo pathway in TFCs increased total TFC number, thereby increasing the number of TFs created and resulting in higher ovariole number.

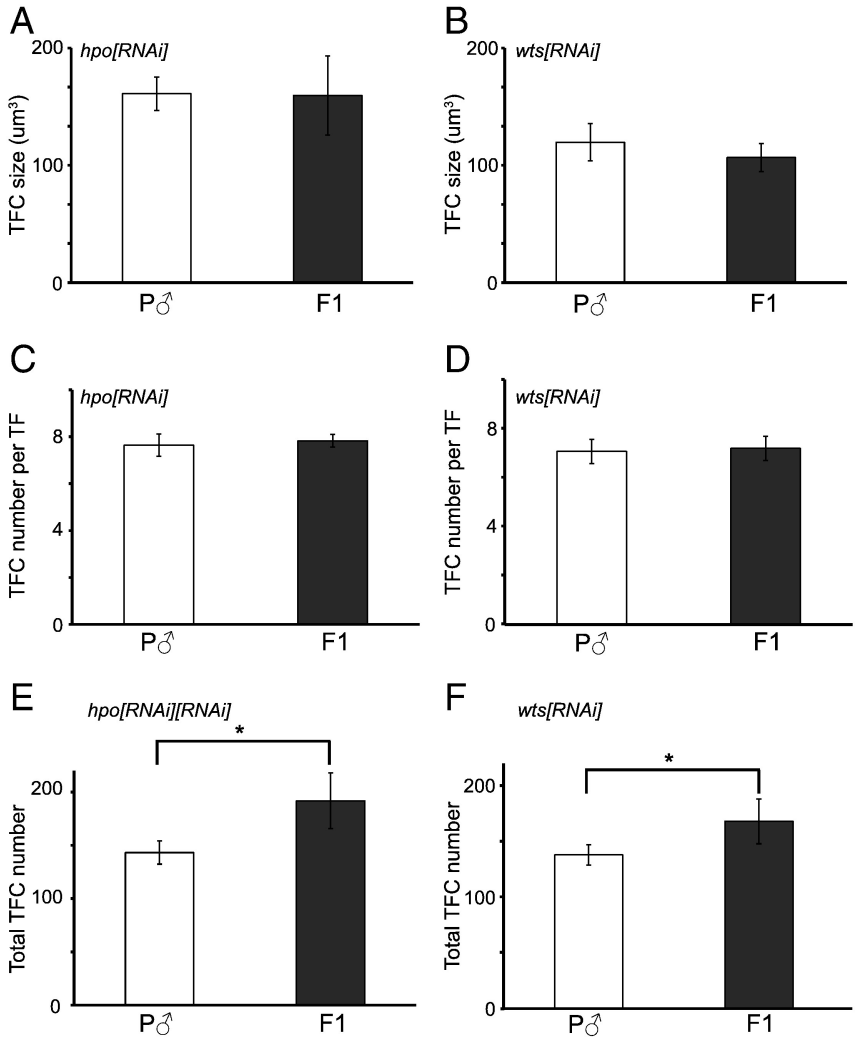

Figure 2.6. Decreasing Hippo pathway activity in TFCs increases total TFC number, without affecting cell size or sorting. (A–B) TFC volume of larval–pupal stage ovaries expressing *hpo*-RNAi (A) or *wts*-RNAi (B) with the *bab:GAL4* driver (Figure A.3) compared to parental strain *y1v1; UAS-RNAi*. *hpo*: $F_{(1,76)} = 0.0066, p = 0.93$; *wts*: $F_{(1,80)} = 1.6, p = 0.23$. (C–D) TFC number per TF of larval–pupal stage ovaries expressing *hpo*-RNAi (C) or *wts*-RNAi (D) compared to parental strains. *hpo*: $F_{(1,112)} = 0.32, p = 0.58$; *wts*: $F_{(1,102)} = 0.13, p = 0.72$. (E–F) Total TFC number of larval–pupal stage ovaries expressing (E) *hpo*-RNAi and (F) *wts*-RNAi compared to parental strain. $n = 5$ per genotype for analysis. * $p < 0.05$. Error bars indicate 95% confidence interval.

Ovariole number differences between D. melanogaster *and* D. yakuba *result from differences in TFC number*

Because we found that TFC number was a key regulator of TF number and thus ovariole number in *D. melanogaster*, we hypothesized that evolutionary changes in TFC number could be responsible for ovariole number differences in different Drosophila species. To test this hypothesis, we examined TFC number in *D. yakuba* (Figure 2.7A, B). This species diverged from the lineage containing *D. melanogaster* 4-6 million years ago (Li et al., 1999), and has an average of 14 ovarioles per ovary (Markow and O'Grady, 2007). We first confirmed that this difference in adult ovariole number correlated with a difference in TF number in larval-pupal stage ovaries (Figure 2.7C, E, $p<0.05$). Consistent with our hypothesis, this reduced TF number was the result of a smaller total number of TFCs (Figure 2.7D, $p<0.01$), which were organized into TFs that contained the same number of TFCs per TF as *D. melanogaster* (Figure 2.7E, $p=0.72$). This shows that the developmental basis of evolutionary change in ovariole number between these two species is a change in proliferation of a specific cell population within the ovary, the TFCs.

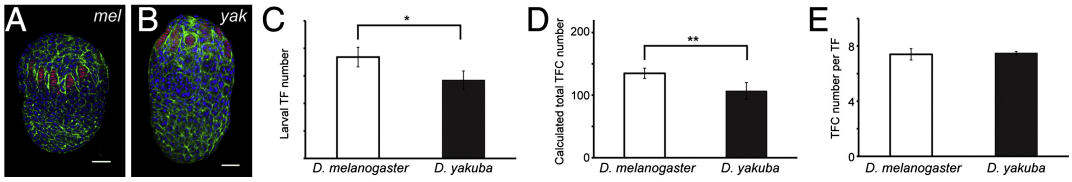

Figure 2.7. TF number, TFC number and TF morphogenesis in *D. yakuba*. Larval–pupal stage ovaries in *D. melanogaster* (A) and *D. yakuba*(B). (C) TF number at larval–pupal stage of *D. yakuba* and *D. melanogaster* . (D) TFC number at larval–pupal stage in *D. yakuba*and *D. melanogaster*. (E) TFC number per TF at larval–pupal stage in *D. yakuba* and *D. melanogaster* ($F_{(1, 148)} = 0.1323, p = 0.72$). Animals were reared at 25 °C for all experiments. In (A, B) anterior is up and scale bar = 20 μm. * $p < 0.05$, ** $p < 0.01$. Error bars indicate 95% confidence interval. Apparent morphological differences between (A) and (B) are an artifact of flattened preparation in (B).

Adult ovariole number and larval TF number decrease in response to lower rearing temperature or decreased nutrition

Finally, we asked if temperature- and nutrition-dependent phenotypic plasticity in ovariole number could proceed through the same developmental mechanisms as genetic variation. Previous studies reported an effect of temperature on ovariole number in *D. melanogaster*, in both wild and laboratory populations (Chakir et al., 2007; Delpuech et al., 1995; Hodin and Riddiford, 2000; Moreteau et al., 1997). Similarly, nutrient intake can also affect ovariole number in *D. melanogaster*: increasing yeast content in the medium increases ovariole number (Bergland et al., 2008), and relatively reduced nutrient levels results in reduced ovariole number (Hodin and Riddiford, 2000; Robertson, 1957). To understand the developmental causes for temperature-induced differences in ovariole number, we analyzed OregonR flies reared at 18°C and 25°C on standard fly medium (Figure A.1A). To investigate the developmental basis for nutrition- dependent reduction in ovariole number, we raised OregonR flies at 25°C on a diet with one quarter the nutrient level of control flies ("quarter food"). In both of these conditions we counted adult ovariole number per ovary and observed, as expected, a significant decrease in ovariole number at 18°C compared to 25°C, and on full medium compared to quarter food ($p<0.001$ for both comparisons) (Figure 2.8A). Similarly, larval-pupal stage TF number corresponded with adult ovariole number in all conditions (Figure 2.8B). The difference was statistically significant in both cases ($p<0.05$ for temperature comparisons and $p<0.01$ for nutrition comparison). This confirms that the decrease in adult ovariole number caused by lower rearing temperature or reducing nutritional intake is a result of reduced larval TF number.

Nutrition affects ovariole number by altering TFC number

We asked whether a second environmental variable, nutrition, also affected ovariole number via the same developmental processes as those altered in our temperature experiments. We found that in fact, variation of different developmental parameters was involved. Flies raised on quarter food had significantly smaller and fewer TFCs than controls (Figure 2.8D, E; $p<0001$ in both cases). This is consistent with previous observations that limiting nutrition reduces both cell size and cell number in epithelial tissues (Neel, 1940; Robertson, 1959) (Figure 2.8C, A.5). However, in contrast to the temperature experiments, the number of TFCs per TF was not significantly different between quarter food-raised flies and full food-raised controls (Figure 2.8F; $p=0.96$). This indicates that, similar to what we observed when altering cell size with the $S6K^{TE}$ alleles (Figure 2.4A, A.4A), altering cell size via nutrition does have a significant impact on TF morphogenesis. The largest contributor to reduced ovariole number in flies raised on quarter-food is therefore the reduction in total TF number (Figure 2.8E), which results in fewer TFs being formed.

Rearing temperature does not affect ovariole number by altering TFC number

We next examined TFC size, TFC number per TF, and total TFC number in ovaries of larvae reared at different temperatures. Because temperature correlates negatively with cell size in somatic epithelial tissues (Azevedo et al., 2002) (Figure 2.8C), we expected that TFCs would also be enlarged by a colder rearing temperature. Surprisingly however, we found no significant difference in TFC size between the two rearing temperatures ($p=0.58$) (Figure 2.8D). As temperature also affects cell cycle and therefore might be

expected to change total cell number, we analyzed total TFC number per ovary at 18°C and 25°C. In wing cell populations, cell number is not affected by temperature (Azevedo et al., 2002) (Figure A.2). Similarly, no differences were observed in total TFC number between larvae reared at 18°C and 25°C (Figure 2.8E; $p=0.45$). This demonstrates that, unlike the species-specific differences in ovariole number, the temperature effect on ovariole number is not achieved by changing the number or size of TFCs. Furthermore, the contrast with the temperature effects observed on wing cell size (Figure A.5) indicates that temperature-induced changes in development can be tissue-specific.

Rearing temperature affects ovariole number by altering TFC number per TF

Even though there was a significant decrease in TF number in larval ovaries reared at 18oC compared with 25°C, there was no corresponding significant decrease in total TFC number. This suggests that temperature-induced changes in TF morphogenesis might account for differences in total TF number. Accordingly, we found a significant increase in TFC number per TF in ovaries from larvae reared at 18°C ($p<0.01$) (Figure 2.8F). This suggests that during early ovarian morphogenesis, the size and starting number of TFCs is similar regardless of the temperature. However, as morphogenesis proceeds and TFs form, lower temperatures result in changes to the mechanism that organizes cells, such that a larger number of TFCs are incorporated into each TF. As a result, fewer TFs are formed at lower temperatures.

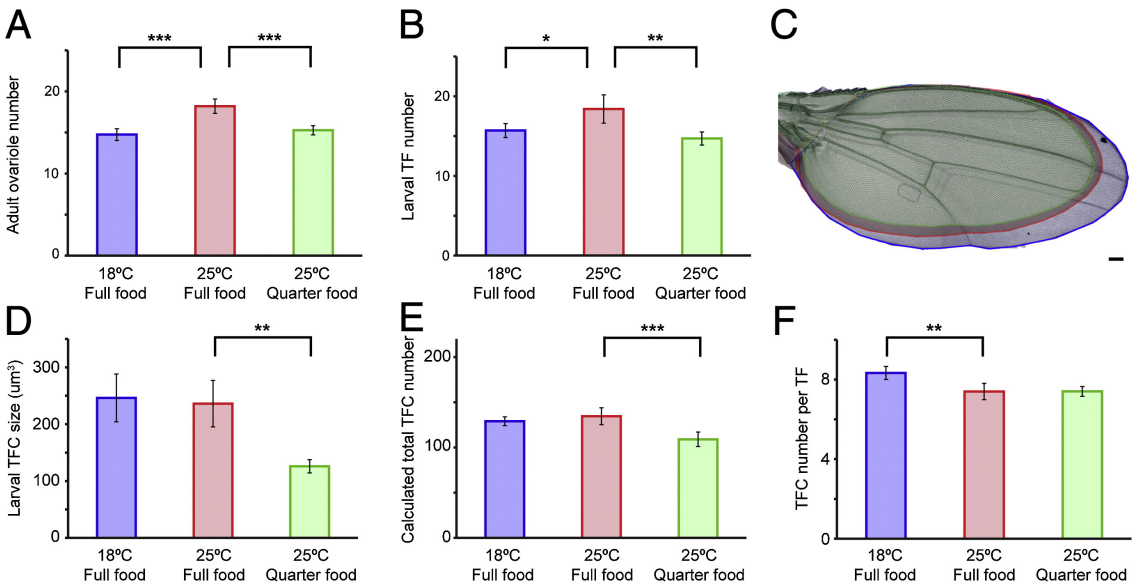

Figure 2.8. The effects of temperature and nutrition on ovariole number, TF number and TFC morphogenesis. (A) Ovariole number decreases at colder temperatures and in flies raised on quarter food. Mean ovariole number of OregonR flies reared at 18 °C (blue), 25 °C (red) and on quarter food (green). (B) TF number at larval–pupal stage of animals reared at 18 °C, 25 °C and on quarter food. (C) Wing size increases at colder temperatures and decreases with reduced nutrition. Outlines of total adult wing surface area of flies reared at 18 °C, 25 °C, and on quarter food; n = 5 for all conditions. Scale bar = 100 μm. Anterior is to the left. (D) TFC size in larval–pupal stage OregonR ovaries reared at 18 °C, 25 °C, and on quarter food (between temperatures $F_{(1,57)} = 0.3288$, $p = 0.58$; between nutritional regimes $F_{(1,177)} = 25.69$, $p < 0.001$). (E) Total TFC number of larval–pupal stage OregonR ovaries reared at 18 °C, 25 °C and on quarter food (between temperatures $p = 0.45$; between nutritional regimes $p < 0.001$). (F) TFC number per TF of larval–pupal stage OregonR ovaries reared at 18 °C, 25 °C and on quarter food between temperatures $F_{(1,182)} = 12.22$, $p < 0.01$; between nutritional regimes $F_{(1,67)} = 0.0019$, $p = 0.96$). $n = 40$ adults per temperature for adult ovariole counts, and $n = 10$ larvae per temperature for TF number counts. Error bars indicate 95% confidence interval. * $p < 0.05$, ** $p < 0.01$, *** $p < 0.001$.

2.5 Discussion

Here we have shown that two distinct developmental mechanisms can alter ovariole number: the establishment of total TFC number (Figure 2.9A), and the local cell–cell sorting process during TF formation (Figure 2.9B). These two processes appear to be differently employed to alter ovariole number. Specifically, by genetically altering the activity of developmental growth pathways, we observed that change in ovariole number was achieved by changes in total TFC number, rather than by changing TFC number per TF. Similarly, changes in TFC number appeared responsible for ovariole number differences between two *Drosophila* species, and for starvation-induced reduction in ovariole number. In contrast, temperature-induced differences in ovariole number were caused by changes in TFC number per TF, rather than changes in total TFC number or TFC size. We postulate that at least some of the genetic changes underlying species-specific ovariole number may alter total TFC number, while temperature-dependent variation may result from differences in TFC sorting during TF formation.

In this work we have examined specifically the TFC population of the somatic ovary. Previous work has analyzed total ovarian cell number in relation to ovariole number, and did not always find a direct correlation (Hodin and Riddiford, 2000). We therefore suggest that total ovarian cell number is unlikely to be the parameter targeted for evolutionary variation in this trait. Consistent with the hypothesis that total ovarian cell number is not necessarily a useful predictor of ovariole number, *Drosophila mauritiana* has fewer ovarioles than *Drosophila simulans*, but more total ovarian cells than *D. simulans* (Hodin and Riddiford, 2000). Thorax length (a proxy index for body size) can correlate positively with ovariole number, but this correlation is strong only

under poor nutritional conditions (Bergland et al., 2008): when grown on food with high yeast concentrations, genetic correlations between thorax length and ovariole number are not significant (Telonis-Scott et al., 2005; Wayne and Mackay, 1998). Our dissection of the response of cellular populations and processes to ovariole number variation suggests that the specific ovarian cell population likely to be the target of evolutionary change is the TFC population. Further studies will be needed to determine if modification of the TFC population is a conserved mechanism of evolutionary change in insect species that differ in ovariole number.

Tissue-specific response to temperature and constitutively active S6K

While investigating the mechanisms underlying ovariole number change, we identified tissue-specific responses to both temperature and overexpression of constitutively active *S6K*. Larval rearing temperature affects overall body size of *D. melanogaster* by causing a change in cell size of the epidermal cells (Azevedo et al., 2002) (Figure 2.9C). When the same strain of flies are reared at colder temperatures, the flies are larger, and the cells that compose the epidermal tissues are larger, but there is no difference in cell number. In contrast, we did not observe cell size differences in the ovarian TFC cells, but rather observed a change in the cell–cell sorting behavior during TF formation.

S6K activity in the *Drosophila* wing influences cell size without affecting cell number (Montagne et al., 1999b). Our analysis showed that constitutively active *S6K* activity could also increase TFC size, but this increase was only statistically significant with the $S6K^{TE}$ allele. In contrast to the wing, however, constitutive *S6K* activity in TFCs significantly increased cell number. The

mammalian *S6K* orthologues S6K1 and S6K2 have been implicated in proliferation in some tissues but to our knowledge S6K has not previously been reported to influence cell proliferation in *Drosophila*.

Interestingly, while constitutively active *S6K* significantly increased TFC number, it also decreased TFC number per TF. This was true even for the *S6KSTDE* allele, where cell size was not significantly increased compared to controls. Since a clear correlation between TFC size and number of cells per TF was not observed (Figure A.5), TF size may not contribute significantly to regulating TF number (Figure 2.9C). Instead, it is possible that Insulin or TOR signaling, which both act via S6K may also be involved in the process of cell–cell sorting of TFCs.

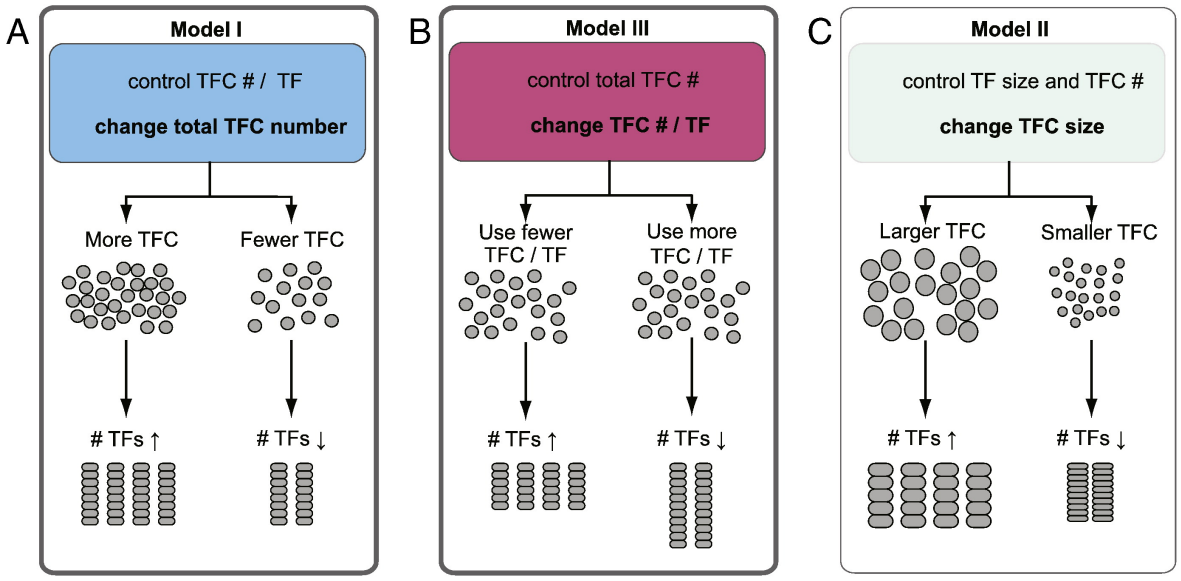

Figure 2.9. Models for developmental parameters that determine ovariole number. (A) Model I: TFC number determines TF number. This model predicts that ovariole number variation is achieved through changes in total TF cell number, but not by altering TF cell number per TF. (B) Model II: TFC number per TF determines TF number. Under this model, variation in ovariole number occurs by changes in TF Cell number per TF, regardless of total TF cell number. (C) Model III: TF morphogenesis controls for TF size. This model predicts that the TF morphogenesis program detects and controls overall TF size; changes in ovariole number would therefore come about through differences in TFC size. This would be predicted to have a secondary effect on TF cell number per TF, such that TFs with larger cells would have fewer cells per TF; however, our data do not support this corollary of Model III (Figure A.4). Our data suggest that growth pathway activity can affect ovariole number primarily via Model I and to a lesser extent via III, and that both nutritional intake and genetic variation between species may change ovariole number via these developmental mechanisms. In contrast, temperature effects on ovariole number in *D. melanogaster* proceed via Model II.

The developmental mechanisms influencing evolutionary change in ovariole number

The ovaries of all insects are composed of ovarioles, and ovariole number changes frequently in insect evolution (Büning, 1994). One of the best-studied examples of ovariole number change is in honeybees, where females develop into queens with hundreds of ovarioles, or workers with only five to ten ovarioles, depending on larval nutrition (Haydak, 1970). The developmental process that ultimately results in ovariole number difference between queens and workers is increased apoptosis in worker ovaries during late larval instars, which actively reduces ovarian structures, and higher ovarian cell proliferation in queens (Reginato and Cruz-Landim, 2003; Reginato and Da Cruz-Landim, 2002). However, it is unclear which specific cell population is the dominant contributor to either apoptosis or proliferation in shaping honeybee ovariole number (Capella and Hartfelder, 1998; Reginato and Da Cruz-Landim, 2002). In contrast to honeybees, apoptosis is not a regulator of ovariole number in *Drosophila* species (Hodin and Riddiford, 2000), but our now data demonstrate that higher TFC proliferation can also increase ovariole number in *D. melanogaster*. This suggests that proliferation control of the TFC population may be a developmental process that is a target of evolutionary change in ovariole number in *Drosophila*, and perhaps in other insects.

Ovariole number in Drosophilid flies can change relatively rapidly within a clade. For example, the *melanogaster* subgroup contains *D. simulans*, *D. mauritiana*, and *D. sechellia*, three species that diverged from a common ancestor less than one million years ago., Their species-specific ovariole numbers are approximately 35, 28, and 17 respectively, and are proportional to fecundity: *D. simulans* is the most fecund of these three species, and *D. sechellia* the least, under standard laboratory rearing conditions(R

kha et al., 1997). These Drosophilids do not display a difference in apoptosis in the developing ovary, but rather have different numbers of total ovarian cells in late larval stages(Hodin and Riddiford, 2000), consistent with the differences in total TFC number that we observed here for *D. melanogaster* and *D. yakuba*. This further supports our hypothesis that TFC proliferation, rather than differential apoptosis, is a developmental process subject to evolutionary change in Drosophilid ovariole number. Because developmental studies on this group have thus far been limited, future work could take advantage of this clade as an opportunity to study the developmental basis for ovariole number variation across shorter evolutionary time scales.

Cell types and evolutionary change

Evolutionary change in *Drosophila* wing size occurs through changes in both cell number and cell size, where selective pressures are proposed to act on the size of the entire wing, rather on specific mechanisms of cell proliferation or growth (Zwaan et al., 2000). Dipteran wing development comprises a continuous, interlocked set of processes, in which proliferation, growth and patterning of all wing disk cells show a high degree of coupling throughout development (Baena-Lopez and Garcia-Bellido, 2006, Garcia-Bellido and Garcia-Bellido, 1998, Rafel and Milan, 2008 and Resino and Garcia-Bellido, 2004). By contrast, in ovariole development discrete steps of proliferation, patterning, movement and sorting by one of many distinct ovarian cell types are required to produce TFs. Each step of TF formation is relatively autonomous with respect to the behaviors of other ovarian cell types during morphogenesis, and to global body-wide processes of growth and patterning (Green & Extavour, unpublished observations; Boyle and DiNardo, 1995, Gilboa and Lehmann, 2006, Kerkis, 1931, King, 1970, Li et al.,

2003 and Riechmann et al., 1998). TFC behavior may thus be able to change in response to a particular evolutionary pressure, without large effects on the other aspects of ovarian or general somatic development. In this context, *Drosophila* ovaries provide an interesting model for addressing the role of different cell types in organ size evolution.

In summary, we have taken a developmental approach to a long-standing question regarding the evolution of a quantitative fitness trait, and shed new light on the specific cell population likely to be the target of evolutionary change in ovariole number. We hypothesize that the most promising candidate pathways for future investigation of species-specific genetic changes affecting ovariole number are pathways that control growth and cell proliferation in TFCs. These may include cell cycle genes, long-range signaling molecules, and organ-level proliferation and growth control pathways. Consistent with this hypothesis, several such genes, including the insulin receptor, are contained in the *Drosophila* QTL that have been identified as linked to inter- and intraspecies variation in this trait (Orgogozo et al., 2006, Wayne and McIntyre, 2002 and Wayne et al., 2001), and insulin pathway genes are present in some honeybee QTL linked to ovariole number differences (Hunt et al., 2007). Intriguingly, differential activity of the insulin pathway can alter ovariole number in both *D. melanogaster* (Green & Extavour, unpublished observations;Richard et al., 2005 and Tu and Tatar, 2003) and in honeybees (Mutti et al., 2011, Patel et al., 2007 and Wolschin et al., 2011). Our work provides novel developmental and cell biological tools to test the hypotheses that these and other genes have been the direct targets of evolutionary change leading to ovariole number variation.

2.7 References

Azevedo, R.B.R., French, V., and Partridge, L. (2002). Temperature modulates epidermal cell size in Drosophila melanogaster. J Insect Physiol *48*, 231–237.

Baena-López, L.A., Baonza, A., and García-Bellido, A. (2005). The orientation of cell divisions determines the shape of Drosophila organs. Curr Biol *15*, 1640–1644.

Barcelo, H., and Stewart, M.J. (2002). Altering Drosophila S6 kinase activity is consistent with a role for S6 kinase in growth. Genesis *34*, 83–85.

Barnes, A.I., Boone, J.M., Jacobson, J., Partridge, L., and Chapman, T. (2006). No extension of lifespan by ablation of germ line in Drosophila. Proc Biol Sci *273*, 939–947.

Bergland, A.O., Genissel, A., Nuzhdin, S. V, and Tatar, M. (2008). Quantitative trait loci affecting phenotypic plasticity and the allometric relationship of ovariole number and thorax length in Drosophila melanogaster. Genetics *180*, 567–582.

Brand, A.H., and Perrimon, N. (1993). Targeted gene expression as a means of altering cell fates and generating dominant phenotypes. Development *118*, 401–415.

Cabrera, G.R., Godt, D., Fang, P.-Y., Couderc, J.-L., and Laski, F.A. (2002). Expression pattern of Gal4 enhancer trap insertions into the bric à brac locus generated by P element replacement. Genesis *34*, 62–65.

Capella, I.C.S., and Hartfelder, K. (1998). Juvenile hormone effect on DNA synthesis and apoptosis in caste-specific differentiation of the larval honey bee (Apis mellifera L.) ovary. J. Insect Physiol. *44*, 385–391.

Chakir, M., Moreteau, B., Capy, P., and David, J.R. (2007). Phenotypic variability of wild living and laboratory grown Drosophila: Consequences of nutritional and thermal heterogeneity in growth conditions. J. Therm. Biol. *32*, 1–11.

Cohet, Y., and David, J. (1978). Control of the adult reproductive potential by preimaginal thermal conditions. A study in Drosophila melanogaster. Oecologia *36*, 295–306.

Coyne, J.A., Rux, J., and David, J.R. (1991). Genetics of morphological differences and hybrid sterility between Drosophila sechellia and its relatives. Genet Res *57*, 113–122.

David, J.R. (1970). Le nombre d'ovarioles chez Drosophila melanogaster: relatiion avec la fécondité et valeur adaptive. Arch. Zool. Exp. Gen. *111*, 357–370.

Delpuech, J.-M., Moreteau, B., Chiche, J., Pla, E., Vouidibio, J., and David, J.R. (1995). Phenotypic plasticity and reaction norms in temperate and tropical populations of

Drosophila melanogaster: Ovarian size and developmental temperature. Evolution (N. Y). *49*, 670–675.

Dong, J., Feldmann, G., Huang, J., Wu, S., Zhang, N., Comerford, S.A., Gayyed, M.F., Anders, R.A., Maitra, A., and Pan, D. (2007). Elucidation of a Universal Size-Control Mechanism in Drosophila and Mammals. Cell *130*, 1120–1133.

Fenton, T.R., and Gout, I.T. (2011). Functions and regulation of the 70kDa ribosomal S6 kinases. Int J Biochem Cell Biol *43*, 47–59.

Forbes, A.J., Lin, H., Ingham, P.W., and Spradling, A.C. (1996). hedgehog is required for the proliferation and specification of ovarian somatic cells prior to egg chamber formation in Drosophila. Development *122*, 1125–1135.

French, V., Feast, M., and Partridge, L. (1998). Body size and cell size in Drosophila: the developmental response to temperature. J. Insect Physiol. *44*, 1081–1089.

Gilboa, L., and Lehmann, R. (2006). Soma-germline interactions coordinate homeostasis and growth in the Drosophila gonad. Nature *443*, 97–100.

Godt, D., and Laski, F.A. (1995). Mechanisms of cell rearrangement and cell recruitment in Drosophila ovary morphogenesis and the requirement of bric à brac. Development *121*, 173–187.

Harvey, K.F., Pfleger, C.M., and Hariharan, I.K. (2003). The Drosophila Mst ortholog, hippo, restricts growth and cell proliferation and promotes apoptosis. Cell *114*, 457–467.

Hodin, J., and Riddiford, L.M. (2000). Different mechanisms underlie phenotypic plasticity and interspecific variation for a reproductive character in drosophilids (Insecta: Diptera). Evolution (N. Y). *54*, 1638–1653.

Huang, J., Wu, S., Barrera, J., Matthews, K., and Pan, D. (2005). The Hippo signaling pathway coordinately regulates cell proliferation and apoptosis by inactivating Yorkie, the Drosophila Homolog of YAP. Cell *122*, 421–434.

James, A.C., Azevedo, R.B., and Partridge, L. (1995). Cellular basis and developmental timing in a size cline of Drosophila melanogaster. Genetics *140*, 659–666.

Jefferies, H.B., Fumagalli, S., Dennis, P.B., Reinhard, C., Pearson, R.B., and Thomas, G. (1997). Rapamycin suppresses 5'TOP mRNA translation through inhibition of p70s6k. EMBO J *16*, 3693–3704.

Karpowicz, P., Perez, J., and Perrimon, N. (2010). The Hippo tumor suppressor pathway regulates intestinal stem cell regeneration. Development *137*, 4135–4145.

L. Lindsley, D., and G. Zimm, G. (1992). The genome of Drosophila melanogaster. 1133.

Lawlor, M.A., Mora, A., Ashby, P.R., Williams, M.R., Murray-Tait, V., Malone, L., Prescott, A.R., Lucocq, J.M., and Alessi, D.R. (2002). Essential role of PDK1 in regulating cell size and development in mice. EMBO J *21*, 3728–3738.

Li, M.A., Alls, J.D., Avancini, R.M., Koo, K., and Godt, D. (2003). The large Maf factor Traffic Jam controls gonad morphogenesis in Drosophila. Nat Cell Biol *5*, 994–1000.

Li, Y.J., Satta, Y., and Takahata, N. (1999). Paleo-demography of the Drosophila melanogaster subgroup: application of the maximum likelihood method. Genes Genet. Syst. *74*, 117–127.

Markow, T.A., and O'Grady, P.M. (2007). Drosophila biology in the genomic age. Genetics *177*, 1269–1276.

Montagne, J., Stewart, M.J., Stocker, H., Hafen, E., Kozma, S.C., and Thomas, G. (1999a). Drosophila S6 kinase: a regulator of cell size. Science *285*, 2126–2129.

Montagne, J., Stewart, M.J., Stocker, H., Hafen, E., Kozma, S.C., and Thomas, G. (1999b). Drosophila S6 kinase: a regulator of cell size. Science (80-.). *285*, 2126–2129.

Moreteau, B., Morin, J.P., Gibert, P., Pétavy, G., Pla, E., and David, J.R. (1997). Evolutionary changes of nonlinear reaction norms according to thermal adaptation: a comparison of two Drosophila species. C R Acad Sci III, Sci Vie *320*, 833–841.

Orgogozo, V., Broman, K.W., and Stern, D.L. (2006). High-resolution quantitative trait locus mapping reveals sign epistasis controlling ovariole number between two Drosophila species. Genetics *173*, 197–205.

Orr, H.A. (2009). Fitness and its role in evolutionary genetics. Nat Rev Genet *10*, 531–539.

Partridge, L., Langelan, R., Fowler, K., Zwaan, B., and French, V. (1999). Correlated responses to selection on body size in Drosophila melanogaster. Genet. Res. *74*, 43–54.

R kha, S., Moreteau, B., Coyne, J.A., and David, J.R. (1997). Evolution of a lesser fitness trait: egg production in the specialist Drosophila sechellia. Genet. Res. *69*, 17–23.

Reginato, R.D., and Cruz-Landim, C. (2003). Ovarian growth during larval development of queen and worker of Apis mellifera (Hymenoptera: Apidae): a morphometric and histological study. Braz J Biol *63*, 121–127.

Reginato, R.D., and Da Cruz-Landim, C. (2002). Morphological characterization of cell death during the ovary differentiation in worker honey bee. Cell Biol. Int. *26*, 243–251.

Sahut-Barnola, I., Godt, D., Laski, F.A., and Couderc, J.L. (1995). Drosophila ovary morphogenesis: analysis of terminal filament formation and identification of a gene required for this process. Dev. Biol. *170*, 127–135.

Telonis-Scott, M., McIntyre, L.M., and Wayne, M.L. (2005). Genetic architecture of two fitness-related traits in Drosophila melanogaster: ovariole number and thorax length. Genetica *125*, 211–222.

Wayne, M.L., and Mackay, T.F. (1998). Quantitative genetics of ovariole number in Drosophila melanogaster. II. Mutational variation and genotype-environment interaction. Genetics *148*, 201–210.

Wayne, M.L., and McIntyre, L.M. (2002). Combining mapping and arraying: An approach to candidate gene identification. Proc Natl Acad Sci USA *99*, 14903–14906.

Wayne, M.L., Hackett, J.B., Dilda, C.L., Nuzhdin, S. V, Pasyukova, E.G., and Mackay, T.F. (2001). Quantitative trait locus mapping of fitness-related traits in Drosophila melanogaster. Genet. Res. *77*, 107–116.

Wieschaus, E., and Szabad, J. (1979). The development and function of the female germ line in Drosophila melanogaster: a cell lineage study. Dev. Biol. *68*, 29–46.

Wu, S., Huang, J., Dong, J., and Pan, D. (2003). hippo encodes a Ste-20 family protein kinase that restricts cell proliferation and promotes apoptosis in conjunction with salvador and warts. Cell *114*, 445–456.

Zwaan, B.J., Azevedo, R.B., James, A.C., Van 't Land, J., and Partridge, L. (2000). Cellular basis of wing size variation in Drosophila melanogaster: a comparison of latitudinal clines on two continents. Heredity (Edinb). *84 (Pt 3)*, 338–347.

Chapter III:

The Hippo pathway regulates homeostatic growth of stem cell niche precursors in the *Drosophila* ovary

The contents of this chapter are reprinted from Sarikaya DP and Extavour CG. The Hippo pathway regulates homeostatic growth of stem cell niche precursors in the Drosophila ovary. *PLOS Genetics* 11(2): e1004962. Copyright 2015 with permission.

3.1 Abstract

The Hippo pathway regulates organ size, stem cell proliferation and tumorigenesis in adult organs (Halder and Johnson 2011, Tumaneng, Russell et al. 2012). Whether the Hippo pathway influences establishment of stem cell niche size to accommodate changes in organ size, however, has received little attention (Ramos and Camargo 2012). Here, we ask whether Hippo signaling influences the number of stem cell niches that are established during development of the *Drosophila* larval ovary (Gancz, Lengil et al. 2011, Gancz and Gilboa 2013), and whether it interacts with the same or different effector signaling pathways in different cell types. We demonstrate that canonical Hippo signaling regulates autonomous proliferation of the soma, while a novel *hippo*-independent activity of Yorkie regulates autonomous proliferation of the germ line. Moreover, we demonstrate that Hippo signaling mediates non-autonomous proliferation signals between germ cells and somatic cells, and contributes to maintaining the correct proportion of these niche precursors. Finally, we show that the Hippo pathway interacts with different growth pathways in distinct somatic cell types, and interacts with EGFR and JAK/STAT pathways to regulate non-autonomous proliferation of germ cells. We thus provide evidence for novel roles of the Hippo pathway in establishing the precise balance of soma and germ line, the appropriate number of stem cell niches, and ultimately regulating adult female reproductive capacity.

3.2 Introduction

The Hippo pathway is a tissue-intrinsic regulator of organ size, and is also implicated in stem cell maintenance and cancer (Barry and Camargo 2013). An outstanding question in the field is whether the Hippo pathway regulates proliferation of cells comprising stem cell niches during development in order to ensure that adult organs have an appropriate number of stem cells and stem cell niches (Ramos and Camargo 2012). The adult *Drosophila* ovary is an extensively studied stem cell niche system. In this organ, specialized somatic cells regulate the proliferation and differentiation of germ line stem cells (GSCs) throughout adult reproductive life (reviewed in Eliazer and Buszczak 2011). The fact that GSCs are first established in larval stages raises the question of how the correct numbers of GSCs, and their associated somatic niche cells, are achieved during larval development. To date, only the Ecdysone, Insulin and EGFR pathways have been implicated in this process (Gancz, Lengil et al. 2011, Gancz and Gilboa 2013, Matsuoka, Hiromi et al. 2013). Here, we investigate the role of the Hippo pathway in regulating proliferation of somatic cells and GSC niche precursors to establish correct number of GSC niches.

Our current understanding of the Hippo pathway is focused on the core kinase cascade and upstream regulatory members. The Hippo pathway's upstream regulation is mediated by a growth signal transducer complex comprising Kibra, Expanded and Merlin (Hamaratoglu, Willecke et al. 2006, Baumgartner, Poernbacher et al. 2010, Genevet, Wehr et al. 2010, Yu, Zheng et al. 2010) and the planar cell polarity regulators Fat (Bennett and Harvey 2006, Silva, Tsatskis et al. 2006, Willecke, Hamaratoglu et al. 2006) and Crumbs (Grzeschik, Parsons et al. 2010, Robinson, Huang et al. 2010). Regulation of Hippo signaling further upstream of these factors appears to be cell type-specific (Reddy and Irvine 2011). When the core kinase cascade is

active, the kinase Hippo (Hpo) phosphorylates the kinase Warts (Wts) (Udan, Kango-Singh et al. 2003, Wu, Huang et al. 2003). Phosphorylated Wts then phosphorylates the transcriptional coactivator Yorkie (Yki), which sequesters Yki within the cytoplasm (Huang, Wu et al. 2005). In the absence of Hpo kinase activity, unphosphorylated Yki can enter the nucleus and upregulate proliferation-inducing genes (Huang, Wu et al. 2005, Nolo, Morrison et al. 2006, Thompson and Cohen 2006, Wu, Liu et al. 2008). The Hippo pathway affects proliferation cell-autonomously in the eye and wing imaginal discs, glia, and adult ovarian follicle cells in *Drosophila* (Udan, Kango-Singh et al. 2003, Wu, Huang et al. 2003, Meignin, Alvarez-Garcia et al. 2007, Polesello and Tapon 2007, Reddy and Irvine 2011), as well as in liver, intestine, heart, brain, breast and ovarian cells in mammals (Striedinger, VandenBerg et al. 2008, Zhang, Ji et al. 2009, Hall, Wang et al. 2010, Zhao, Li et al. 2010, Heallen, Zhang et al. 2011, Zhou, Zhang et al. 2011). Hippo pathway is often improperly regulated in cancers of these tissues, which display high levels and ectopic activation of the human ortholog of Yki, YAP (Zhao, Wei et al. 2007, Hall, Wang et al. 2010, Zhang, George et al. 2011, Zhou, Zhang et al. 2011). Upregulation of YAP is also commonly observed in a variety of mammalian stem cell niches, where YAP can be regulated in a Hippo-independent way to regulate stem cell function (reviewed in Ramos and Camargo 2012). Interestingly, germ line clones lacking Hippo pathway member function do not cause germ cell tumors in the adult *Drosophila* ovary, which has led to the hypothesis that Hippo signaling functions only in somatic cells but not in the germ line (Sun, Zhao et al. 2008, Yu, Poulton et al. 2008).

More recently, it has become clear that the Hippo pathway can regulate proliferation non-autonomously: Hippo signaling regulates secretion of JAK/STAT and EGFR ligands in *Drosophila* intestinal stem cells (Karpowicz, Perez et al. 2010, Ren, Wang et al. 2010, Shaw,

Kohlmaier et al. 2010), and of EGFR ligands in breast cancer cell lines (Zhang, Ji et al. 2009), and the resulting changes in ligand levels affect the proliferation of surrounding cells non-autonomously. How autonomous and non-autonomous effects of the Hippo pathway coordinate differentiation and proliferation of multiple cell types has nonetheless been poorly investigated. Moreover, most studies address the Hippo pathway's role in adult stem cell function, but whether Hippo signaling also plays a role in the early establishment of stem cell niches during development remains unknown.

Here we use the *Drosophila* larval ovary as a model to address both of these issues. Adult ovaries comprise egg-producing structures called ovarioles, each of which houses a single GSC niche. The GSC niche is located at the anterior tip of each ovariole, and produces new oocytes throughout adult life. The niche cells include both GSC and differentiated somatic cells called cap cells (King 1970). Each GSC niche lies at the posterior end of a stack of seven or eight somatic cells termed terminal filaments (TFs). Somatic stem cells located close to the GSCs serve as a source of follicle cells that enclose each developing egg chamber during oogenesis (Eliazer and Buszczak 2011). All of these cell types originate during larval development, when the appropriate number of stem cells and their niches must be established. The larval ovary thus serves as a compelling model to address issues of homeostasis and stem cell niche development.

TFs serve as beginning points for ovariole formation and thus establish the number of GSC niches (Godt and Laski 1995). TFs form during third instar larval (L3) development by the intercalation of terminal filament cells (TFCs) into stacks (TFs) (Figure 3.1A; (Godt and Laski 1995)). TFCs proliferate prior to entering a TF, and cease proliferation once incorporated into a TF (Sahut-Barnola, Dastugue et al. 1996). The morphogenesis and proliferation of TFCs during the third larval instar (L3) is regulated by Ecdysone and Insulin signaling, and by the BTB/POZ

factor *bric-à-brac* (*bab*) (Godt and Laski 1995, Hodin and Riddiford 1998, Gancz, Lengil et al. 2011, Bartoletti, Rubin et al. 2012, Gancz and Gilboa 2013, Green II and Extavour 2014). Intermingled cells (ICs) arise from somatic cells that are in close contact with the germ cells (GCs) during L2, and proliferate throughout larval development (Li, Alls et al. 2003) (Figure 3.1A). ICs regulate GC proliferation and differentiation and are thought to give rise to escort cells in the adult niche (Song, Call et al. 2007, Gancz, Lengil et al. 2011, Gancz and Gilboa 2013). Both Insulin and EGFR signaling promote the proliferation of ICs (Green II and Extavour 2012, Gancz and Gilboa 2013). Finally, larval GCs give rise to GSCs and early differentiating oocytes. GCs proliferate during development and do not differentiate until mid-L3, when the GSCs are specified in niches that form posterior to the TFs (Gilboa and Lehmann 2006, Gancz, Lengil et al. 2011, Gancz and Gilboa 2013), and the remaining GCs begin to differentiate as oocytes. GCs secrete Spitz, an EGFR ligand, and promote proliferation of ICs (Gilboa and Lehmann 2006). In addition, activation of Insulin and Ecdysone signaling in ICs regulates timing of early GC differentiation and cyst formation (Gancz, Lengil et al. 2011, Gancz and Gilboa 2013), though the identity of the IC-to-GC signal is unknown. ICs can non-autonomously regulate the proliferation of GCs both positively and negatively through Insulin and EGFR signaling respectively (Gilboa and Lehmann 2006, Gancz and Gilboa 2013, Matsuoka, Hiromi et al. 2013).

We previously showed that *hpo* and *wts* regulate TFC number in a cell-autonomous manner (Sarikaya, Belay et al. 2012). Here we demonstrate a role for canonical Hippo pathway activity in regulating both TFCs and ICs. We also provide evidence for three novel roles of Hippo pathway members in ovarian development: First, in contrast to a previous report suggesting that *yki* did not play a role in determining GC number (Sun, Zhao et al. 2008), we

show that non-canonical, *hpo*-independent *yki* activity regulates proliferation of the germ line. Second, we show that Hippo signaling regulates homeostatic growth of germ cells and somatic cells through the JAK/STAT and EGFR pathways. Third, we show that the Hippo pathway interacts with the JAK/STAT pathway to regulate TFC number, and with both the EGFR and JAK/STAT pathways to regulate IC number autonomously and GC number non-autonomously. These data elucidate how Hippo pathway-mediated control of ovarian development establishes an organ-appropriate number of stem cell niches, and thus ultimately influences adult reproductive capacity.

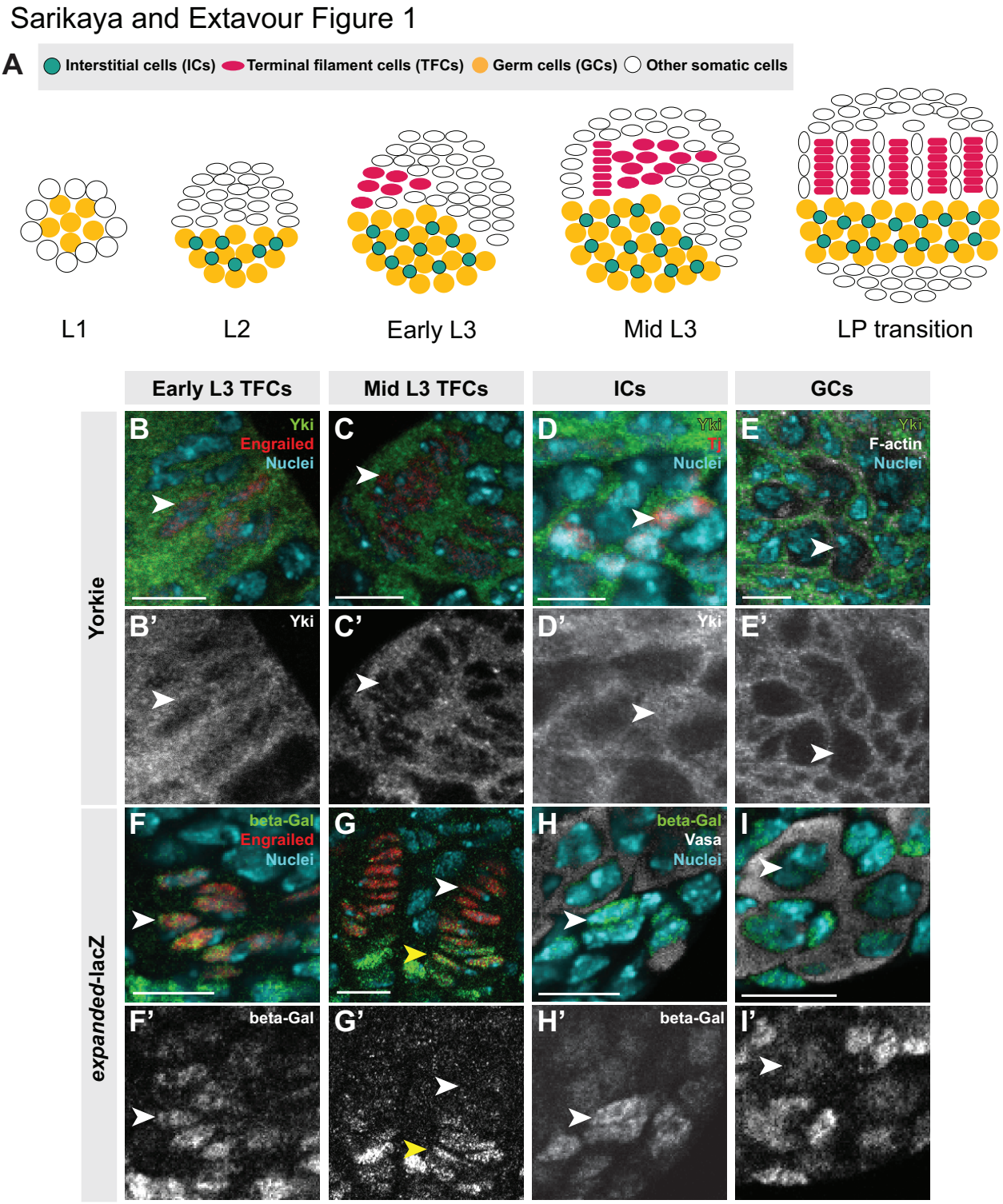

Figure 3.1. Hippo pathway activity is cell-type specific in the larval ovary. (A) Schematic of *Drosophila* larval ovarian development from first instar (L1) to the larval-pupal (LP) transition stage. The L1 larval ovary consists of germ cells (GCs: yellow) surrounded by a layer of somatic cells. As the ovary grows (L2), some somatic cells intermingle with GCs, becoming intermingled cells (ICs: green). Terminal filament cells (TFCs: pink) emerge during early L3, and begin intercalating to form terminal filaments (TFs), whose formation continues until the LP stage. (B-

I) Expression of Yorkie (B-E) and *expanded-lacZ* (F-I) in larval ovarian cell types. See Figure C.2I-J for quantification. (B) TFCs at early L3 that are intercalating into TFs display nuclear Yorkie localization. (C) Once incorporated into TFs, TFCs display cytoplasmic Yorkie localization. (D) ICs have high levels of nuclear and cytoplasmic Yorkie. (E) Yorkie is detectable only at very low levels in GCs. *expanded-lacZ* expression is detected in intercalating TFCs (F), ICs (H) and GCs (I) but not in TFCs once they are incorporated into TFs (G). White arrowheads indicate an example of the specific cell types indicated in each column. Yellow arrowheads indicate cap cells posterior to TFs. Scale bar = 10 μm in B-I'.

3.2 Results

Hpo pathway activity is cell type-specific in the larval ovary

To determine whether Hippo signaling regulates proliferation of the GSC niche precursor cells, we first examined the expression pattern of Hippo pathway members in the larval ovary. Throughout larval development, Hpo was expressed ubiquitously in the ovary (Figure C.1A-C), and Yki was expressed in all somatic cells of the ovary (Figure C.1F-H). However, the subcellular localization of Yki was dynamic during ovariole morphogenesis, and different in distinct somatic cell types. We observed nuclear Yki expression in newly differentiating TFCs (identified by Engrailed expression and elongated cellular morphology) (Figure 3.1B-B', arrowhead; Fig. C.2I), while late stage TFs had very little detectable nuclear Yki (Figure 3.1C-C', arrowhead; Figure C.2I). Since Yki localization in the nucleus indicates low or absent Hippo pathway activity (Huang, Wu et al. 2005), these data suggest that Hpo signaling may promote TFC and TFC-progenitor proliferation before TF formation, and then suppress proliferation in TFCs that have entered TFs. This is consistent with previous reports of the somatic proliferative dynamics of the larval ovary (Sahut-Barnola, Dastugue et al. 1996, Green II and Extavour 2012).

We also assessed Yki activity by analyzing expression of the downstream target genes *expanded* (*ex*) (Huang, Wu et al. 2005), *diap1* (also called *thread*) (Huang, Wu et al. 2005) and *bantam* (Nolo, Morrison et al. 2006). *ex-lacZ* (Figure 3.1F-G, Figure C.2J) and *diap1-lacZ* (Figure C.2A-B, K) were expressed in early TFCs, but ceased expression once TFCs were incorporated into a TF. The *bantam-GFP* sensor is a GFP construct containing *bantam* miRNA target sites, such that low or absent GFP expression indicates *bantam* expression and activity. The sensor was not expressed in early differentiating TFCs, but was expressed in TFCs within a TF (Figure C.2E-F, L). These data are consistent with the subcellular localization of Yki in TFCs.

Yki activity reporters were also expressed in cap cells of the GSC niche, which are immediately posterior to TFs (Figure 3.1G-G', yellow arrowhead).

In ICs, strong cytoplasmic and nuclear expression of Yki was observed throughout development (Figure 3.1D-D'; S2I). Likewise, all Yki activity reporters examined were expressed in ICs (Figure 3.1H-H', Figures C.2C-C', G-G', J-L), consistent with continuous proliferation of these cells throughout larval development.

Hippo signaling regulates terminal filament cell proliferation

The expression patterns described above, and our previous observation that knockdown of *hpo* or *wts* increased TFC number (Sarikaya, Belay et al. 2012), suggested that the Hippo pathway regulates TFC proliferation. To further test this hypothesis, we manipulated activity of the core Hippo pathway members *hpo*, *wts* and *yki* in somatic cells using the *bric-à-brac* (*bab)* and *traffic jam (tj) GAL4* drivers (Cabrera, Godt et al. 2002, Hayashi, Ito et al. 2002). *bab:GAL4* is strongly expressed in TFCs during L3 but only weakly in other somatic cell types (Cabrera, Godt et al. 2002, Sarikaya, Belay et al. 2012). *tj:GAL4* is expressed primarily in somatic cells posterior to the TFs, including ICs, to a lesser extent in newly forming TF stacks during early and mid L3, and in posterior TFCs in late L3 (Figure C.3A-D) (Tanentzapf, Devenport et al. 2007). We note that the expression of Tj in intercalating TFCs is not detected with the Traffic-Jam antibody (Figure C.3E). Antibody staining against Hpo and Yki was used to confirm effectiveness of the RNAi-mediated knockdown under both GAL4 drivers (Figure C.1D-D', I-I'; see Methods for further details of RNAi validation in these and subsequent experiments).

Lowering Hippo pathway activity in somatic cells by expressing RNAi against *hpo* or *wts* under either GAL4 driver significantly increased TFC number (student's t-test was used for this

and all other comparisons: $p<0.05$; Figure 3.2A, Table C1). We previously showed that TFC number correlates with TF number (Sarikaya, Belay et al. 2012). Accordingly, driving RNAi against either *hpo* or *wts* in somatic tissues significantly increased TF number ($p<0.05$; Figure 3.2B, Table C1). Conversely, decreasing Yki activity in somatic cells by expressing *yki* RNAi under either driver significantly reduced both TFC number and TF number ($p<0.05$; Figure 3.2A-B, Table C1).

Somatic overexpression of *hpo* or *yki* under the *bab:GAL4* driver resulted in larval lethality, likely due to the known pleiotropic expression of *bab* in multiple non-ovarian tissues (Cabrera, Godt et al. 2002). However, *tj:GAL4*-driven overexpression of *yki* or *hpo* was viable. Using the *tj:GAL4* driver, we found that somatic *yki* overexpression resulted in a significant increase in both TFC number ($p<0.05$; Figure 3.2A, Table C1) and TF number ($p<0.01$; Figure 3.2B, Table C1), while somatic *hpo* overexpression led to a significant reduction in both TFCs and TFs ($p<0.05$; Figure 3.2A-B, Table C1). A null allele of the Hippo pathway effector *expanded* (ex^{1} (Stern and Bridges 1926)) and a gain of function allele of *yorkie* (yki^{DB02} (Zhao, Wei et al. 2007)) both led to a significant increase in TFC number (Figure C.4A, Table C2), consistent with results obtained from RNAi treatments.

As larval TF number corresponds to the number of GSC niches in the adult (ovariole number) (Sarikaya, Belay et al. 2012), we asked if Hpo signaling might play a role in determining ovariole number. We quantified ovariole number in adults with RNAi-mediated knockdown of Hippo signaling pathway members *hpo*, *wts*, *salvador* (*sav*), *Merlin* (*Mer*), or *ex* in somatic cells. In all cases adult ovariole number was significantly increased ($p<0.01$; Figure 3.2C). Conversely, *yki* knockdown under *tj:GAL4* significantly decreased ovariole number ($p<0.01$; Figure 3.2C).

Adult females of all reported somatic knockdown and overexpression experiments were viable and did not have defects in adult ovarian structure. Adult females expressing *hpo* RNAi under the *tj:GAL4* driver, which had significantly more ovarioles than controls (Figure 3.2B, Table C1), also laid significantly more eggs than controls (Figure 3.2D). Conversely, adult females expressing *yki* RNAi under *tj:GAL4* driver laid significantly fewer eggs than controls, and some appeared to be entirely sterile (Figure 3.2D). This shows that by regulating somatic gonad cell number in the larval ovary, the Hippo pathway can influence adult female reproductive capacity.

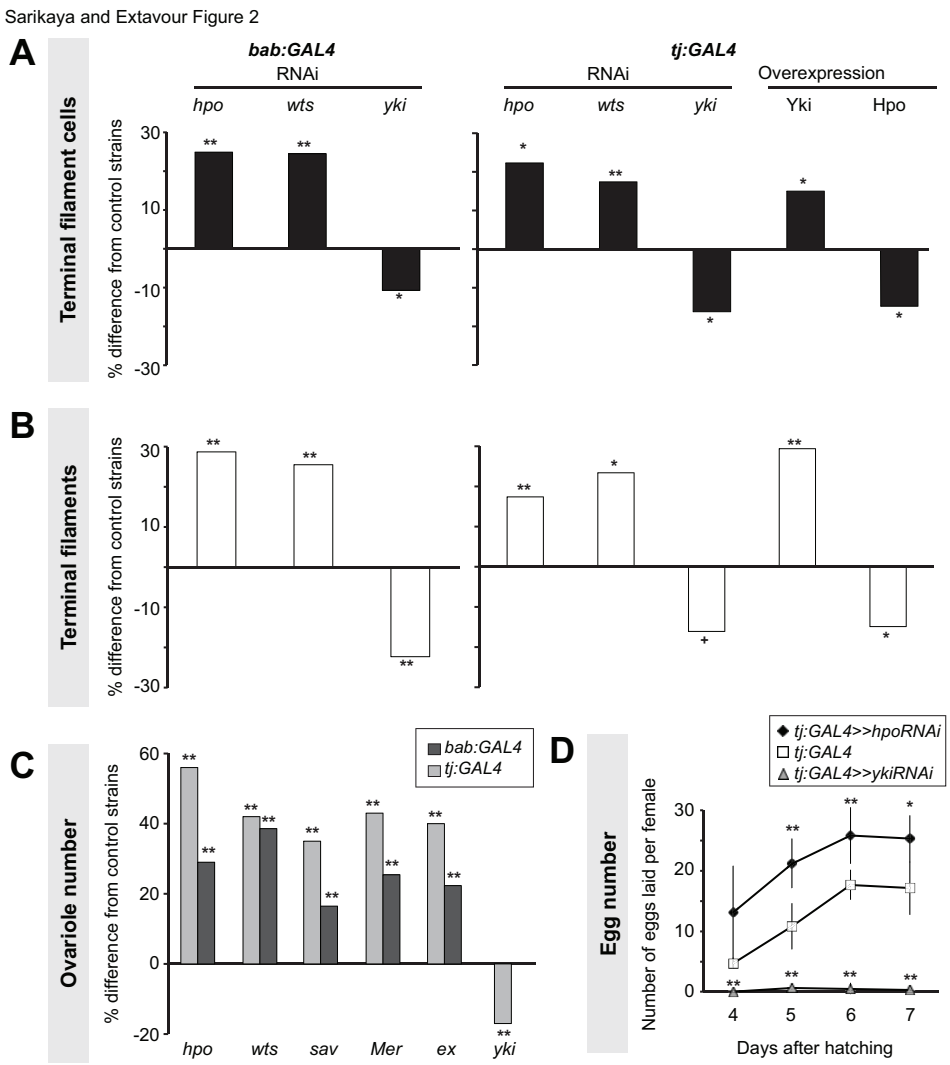

Figure 3.2. Hippo pathway influences proliferation of TFCs, thereby influencing ovariole number. Changes in (A) TFC or (B) TF number in LP ovaries expressing UAS-induced RNAi against *hpo*, *wts* or *yki*, or overexpressing *hpo* or *yki* under the *bab:GAL4* or *tj:GAL4* drivers. Here and in Figures 3.3-6, C.4 and C.5, bar graphs show percent difference from control genotypes of the indicated cell type or structure in each of the experimental genotypes, which are those that carry both *UAS* and *GAL4* constructs. Control genotypes are either parental strains or siblings carrying a balancer chromosome instead of the GAL4 construct (see Methods). When statistical comparisons were performed to parental strains, values from the two parental strains were averaged and percent difference from the average was plotted. Statistical significance was calculated using a student's two-tailed t-test with unequal variance. ** $p<0.01$, * $p<0.05$, + $p<0.01$ against the UAS parental line and $p=0.08$ against the GAL4 parental line. n=10 for each genotype. Numerical data can be found in Table S1. (C) Changes in adult ovariole number in individuals expressing *hpo*, *wts*, *sav*, *Mer*, *ex* or *yki* RNAi under *bab:GAL4* (dark grey bars) or *tj:GAL4* (light grey bars) drivers. ** $p< 0.01$ against controls. n=20 for each genotype. (D) Average egg counts from females four to seven days after hatching of *tj:GAL4* (control, white squares), *tj:GAL4* driving hpo^{RNAi} (black diamonds), *tj:GAL4* driving yki^{RNAi} (grey triangles). Error bars indicate confidence intervals. * $p<0.05$, ** $p<0.01$. n = 5 vials containing 3 females per vial.

Hippo signaling regulates interstitial cell proliferation

We next asked whether the Hippo pathway also influenced the proliferation of ICs, which do not contribute to TF formation but are in direct contact with germ cells and are thought to give rise to somatic stem cells or escort cells (Song, Call et al. 2007, Gancz, Lengil et al. 2011, Gancz and Gilboa 2013). Larval-pupal transition (LP) stage ICs were identified by antibody staining against Traffic Jam, which is specific to ICs at this stage of development (Lin et al., 2003). Altering Hippo pathway activity in somatic cells had the same overall effects on IC number as on TFC number: knocking down *hpo* or *wts* or overexpressing Yki resulted in a significant increase in IC number (*hpo* or *wts* RNAi: $p<0.05$ for *bab:GAL4* and $p<0.01$ for *tj:GAL4*; *yki* overexpression: $p<0.01$ for both drivers; Figure 3.3A, D-I, M-N Table C3). Conversely, RNAi against *yki* or overexpression of *hpo* in the soma significantly reduced IC number ($p<0.01$; Figure 3.3A, J-L, Table C3). As observed for TFC number, IC numbers in ex^{1} or yki^{DB02} backgrounds were significantly increased (Figure C.4, Table C2), consistent with the RNAi data. Ovarian morphogenesis, including TF, ovariole and GSC niche formation, was normal in most cases (Figure 3.3D-N). However, the 150% increase in IC number caused by *yki* overexpression correlated with failure of swarm cell migration in some ovaries (Figure 3.3M–N, arrowhead; n= 2/10), suggesting that excessive proliferation of ICs above a certain threshold cannot be accommodated by the ovary, leading to disrupted ovariole morphogenesis.

Because the *tj:GAL4* and *bab:GAL4* drivers are expressed in both ICs and TFCs (albeit at varying levels), we could not use these tools to determine whether ICs and TFCs influence each others' proliferation non-autonomously. Thus, we tested the utility of *ptc:GAL4*, which is expressed in ICs (albeit at low levels) but not in TFCs (Figure C5A-C), and *hh:GAL4*, which is expressed in a subset of TFCs during and after TF stacking but not in ICs (Figure C5D-F), for

this purpose. However, when we drove RNAi against *hpo* or *wts* using either driver, we did not observe any significant changes in IC, TFC or TF number compared to controls (Figure C.5G-H; Table C5). This is likely due to the facts that (1) *hh:GAL4* expression in TFCs arises after TFC proliferation has essentially completed (Figure C.5D-F); and (2) *ptc:GAL4* expression is extremely weak in ICs (Figure C.5A-C). We therefore cannot rule out the hypothesis that TFC or IC proliferation has a non-autonomous influence on the other of these two somatic cell types.

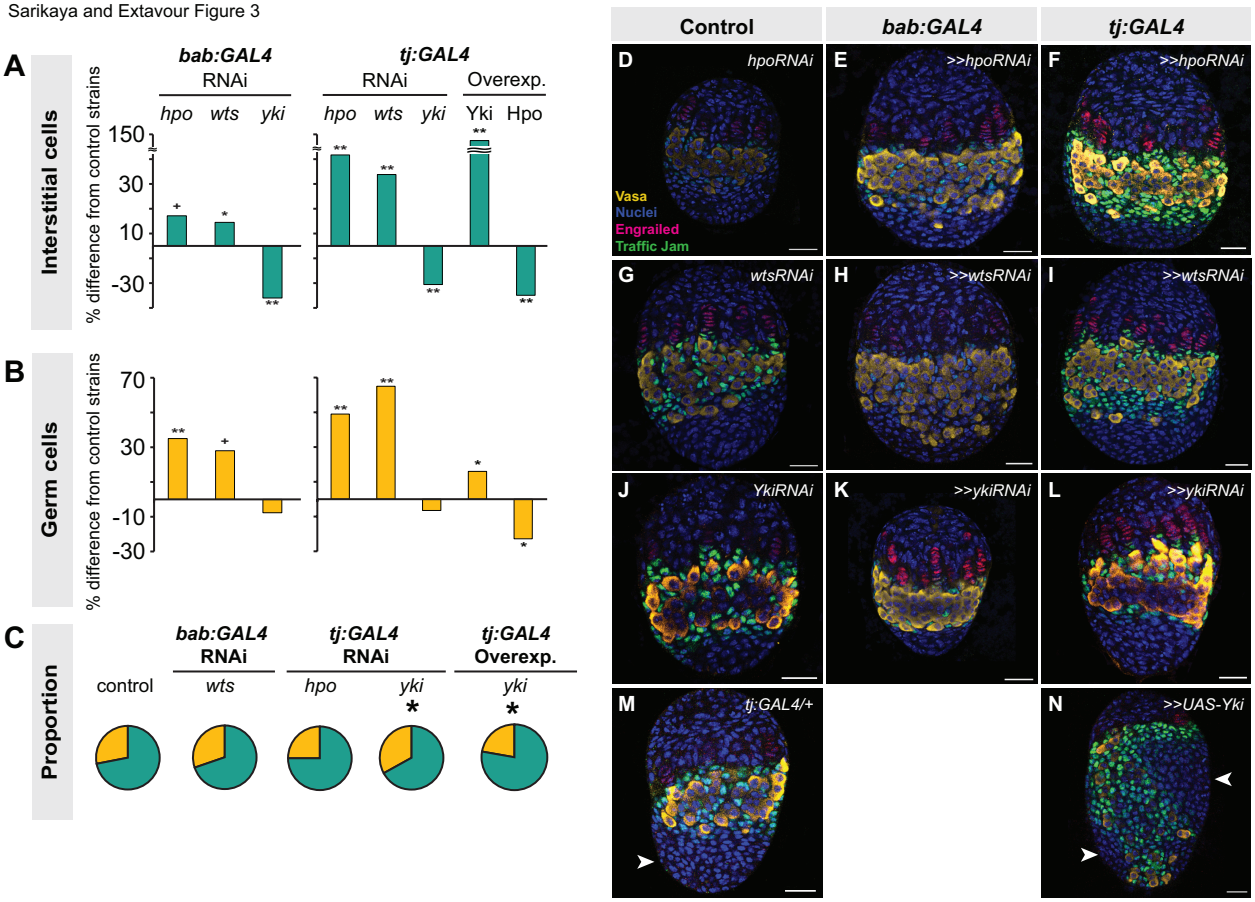

Figure 3.3. Altering Hippo pathway activity in somatic cells changes IC and GC number. Changes in (A) IC or (B) GC number in ovaries expressing *hpo*, *wts* or *yki* RNAi, or overexpressing *hpo* or *yki* under the *bab:GAL4* or *tj:GAL4* drivers. Bar graphs are as explained in Figure 2 legend. ** $p<0.01$, * $p<0.05$, + $p=0.05$ against the UAS parental line and $p<0.05$ against the GAL4 parental line. n=10 for each genotype. Numerical values can be found in Table S3. (C) Pie charts of proportions of ICs (green) and GCs (yellow) in ovaries under indicated selected experimental conditions. * $p<0.05$. Numerical values can be found in Table S6; pie charts for all experimental conditions shown in Figure S7. (D-N) LP stage larval ovaries representative of control and experimental samples used to obtain cell type counts. Scale bar = 10 μm.

Germ cell proliferation is regulated by yki *in a* hpo/wts-*independent manner*

Having observed apparently canonical Hippo pathway activity in the somatic gonad cells, we next asked whether this pathway operated similarly in germ cells, and found a number of significant differences. First, unlike the dynamic expression of Yki in somatic ovarian cells, we detected only extremely low levels of Yki in GCs throughout development (Figures 3.1E, E', C.1F-H, C.2I). The *bantam*-GFP sensor also suggested low or absent Yki activity in GCs (Figure C.2H-H', L). However, we did observe expression of the *expanded-lacZ* (Figures 3.1I-I', C.2J) and *diap1-lacZ* (Figures C.2D-D', C.2K) reporters in the GCs. We thus performed functional experiments to evaluate the roles of Yki and other Hpo pathway members in GCs.

We disrupted Hippo pathway activity in GCs using the germ line-specific driver *nos:GAL4* (Figure C.3E-H). In contrast to the overproliferation of somatic cell types observed in the experiments described above, driving RNAi against *hpo* or *wts* in the germ line did not significantly change GC number (Figure 3.4A; Table C3). However, driving *yki* RNAi in the germ line significantly reduced GC number ($p<0.01$; Figure 3.4A), and a second independent RNAi line (Dietzl, Chen et al. 2007, Ni, Liu et al. 2009) yielded similar results ($p<0.05$; Table C3). Conversely, overexpression of *yki* in GCs led to a significant increase in GCs ($p<0.01$, Figure 3.4A). Although *hpo* RNAi had no effect on GC number (Figure 3.4A, Table C3), *hpo* overexpression significantly decreased GC number ($p<0.01$; Figure 3.4A). Interestingly, we observed a non-autonomous increase in ICs in when *yki* was overexpressed in GCs, but not in the other experimental conditions ($p<0.05$, Table C3).

To validate our findings from the *hpo* and *yki* RNAi experiments, we induced *hpo* (Jia, Zhang et al. 2003) and *yki* (Huang, Wu et al. 2005) null mutant GC clones in L1 larvae and compared the clone sizes (number of cells per clone) of homozygous mutant clones and their

homozygous wild type twin spot clones in late L3 ovaries. Consistent with our RNAi analysis, hpo^{BF33} clones were not significantly different in size from controls (Figure 3.4F, H), but yki^{B5} clones were significantly smaller than controls ($p<0.01$; Figure 3.4F, I). Taken together, both RNAi and clonal analysis data suggest that *yki* but not *hpo* is involved in regulating GC number.

We therefore sought further evidence that *yki* activity in the germ line was independent of *hpo*. The FERM domain protein Expanded can bind to Yki independently of Hpo or Wts to sequester Yki to the cytoplasm of *Drosophila* eye imaginal disc and S2 cells (Badouel, Gardano et al. 2009), or alternatively can bind to and sequester Yki by forming a complex with Hpo and Wts in *Drosophila* wing imaginal discs (Oh, Reddy et al. 2009). To determine if one of these mechanisms might be operating in GCs, we knocked down *ex* alone, or *hpo*, *wts* and *ex* together in GCs. We did not observe significant changes in GC number under either condition (Figure 3.4A; Table C3), suggesting that these phosphorylation-independent mechanisms do not regulate Yki in GCs. Consistent with this hypothesis, we found that overexpression of yki^{S168A}, an allele of Yki that is impervious to Wts-mediated phosphorylation (Oh and Irvine 2008), also significantly increased GC number (Figure 3.4A). To our knowledge, the only other identified *hpo*-independent mechanism of *yki* regulation in *Drosophila* is via the kinase Hipk, which phosphorylates Yki and induces nuclear translocation in *Drosophila* wing imaginal discs (Poon, Zhang et al. 2012). However, knocking down *hipk* in GCs also did not affect GC number (Figure 3.4A). Finally, we asked if Yki might still operate together with the transcription factor Scalloped (Sd)/TEAD in germ cells, as has been shown in somatic cells of *Drosophila* and mammals (Goulev, Fauny et al. 2008, Wu, Liu et al. 2008, Zhang, Ren et al. 2008). Knocking down *sd* in GCs significantly reduced GC number ($p<0.01$, Figure 3.4A), suggesting that a Yki/Sd complex could play a role in GC proliferation.

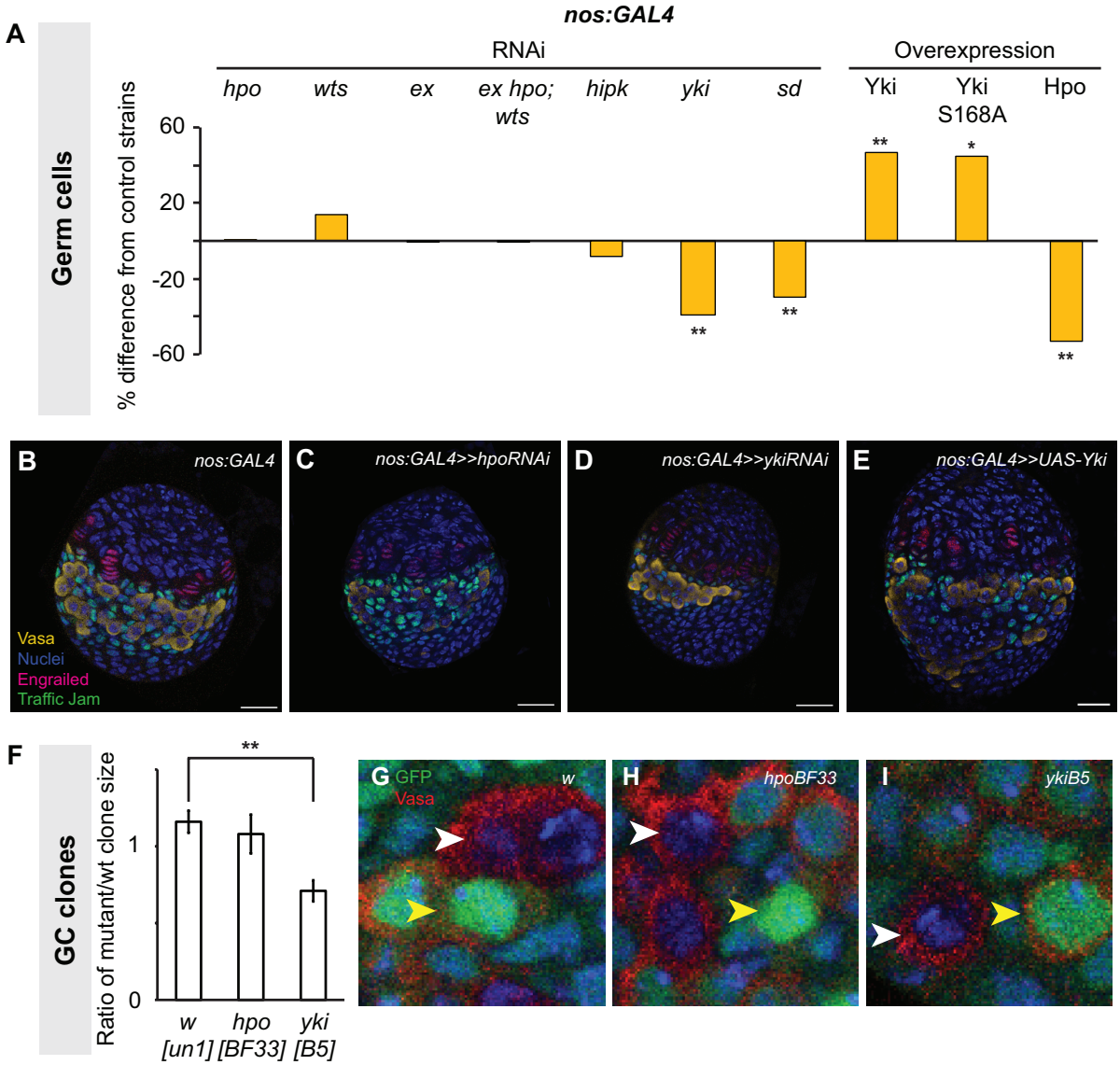

Figure 3.4. Yorkie activity regulates GC number. Changes in (A) GC number in ovaries expressing *hpo*, *wts*, *ex*, *hpo/wts/ex* triple, *hipk*, *yki or sd* RNAi, or overexpressing *hpo*, *yki or* yki^{S168A} under the *nos:GAL4* driver. Bar graphs are as explained in Figure 2 legend. * $p<0.05$, ** $p<0.01$ against controls. n=10 for each genotype. Numerical values can be found in Table S2. (B-E) LP stage larval ovaries representative of control and experimental samples used to obtain cell type counts. Scale bar = 10 μm. (F) Ratio of size (number of cells per clone) of homozygous mutant versus homozygous wild type twin spot clones for control (w^{un-1}), hpo^{BF33} and yki^{B5} alleles. ** $p<0.01$ against control. (G-I) LP stage larval ovaries representative of control and experimental samples for clonal analysis showing GCs (Vasa, red), homozygous wild type clones (strong GFP expression; yellow arrowhead), and clones homozygous for tested alleles (no GFP; white arrowhead). n=10 for each genotype.

A reduction in GC number could be caused by altered GC proliferation, or by premature differentiation of GCs into oocytes, as has been observed for loss of function mutations in members of the Ecdysone and Insulin signaling pathways (Gancz, Lengil et al. 2011, Gancz and Gilboa 2013). To ask if altered *yki* activity was causing changes in GC number by affecting the timing of oocyte differentiation, we assayed for fusome morphology, an indicator for early cyst cells, in ovaries expressing RNAi against *yki* or overexpressing *yki* in GCs (Figure C.6). We observed no overt signs of early differentiation of PGCs and fusome morphology was similar to controls, suggesting that the reduction of GC number induced by *yki* knockdown in GCs is likely due to reduced GC proliferation.

Changing Hpo activity in the soma non-autonomously influences GC number

Given our finding that Hippo signaling pathway members regulate autonomous proliferation of both somatic and germ line cells, we asked if this pathway might also coordinate non-autonomous proliferation of both cell types. Such a mechanism might be expected to operate in order to adjust the numbers of one cell type in response to Hippo signaling-mediated changes in the other, which would ensure an appropriate number of operative stem cell niches (Gancz, Lengil et al. 2011). To test this hypothesis, we analyzed GC number in conditions where Hippo pathway activity was altered in the somatic cells. Non-autonomous positive regulation of GC number by ICs has been documented, but only in ways that also affect GC differentiation (Gilboa and Lehmann 2006). Whether ICs can positively regulate GC proliferation without affecting their differentiation thus remains unknown (Gancz, Lengil et al. 2011, Gancz and Gilboa 2013). We found that increasing somatic cell number by driving *hpo* or *wts* RNAi in the soma also significantly increased GC number ($p<0.01$, $p=0.06$ respectively; Figure 3.3B-I; Table C3).

Strikingly, GC number increased in precise proportion to the IC number increase, whether this increase was as little as 15% (*bab:GAL4>>wts*^{RNAi}; Figure 3.3C, C.7; Tables C3, C6) or as much as 70% (*tj:GAL4>>hpo*^{RNAi}; Figures 3.3C, C.7; Tables C3, C6), resulting in a consistent ratio of ICs to GCs (Figures 3.3C, C.7; Table C6). However, increasing IC number by 150% via somatic overexpression of *yki* prompted only a 10% increase in GC number ($p<0.05$, Figure 3.3B). In this condition, the GC:IC ratio was significantly lower than controls (Figures 3.3C, C.7; Table C6), and GC:IC proportions were not maintained (Figure 3.3C, C7). These results suggest that the Hippo pathway can maintain homeostatic growth of the larval ovary by regulating the number of GCs to accommodate changes of up to 70% in the number of ICs. However, further overproliferation of ICs cannot be matched by proportional GC proliferation.

We then asked if somatic Hippo signaling could also non-autonomously compensate for decreases in IC number via a proportional reduction in GC number. We found that somatic *yki* RNAi significantly decreased IC number ($p<0.05$), but did not significantly decrease GC number ($p=0.29$, Figure 3.3B), thus disrupting the GC:IC ratio (Figures 3.3C, C.7). However, reducing IC number via *hpo* overexpression in the soma yielded a marginally significant decrease in GC number (Figure 3.3A, B). These results suggest that the Hippo pathway's role in non-autonomous proliferation of GCs is primarily operative in cases of somatic cell overproliferation, but that to accommodate significant decreases in IC number by reducing GC numbers, Hippo signaling is not always sufficient and additional mechanisms may be required. The latter may include insulin signaling (Gancz and Gilboa 2013).

Hpo interacts with EGFR signaling in ICs but not TFCs

Finally, we asked which signaling pathways Hippo signaling might interact with in the ovary to regulate proliferation. We also asked whether these pathways were the same or different in distinct somatic cell types (ICs and TFCs). First, we considered the EGFR pathway. The Hippo pathway interacts with the EGFR pathway to regulate non-autonomous control of proliferation in other organs (Zhang, Ji et al. 2009, Ren, Wang et al. 2010, Herranz, Hong et al. 2012, Huang, Nagatomo et al. 2013, Reddy and Irvine 2013). Moreover, the EGFR pathway is known to regulate IC number and to non-autonomously regulate GC number (Gilboa and Lehmann 2006, Matsuoka, Hiromi et al. 2013). We therefore asked whether the Hippo pathway interacted with EGFR signaling in the larval ovary. In wild type larval ovaries we observed, as previously reported (Gilboa and Lehmann 2006), that pMAPK (a readout of EGFR activity) is expressed predominantly in ICs (Figure 3.5A, white arrowhead) and in some TFCs (Figure 3.5A, red arrowhead), but not in GCs (Figure 3.5A, yellow arrowhead). When we knocked down *hpo* in the soma, we detected significantly increased pMAPK expression in the ovary ($p<0.01$; Figure 3.5B-C), most notably in ICs at mid L3 and late L3 stages (Figure 3.5B, white arrowhead), and additionally in some TFCs (Figure 3.5B, red arrowhead). These results suggest that in wild type ovaries Hippo pathway activity may limit EGFR activity in somatic cells.

In order to assess the consequences of *hpo*/EGFR pathway interactions, we conducted double-RNAi knockdowns of *hpo* and either the EGFR receptor (*egfr*) or the EGFR ligand *spitz* (*spi*) in the soma using the *tj:GAL4* driver. To validate the RNAi constructs, we expressed $egfr^{RNAi}$ or spi^{RNAi} under *tj:GAL4,* and observed significant reduction in pMAPK levels in L3 ovaries ($p<0.05$, Figure C.8A). In both *hpo* and *egfr* or *spi* double-RNAi knockdowns, TFC number was not significantly different from *hpo* single knockdowns (Figure 3.5D; Table C4). In addition, TFC number was not altered when we knocked down *egfr* or *spi* alone in the soma

(Table C4). This suggests that the Hippo pathway does not regulate TFC number via EGFR signaling, consistent with the limited pMAPK expression observed in TFCs (Figure 5A, red arrowhead).

In contrast, and consistent with the strong pMAPK expression in ICs (Figure 5A, white arrowhead), *tj:GAL4*-mediated double knockdown of *hpo* and *egfr* partially rescued the *hpo* RNAi-induced overgrowth of ICs ($p<0.05$; Figure 3.5D; Table C4). However, these ovaries still had 35% more ICs than wild type controls ($p<0.01$; Figure 3.5E). Double knockdown of *hpo* and *spi* yielded no significant difference in IC number compared to *hpo* single knockdowns (Figure 3.5D). IC number was unaltered by knockdown of *egfr* or *spi* alone (Table C4). In contrast to the TFCs, the Hippo pathway thus appears to interact with EGFR signaling to regulate IC number.

Finally, we quantified GCs to test whether the EGFR-Hippo signaling interaction in ICs could non-autonomously regulate GCs. Double knockdown of *hpo* and *egfr*, which significantly reduced IC number relative to *hpo* RNAi alone ($p<0.05$; Figure 3.5D; Table C4), also resulted in significantly fewer GCs ($p<0.05$; Figure 3.5D; Table C4), completely rescuing the *hpo* RNAi-induced GC overproliferation (Figure 3.5E; Table C4). Double knockdown of *hpo* and *spi* did not alter IC number relative to *hpo* RNAi alone ($p=0.24$; Figure 3.5D; Table C4), but resulted in near-significant reduction of GCs ($p=0.054$), also yielding a complete rescue of the *hpo* RNAi-induced overproliferation (Figure 3.5E; Table C4). Because the degree of *hpo* RNAi rescue was greater in GCs than in ICs in the *hpo*/*spi* double knockdown , the homeostatic balance of these cell types was no longer maintained (Figure C5F). As previously reported (Gilboa and Lehmann 2006, Matsuoka, Hiromi et al. 2013), we observed a significant increase in GC number when we knocked down *egfr* alone, but not *spi* alone, in the soma (Table C4). Taken together, these results

indicate that *hpo* interacts in the soma with *egfr* signaling, likely through an additional ligand along with *spi*, to regulate both IC number autonomously and GC number non-autonomously.

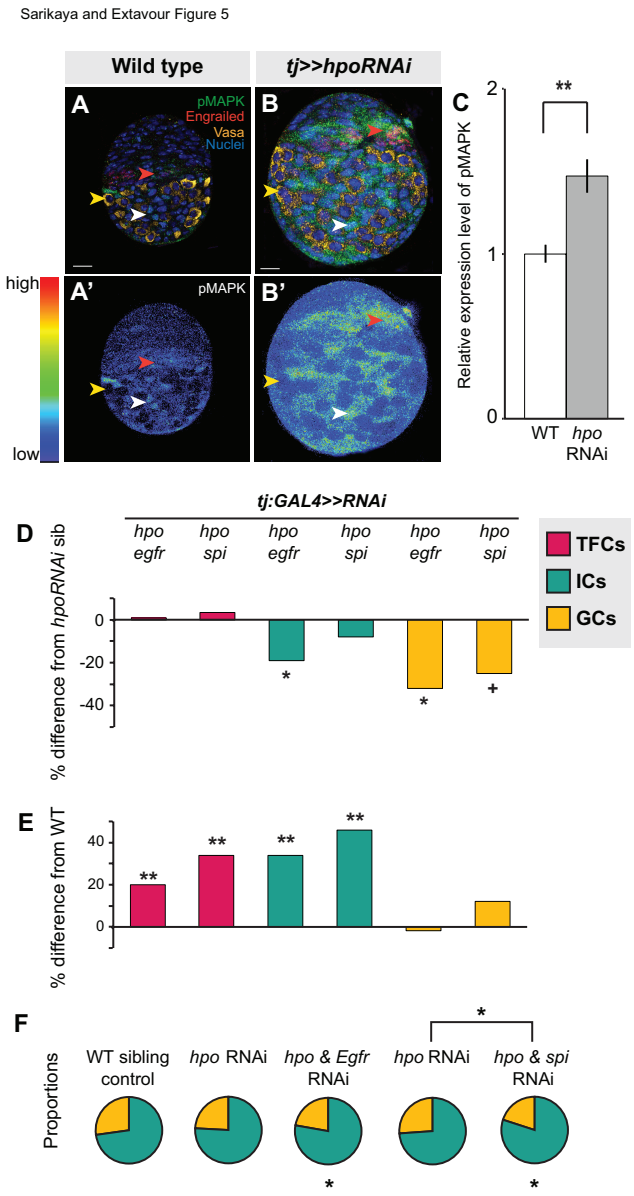

Figure 3.5. The Hippo pathway interacts with the EGFR pathway to regulate IC and GC growth. (A) Expression pattern of EGFR pathway activity marker pMAPK in wild type L3 ovary. Expression is mainly in posterior IC cells. Scale bar = 10 μm and applies also to A'. (B) pMAPK expression in ovary expressing *UAS:hpo*^{RNAi} in the soma, exposed at same laser setting as (A). Scale bar = 10 μm and applies also to B'. (C) Relative intensity of anti-pMAPK fluorescence in wild type compared to *hpo* knockdown experimental (n=8). Overall expression level of pMAPK is higher than controls, most prominently in the ICs. (D-E) Percent difference in TF (red), IC (green), and GC (yellow) number in double RNAi (*hpo* and *egfr*, or *hpo* and *spi*) compared to *hpo* single RNAi sibling controls (D), and wild type sibling controls (E). * $p<0.05$, ** $p<0.01$. Numerical values can be found in Table S4. (F) Pie charts showing proportions of ICs (green) and GCs (yellow) under indicated selected experimental conditions. * $p<0.05$, see Table S6 for numerical values; pie charts for all experimental conditions shown in Figure S7.

Hpo interacts with JAK-STAT signaling in TFCs and ICs

Another characterized interacting partner of the Hippo pathway in various somatic tissues is the JAK/STAT pathway (Karpowicz, Perez et al. 2010, Reddy, Rauskolb et al. 2010, Ren, Wang et al. 2010, Shaw, Kohlmaier et al. 2010, Staley and Irvine 2010, Ohsawa, Sato et al. 2012). We therefore asked whether these two pathways also interact to regulate autonomous and/or homeostatic proliferation in the larval ovary. First, we used detection of Stat92E as a readout of JAK/STAT activity (Sweitzer, Calvo et al. 1995, Yan, Small et al. 1996, Flaherty, Salis et al. 2010). We observed strongest Stat92E expression in posterior somatic cells, including ICs, in wild type ovaries (Figure 3.6A-A'). Knocking down *hpo* in the soma led to significantly higher Stat92E levels ($p<0.01$; Figure 3.6B-C), suggesting that, similar to its interaction with EGFR, Hippo pathway activity normally limits JAK/STAT pathway activity in the larval ovary.

Next, we asked if RNAi against either the JAK/STAT receptor *dome* or the ligand *unpaired* (*upd1*) could rescue the effects of *hpo* RNAi in the soma. While there are three *upd* orthologues in *Drosophila* (Harrison, McCoon et al. 1998, Agaisse, Petersen et al. 2003, Brown, Hu et al. 2003), we focused on *upd1,* as it is known to regulate GC proliferation in the testis (Tulina and Matunis 2001) and thought to be a specific *yki* target in polar cells (Lin, Yeh et al. 2014), which are derivatives of the somatic cells of the ovary. Expressing *dome* or *upd1* RNAi under *tj:GAL4* significantly reduced Stat92E levels in the larval ovary ($p<0.05$ for *dome*, $p=0.06$ for *upd1*; Figure C.8B), confirming functionality of these RNAi lines. In TFCs, double knockdown of *dome* and *hpo*, but not of *upd1* and *hpo*, completely suppressed the *hpo* single knockdown phenotype ($p<0.05$; Figure 3.6D; Table C4). Knocking down *dome* alone in the soma significantly decreased TFC number ($p<0.05$; Table C4), supporting the hypothesis that JAK/STAT signals positively regulate TFC proliferation. These data suggest that Hippo

signaling regulates TFC proliferation via interactions with the JAK/STAT pathway, and that a ligand other than *upd1* mediates this interaction.

We next counted IC and GC number to determine whether JAK/STAT-Hippo pathway interactions regulate ICs proliferation autonomously, and/or GC proliferation non-autonomously. Both *dome*/*hpo* or *upd1*/*hpo* double knockdowns partially rescued the overproliferation caused by knockdown of *hpo* alone ($p<0.01$; Figure 3.6D; Table C4), but these ovaries still had significantly more ICs than wild type controls ($p<0.05$; Figure 3.6E). Both double knockdown conditions also completely rescued the non-autonomous increase in GC number caused by *hpo* RNAi (Figure 3.6D; Table C4). Similar to our experiments on the EGFR pathway, we observed abnormal IC:GC ratios in the *hpo* and *dome* RNAi single knockdowns (Figures 3.6F, C7; Table C6). In summary, Hippo signaling interacts with JAK/STAT signaling via *upd1* to regulate IC:GC homeostasis.

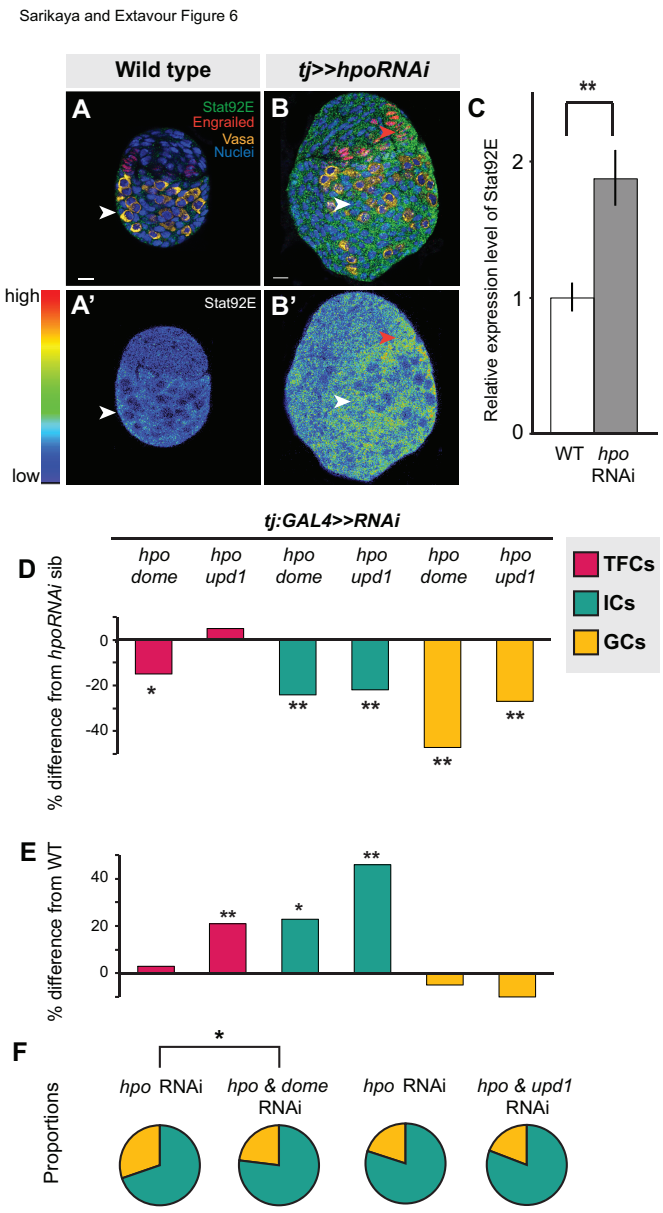

Figure 3.6. Hippo pathway interacts with JAK/STAT pathway to regulate TFC and IC proliferation, and non-autonomous regulation of GC number. (A) Expression pattern of JAK/STAT pathway kinase Stat92E in wild type L3 ovary. Scale bar = 10 μm and applies also to A'. (B) Stat92E expression in ovary expressing *UAS:hpo*^{RNAi} in the soma, exposed at same laser setting as (A). Scale bar = 10 μm and applies also to B'. (C) Relative intensity of anti-Stat92E fluorescence in wild type compared to *hpo* knockdown experiments (n=10). (D-E) Percent difference in TF (red), IC (green), GC (yellow) number in double RNAi (*hpo* and *dome*, or *hpo* and *upd1*) knockdowns compared to *hpo* single RNAi sibling controls (D), and wild type sibling controls (E). * $p<0.05$, ** $p<0.01$. Numerical values can be found in Table S4. (F) Pie charts showing proportions of ICs (green) and GCs (yellow) of *hpo* RNAi control and *hpo* and *dome*/*up1* double RNAi. * $p<0.05$, see Table C6 for numerical values; pie charts for all experimental conditions shown in Figure C.7.

3.4 Discussion

Hippo signaling in somatic cells of the larval ovary

We have shown that canonical cell autonomous Hippo signaling regulates proliferation of two key somatic cell types, TFCs and ICs. Because TFCs form TFs, which are the beginning points of each GSC niche, the number and stacking of TFCs can ultimately influence adult ovariole number and thus reproductive capacity (David 1970, Hodin and Riddiford 2000, Sarikaya, Belay et al. 2012). We previously showed that the differences in ovariole number between *D. melanogaster* and closely related *Drosophila* species results from changes in TFC number (Green II and Extavour 2012, Sarikaya, Belay et al. 2012). This suggests Hippo and JAK/STAT pathway members as novel potential targets of evolutionary change in ovariole number variation. Indeed, loci containing many of these genes have been previously identified in QTL analyses of genomic variation correlated with ovariole number variation (Orgogozo, Broman et al. 2006). Our study thus provides novel experimental validation of previous quantitative genetics approaches to understanding the genetic regulation of ovariole number.

In TFCs, Hippo signaling regulates proliferation by interacting with *dome* but not *upd1*, suggesting that one or both of *upd2* or *upd3* act as ligands for JAK/STAT signaling in this context. Alternatively, a role for *upd1* in TFC number regulation may have been obscured by our use of the *tj:GAL4* driver, since this driver is restricted to cells posterior to TFCs in L3. A potential source of JAK/STAT ligands that would not have been captured by our experiments could be the anterior somatic cells that are in close contact with TFCs. While TFCs establish the number of niches, ICs appear to communicate with and regulate the number of GCs that can populate those niches. We hypothesize that TFCs and ICs do not regulate each others' proliferation non-autonomously. However, we cannot test this hypothesis directly, as to our

knowledge, no GAL4 drivers currently exist that are exclusively expressed in only TFCs or only ICs. Nevertheless, a number of lines of evidence support this hypothesis. First, reducing Hippo pathway activity in a subset of TFCs had no effect on IC number (Figure C.5H; Table C5). Second, a double knockdown of *egfr* and *hpo* under the *tj:GAL4* driver reduced IC number but had no effect on TFC number (Figure 3.5D). Third, loss of *germ cell-less* (*gcl*) function leads to reduced GC and IC numbers (Gilboa and Lehmann 2006), but has no effect on ovariole number (Barnes, Boone et al. 2006). Given that ovariole number is largely determined by TFC number (Sarikaya, Belay et al. 2012), it is likely that *gcl* ovaries have reduced ICs but not reduced TFCs. However, we note that both TFCs and ICs respond to hormonal cues provided by Ecdysone and Insulin signaling (Gancz, Lengil et al. 2011, Gancz and Gilboa 2013). This suggests that growth of these somatic cell types may be accomplished through their response to systemic hormonal cues, rather than through non-autonomous effects of one somatic cell type on another.

While the Hippo pathway regulates proliferation of both ICs and TFCs, each cell type had a unique pattern of Hippo pathway activity during larval development, suggesting that the upstream regulatory cues of Hippo signaling are different for TFCs and ICs. In *Drosophila*, glial cells and wing disc cells activate the Hippo pathway using different combinations of upstream regulators (Reddy and Irvine 2011), indicating that the Hippo pathway can interact with a unique set of upstream regulatory genes depending on the cell type. Addressing these cell type-specific differences in Hippo pathway activation in future studies will elucidate how the Hippo pathway is regulated locally during development of complex organs to establish organ size.

Another notable difference between Hippo pathway operation in ICs and TFCs is its differential interactions with the EGFR and JAK/STAT pathways in distinct ovarian cell types. In *Drosophila* intestinal stem cell development and stem cell-mediated regeneration (Karpowicz,

Perez et al. 2010, Ren, Wang et al. 2010, Shaw, Kohlmaier et al. 2010, Staley and Irvine 2010), as well as in eye imaginal discs (Reddy, Rauskolb et al. 2010, Reddy and Irvine 2013), the Hippo pathway regulates proliferation of these tissues via interactions with both the EGFR and JAK/STAT pathways. In contrast, the Hippo pathway acts in parallel with but independently of both pathways to regulate the maturation of *Drosophila* ovarian follicle cells (Polesello and Tapon 2007, Yu, Poulton et al. 2008). We do not know what mechanisms determine whether the Hippo pathway interacts with EGFR signaling, JAK/STAT signaling, or both in a given cell or tissue type. One mechanism that may be relevant, however, is the differential activation of specific ligands. For example, in the *Drosophila* eye disc, Hippo signaling interacts genetically with EGFR activity induced by *vein*, but not by any of the other three *Drosophila* EGFR ligands (Zhang, Ji et al. 2009). Similarly, constitutively active human YAP can upregulate transcription of *vein*, but not the other three EGFR ligands, in *Drosophila* wing imaginal discs (Zhang, Ji et al. 2009). That fact that spi^{RNAi} driven in the soma does not rescue the hpo^{RNAi} overproliferation phenotype in the ovary may indicate that other ligands, such as *vein*, are required for this EGFR-Hippo signaling interaction, or that the relevant EGFR ligands are expressed by GCs rather than the soma. Our results suggest that the larval ovary could serve as a model to examine whether differential ligand use within a single organ could modulate Hippo pathway activity during development.

Hippo signaling in germ cells of the larval ovary

Previous reports (Sun, Zhao et al. 2008, Yu, Poulton et al. 2008) suggested that the Hippo pathway components were dispensable for the proliferation of adult GSCs. In contrast, we observed that *yki* controls proliferation of the larval GCs, albeit independently of *hpo* and *wts*.

These contrasting results are likely due to the fact that Sun *et al*. (Sun, Zhao et al. 2008) sought to detect conspicuous germ cell tumors in response to reduced Hippo pathway activity, whereas we manually counted GCs and in this way detected significant changes in GC number in response to *yki* knockdown or overexpression. Although *hpo*, *wts*, *ex* or *hipk* RNAi (Figure 3.4A) and *hpo* null clones (Figure 3.4F) suggested that *yki* activity in GCs was independent of the canonical Hippo kinase cascade, overexpression of *hpo* in GCs did decrease GC number (Figure 3.4A). Taken together, our data suggest that although sufficiently high levels of *hpo* are capable of restricting Yki activity in GCs, *hpo* does not regulate *yki* in GCs in wild type ovaries.

A growing body of evidence shows that *hpo*-independent mechanisms for regulating Yki are deployed in stem cells of multiple vertebrate and invertebrate tissues. For example, in mammalian epidermal stem cells, YAP is regulated in a Hpo-independent manner by an interaction between alpha-catenin and adaptor protein 14-43 (Schlegelmilch, Mohseni et al. 2011). Similarly, the C-terminal domain of YAP that contains the predicted *hpo*-dependent phosphorylation sites is dispensable for YAP-dependent tissue growth in postnatal epidermal stem cells in mice (Beverdam, Claxton et al. 2013). Other known Hpo-independent regulators of Yki include the phosphatase PTPN14 and the WW domain binding protein WBP2, which were identified in mammalian cancer cell lines (Chan, Lim et al. 2011, Liu, Yang et al. 2013). The flatworm *Macrostomum ligano* displays a requirement for *hpo*, *sav*, *wts*, *mats* and *yki* in regulating stem cell number and proliferation, although it is unknown whether *yki* operates independently of the core kinase cascade in this system (Demircan and Berezikov 2013). In contrast, however, in the flatworm *Schmidtea mediterranea*, while *yki* plays a role in regulating stem cell numbers, *hpo*, *wts* and *Mer* appear dispensable for stem cell proliferation (Lin and Pearson 2014). We hypothesize that, as in many other stem cell systems, the *Drosophila* germ

line may use Yki regulators that are not commonly used in the soma to regulate proliferation. Further investigation into the Yki interacting partners in GCs will be needed to understand how Yki may be regulated non-canonically in establishing stem cell populations.

A novel role for Hippo signaling in germ line-soma homeostasis

One of the most striking aspects of growth regulation in the larval ovary is the homeostatic growth of ICs and GCs during development. This homeostatic growth is critical to ensure establishment of an appropriate number of GSC niches that each contain the correct proportions of somatic and germ cells. We have summarized the available data on the molecular mechanisms that regulate the number of ICs and GCs (Figure 3.7A) and our current understanding of how these mechanisms operate within and between the cell types that comprise the GSC niche (Figure 3.7B). Previous work has shown that these mechanisms include the Insulin signaling and EGFR pathways. Insulin signaling function in the soma regulates differentiation and proliferation both autonomously in ICs and non-autonomously in GCs (Gancz and Gilboa 2013) (Figure 3.7A, B). The EGFR pathway regulates homeostatic growth of both IC and GC numbers as follows: GCs produce the ligand Spitz that promotes survival of ICs, and ICs non-autonomously represses GC proliferation via an unknown regulator that is downstream of the EGFR pathway (Gilboa and Lehmann 2006) (Figure 3.7A, B). Our results add four critical new elements to the emerging model of soma-germ line homeostasis in the larval ovary (Figure 3.7B, blue elements). First, *yki* positively and cell-autonomously regulates GC number independently of the canonical Hippo signaling pathway. Second, canonical Hippo signaling negatively and cell-autonomously regulates TFC number via JAK/STAT signaling, and IC number via both EGFR and JAK/STAT signaling. Third, JAK/STAT signaling also negatively

regulates IC and TFC number in a cell-autonomous manner. Finally, Hippo signaling contributes to non-autonomous homeostatic growth of ICs and GCs in at least two ways: (1) Yki activity in GCs non-autonomously regulates IC proliferation; and (2) Hippo signaling activity in ICs non-autonomously regulates GC proliferation through the EGFR and JAK/STAT pathways. The latter relationship is, to our knowledge, the first report of a non-autonomous mechanism that ensures that GC number increases in response to increased IC number, without negatively affecting GSC niche differentiation or function.

Finally, we note that although IC number and GC number had been previously observed to affect each other non-autonomously (Gilboa and Lehmann 2006, Gancz and Gilboa 2013), our experiments shed new light on the remarkable degree to which specific proportions of each cell type are maintained, and demonstrate the Hippo pathway's involvement in this precise homeostasis. This proportionality was not maintained, however, in Hippo/ EGFR or Hippo/JAK/STAT pathway double knockdowns (Figures 3.7, C.7). This suggests that Hippo pathway-mediated proportional growth of ICs and GCs requires activity of not only the EGFR pathway, as previously reported (Gilboa and Lehmann 2006), but also of the JAK/STAT pathway in the soma.

The proportional growth of these cell types maintained by the Hippo-EGFR-JAK/STAT pathway interactions we describe here suggests that the soma releases proliferation-promoting factors to the GCs, and that the GCs can process these signals to maintain optimal proportionality. Similarly, when GC number increased via *yki* overexpression in GCs, we noticed that IC number increased non-autonomously. Achieving specific numbers and proportions of distinct cell types within a single organ, and linking these processes to final organ size and function, are largely unexplained phenomena in developmental biology and organogenesis. By using the larval ovary

as a system to address these problems, we have shown not only that the Hippo pathway is involved in these processes, but also that it can display remarkable complexity and modularity in regulating stem cell precursor proliferation and adjusting organ-specific stem cell niche number during development.

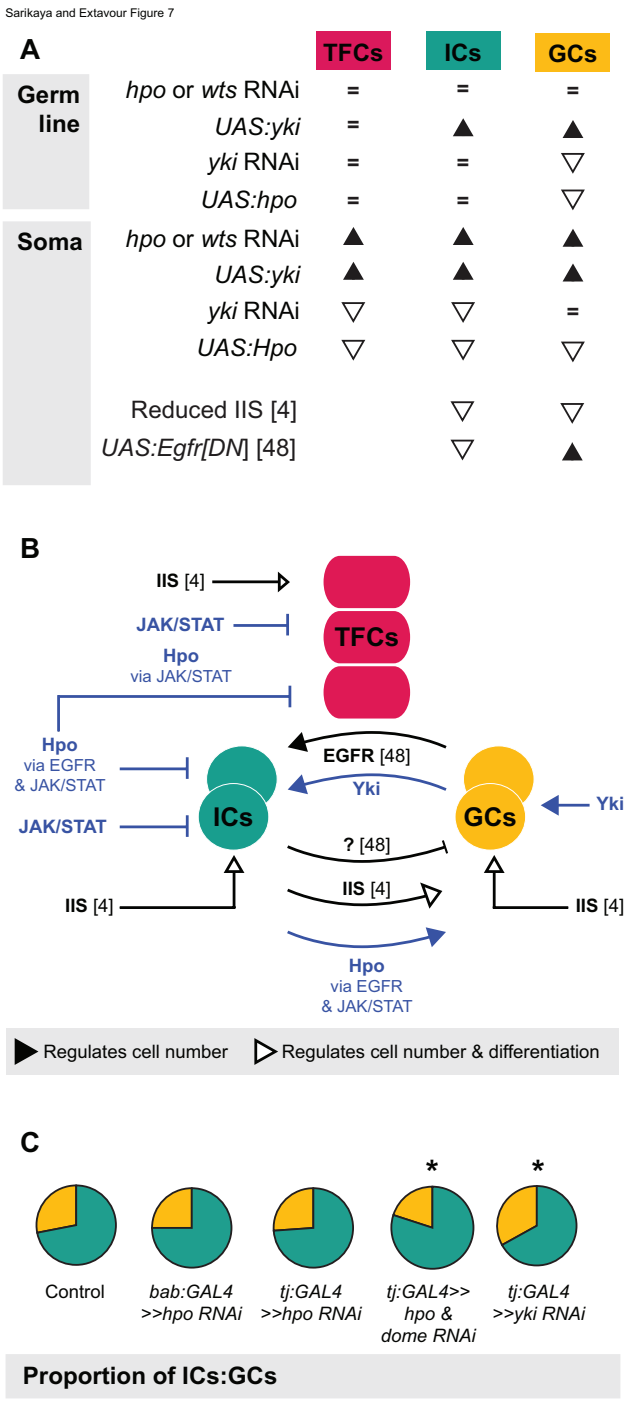

Figure 3.7. The Hippo pathway regulates coordinated growth of the soma and germ line. (A) Summary of changes in TFC, IC and GC numbers when expression of genes from various growth pathways were altered in our study and two other studies (Gilboa and Lehmann 2006, Gancz and Gilboa 2013). Black triangles indicate significant increase; white triangles indicate significant decrease; = indicate no significant change. (B) Model of how Hippo pathway influences coordinated proliferation of somatic cells and germ cells in the larval ovary. Contributions of the present study are indicated in blue; elements of the model derived from other studies (Gilboa and Lehmann 2006, Gancz and Gilboa 2013) are indicated in black. The Hippo pathway interacts with JAK/STAT to regulate proliferation of TFCs, and interacts with

EGFR and JAK/STAT pathways to regulate autonomous proliferation of ICs and non-autonomous proliferation of GCs. In addition, *yki* acts independently of *hpo* to influence proliferation of GCs in a non-canonical manner. (C) Summary of representative IC (green)/GC (yellow) proportions observed in our experiments, further elaborated in Figure S7. Proportions of ICs and GCs are similar to controls when we knock down *hpo* or *wts* alone in the soma, but disrupting both *hpo* and EGFR or JAK/STAT pathway members leads to loss of proportional growth. Asterisk denotes $p<0.05$. See Table S6 for numerical values.

3.5 Materials and Methods

Fly stocks

Flies were reared at 25ºC at 60% humidity with food containing yeast and in uncrowded conditions as previously described (Sarikaya, Belay et al. 2012). The following RNAi lines from the Bloomington Stock Center (B) (Ni, Liu et al. 2009) or the Vienna Drosophila RNAi Center (VDRC) (Dietzl, Chen et al. 2007) were used for knockdown: B33614 (*UAS:hpo*^{RNAi}), B34064 (*UAS:wts*^{RNAi}), B34067 (*UASyki*^{RNAi}), VDRC104523 (*UAS:yki*^{RNAi}), VDRC109281 (*UAS:ex*^{RNAi}), VDRC43267 (*UAS:egfr*^{RNAi}), VDRC19717 (*UAS:dome*^{RNAi}), B35363 (*UAS:hipk*^{RNAi}), B35481 (*UAS:sd*^{RNAi}). For overexpression of *hpo* or *yki* we used *w***; UAS:hpo/TM3 Sb* (Wu, Huang et al. 2003) and *w***; UAS:yki/TM6B* (Huang, Wu et al. 2005) (courtesy of D. Pan, Johns Hopkins University). GAL4 lines used were: *w; P{GawB}bab1*$^{Pgal4-2}$*/TM6, Tb*^{1} (*bab:GAL4*, B6803), *P{UAS-Dcr-2.D}1, w*^{1118}*; P{GAL4-nos.NGT}40* (*nos:GAL4*, B25751), *y w; P{w*$^{+mW.hs}$*=GawB}NP1624* (*tj:GAL4*, Kyoto Stock Center, K104-055), *y w hs:FLP*^{122}*; Sp/CyO; hh:GAL4/TM6B* (*hh:GAL4*, courtesy of L. Johnston, Columbia University), *w; P{w*$^{+mW.hs}$*=GawB}ptc*$^{559.1}$ (*ptc:GAL4*, B2017). For GAL4 expression domain analysis, GAL4 lines were crossed to *w; P{w*$^{+mC}$*=UAS-GFP.S65T}T2* (B1521). For clonal analysis of *hpo* and *yki* null alleles, the following lines were used: *w*^{1118}*; P{ry*$^{+t7.2}$*=neoFRT}*$_{42D}$ *P{w*$^{+mC}$*=Ubi GFP(S65T)nls}2R/CyO* (B5626), *w*^{1118}*; P{ry*$^{+t7.2}$*=neoFRT}*$_{42D}$ *P{w*$^{+t*}$ *ry*$^{+t*}$*=white-un1}*$_{47A}$ (B1928), *P{ry*$^{+t7.2}$*=hsFLP}1, w*^{1118}*; Adv[*^{1}*]/CyO* (B6), *hsFLP12 w***; P{ry*$^{+t7.2}$*=neoFRT}42D yki*^{B5}*/CyO* (Huang, Wu et al. 2005) (courtesy of D. Pan, Johns Hopkins University), and *y** *w***; P{ry*$^{+t7.2}$*=neoFRT}*$_{42D}$ *hpo*^{BF33}*/CyO (y+)* (Jia, Zhang et al. 2003) (Courtesy of J. Jiang, University of Texas Southwestern Medical Center). For analysis of cell type numbers in flies homozygous

for loss of function Hippo pathway alleles, we used ex^{1} (B295; (Stern and Bridges 1926)) and *y*w*eyFLP; FRT*^{42D} *yki*^{DBO2} */ CyO* (Courtesy of K-L Guan, UCSD; (Zhao, Wei et al. 2007)) .

Validation of RNAi lines was provided by data from a number of independent experiments, as follows: (1) Immunohistochemistry against Hpo or Yki showed that RNAi against these genes reduced protein levels to levels indistinguishable from background in whole mounted larval ovaries (Figure S1D, I). (2) Germ line clones of null alleles of *hpo* (*hpo*^{BF33} (Jia, Zhang et al. 2003)) or *yki* (*yki*^{B5} (Huang, Wu et al. 2005)) had the same effect on germ cell number as RNAi against these genes driven in the germ line (Figure 4F). (3) A null allele of *expanded* (Stern and Bridges 1926) had the same effect on TFC number, GC number and IC number as RNAi against Hippo pathway activity (Figure S4, Table S2). (4) Two different *yki* RNAi lines had the same effect on GC number (Table S3). (5) Expression of pMAPK and Stat92E in the larval was reduced by RNAi against *egfr* or *spi* and *dome* or *upd1*, respectively (Figure S8). In addition, the *wts*^{RNAi} and *dome*^{RNAi} lines we used here have been independently validated by other studies (Mummery-Widmer, Yamazaki et al. 2009, Jukam, Xie et al. 2013).

Immunohistochemistry

Larvae were all reared at 25ºC at 60% humidity. Larval fat bodies were dissected in 1xPBS with 0.1% Triton-X, and fixed in 4% PFA in 1xPBS for 20 minutes at room temperature or overnight at 4ºC. For tissues stained with the rat-Hippo antibody (courtesy of N. Tapon, London Research Institute), fat body tissue was fixed in freshly made PLP fixative (Grzeschik, Parsons et al. 2010) for 20 minutes. Tissues were stained as previously described (Sarikaya, Belay et al. 2012). Primary antibodies were used in the following concentrations: Mouse anti-Engrailed 4D9 (1:50, Developmental Studies Hybridoma Bank), guinea pig anti-Traffic Jam (1:3000-5000, courtesy of

D. Godt, University of Toronto), rabbit anti-Vasa (1:500, courtesy of P. Lasko, McGill University), rabbit anti-Yorkie (1:400, courtesy of K. Irvine, Rutgers University), rat anti-Hippo (1:100, courtesy of N. Tapon, London Research Institute), chicken anti-Beta-galactosidase (1:200, Abcam), mouse anti-Alpha spectrin 3A9 (1:5, Developmental Studies Hybridoma Bank), rabbit anti-dpErk (1:300, Cell Signaling), rabbit anti-Stat92E (1:200, courtesy of E. Bach, New York University). We used goat anti-guinea pig Alexa 488, anti-mouse Alexa 488, Alexa 555, and Alexa 647, anti-rabbit Alexa 555, Alexa 647, anti-rat Alexa 568, and anti-chicken Alexa 568 at 1:500 as secondary antibodies (Life Technologies). All samples were stained with 10 mg/ml Hoechst 33342 (Sigma) at 1:500 to visualize nuclei, and some samples were stained with 0.1 mg/ml FITC-conjugated Phalloidin (Sigma) at 1:200 to visualize cell outlines. For GAL4 crosses, we crossed virgin females carrying the GAL4 construct with males carrying the UAS construct, and analyzed F1 LP stage larvae. Samples were imaged with Zeiss LSM 700, 710 or 780 confocal microscopes at the Harvard Center for Biological Imaging. Each sample was imaged in z-stacks of 1 μm thickness. For expression level analysis, laser settings were normalized to the secondary only control conducted in parallel to the experimental stain. Expression levels were quantified using Image J (NIH) and were normalized to nuclear stain intensity to control for staining level differences between samples.

Cell type, ovariole number and egg-laying quantification

White immobile pupae were collected from uncrowded tubes (<100 larvae) for cell number analysis. All cell counts were obtained manually using Volocity (Perkin Elmer) after samples were randomized and coded to prevent bias; cells stained with Vasa were counted for germ cell number, and cells stained with Traffic Jam were counted for interstitial cell number. TF number

and total TFC number were collected as described in (Sarikaya, Belay et al. 2012). Experimental crosses were compared to parental GAL4 and RNAi strains using a student's t-test with unequal variance performed in Microsoft Excel. Changes in number were not considered significant unless *p* values were significant for both parental strains. For crosses where one or both parents were heterozygous for balanced GAL4 and/or UAS elements, sibling data from F1s carrying balancer chromosomes, rather than parental data, was collected as a control.

Adult ovariole number was counted in mated females that were 3-5 days post hatching from uncrowded vials kept in 25 ºC at 60% humidity. Adult ovaries were dissected in 1xPBS containing 0.1% Triton-X, and ovariole number was counted under a dissecting microscope by teasing apart ovariole strands using a tungsten needle. F1 ovariole number was compared to the ovariole number of siblings carrying balancer chromosomes for *bab:GAL4*, and to the *tj:GAL4* parental line for the *tj:GAL4* crosses.

Adult fecundity was measured by placing three females and one male in a vial for 24 hours, and counting total egg number per vial. Five replicates (vials) were performed for each treatment. The egg count was divided by the number of females to obtain the average egg number per female per 24 hours.

Clonal analysis

P0 flies were mated (for *yki*^{B5} clones: *w*^{1118}*; P{ry*$^{+t7.2}$*=neoFRT}*$_{42D}$ *P{w*$^{+mC}$*=Ubi GFP(S65T)nls}2R/CyO* x *hsFLP12 w***; P{ry*$^{+t7.2}$*=neoFRT}42D yki*^{B5}*/CyO*; for *hpo*^{BF33} clones: *P{ry*$^{+t7.2}$*=hsFLP}1, w*^{1118}*; P{ry*$^{+t7.2}$*=neoFRT}*$_{42D}$ *P{w*$^{+mC}$*=Ubi GFP(S65T)nls}2R/CyO* x *y** *w***; P{ry*$^{+t7.2}$*=neoFRT}*$_{42D}$ *hpo*^{BF33}*/CyO (y+)*; for control *w* clones: *P{ry*$^{+t7.2}$*=hsFLP}1, w*^{1118}*; P{ry*$^{+t7.2}$*=neoFRT}*$_{42D}$ *P{w*$^{+mC}$*=Ubi GFP(S65T)nls}2R/CyO* x *w*^{1118}*; P{ry*$^{+t7.2}$*=neoFRT}*$_{42D}$ *P{w*$^{+t*}$

ry$^{+t7.2}$*=white-un1}47A*) and F1 eggs were collected for 8-12 hours at 25 ºC. L1 larvae were heat shocked at 37ºC for 1 hour 36-48 hours after egg laying. Late L3 to LP stage ovaries were dissected, stained with 10 mg/ml Hoechst 4333 (Sigma) at 1:500, FITC-conjugated anti-GFP (1:500, Life Technologies), and rabbit anti-Vasa (1:500, courtesy of P. Lasko, McGill University), and imaged. GFP-negative mutant GC clone size (number of cells per clone) and GFP++ wild type twin spot clone size were counted manually.

3.6 Acknowledgements

We thank Erika Bach, Dorothea Godt, Ken Irvine, Jin Jiang, Laura Johnston, Paul Lasko, Duojia Pan, Kun-Liang Guan and Nick Tapon for kindly sharing reagents. This work was supported by National Institutes of Health grant 1R01 HD073499 to CGE. DPS is supported by a post-graduate scholarship from the Natural Sciences and Engineering Research Council of Canada (NSERC) and a pre-doctoral fellowship from Fonds de la santé de Québec (FRSQ).

3.7 References

Agaisse, H., U. M. Petersen, M. Boutros, B. Mathey-Prevot and N. Perrimon (2003). "Signaling role of hemocytes in *Drosophila* JAK/STAT-dependent response to septic injury." Developmental Cell **5**(3): 441-450.

Badouel, C., L. Gardano, N. Amin, A. Garg, R. Rosenfeld, T. Le Bihan and H. McNeill (2009). "The FERM-domain protein Expanded regulates Hippo pathway activity via direct interactions with the transcriptional activator Yorkie." Developmental Cell **16**(3): 411-420.

Barnes, A. I., J. M. Boone, J. Jacobson, L. Partridge and T. Chapman (2006). "No extension of lifespan by ablation of germ line in *Drosophila*." Proceedings of the Royal Society of London. Series B: Biological Sciences **273**(1589): 939-947.

Barry, E. R. and F. D. Camargo (2013). "The Hippo superhighway: signaling crossroads converging on the Hippo/Yap pathway in stem cells and development." Current Opinion in Cell Biology **25**(2): 247-253.

Bartoletti, M., T. Rubin, F. Chalvet, S. Netter, N. Dos Santos, E. Poisot, M. Paces-Fessy, D. Cumenal, F. Peronnet, A. M. Pret and L. Theodore (2012). "Genetic basis for developmental homeostasis of germline stem cell niche number: a network of Tramtrack-Group nuclear BTB factors." PloS ONE **7**(11): e49958.

Baumgartner, R., I. Poernbacher, N. Buser, E. Hafen and H. Stocker (2010). "The WW Domain Protein Kibra Acts Upstream of Hippo in *Drosophila*." Developmental Cell **18**(2): 309-316.

Bennett, F. C. and K. F. Harvey (2006). "Fat cadherin modulates organ size in *Drosophila* via the Salvador/Warts/Hippo signaling pathway." Current Biology **16**(21): 2101-2110.

Beverdam, A., C. Claxton, X. Zhang, G. James, K. F. Harvey and B. Key (2013). "Yap controls stem/progenitor cell proliferation in the mouse postnatal epidermis." The Journal of Investigative Dermatology **133**(6): 1497-1505.

Brown, S., N. Hu and J. C. Hombria (2003). "Novel level of signalling control in the JAK/STAT pathway revealed by in situ visualisation of protein-protein interaction during *Drosophila* development." Development **130**(14): 3077-3084.

Cabrera, G. R., D. Godt, P. Y. Fang, J. L. Couderc and F. A. Laski (2002). "Expression pattern of Gal4 enhancer trap insertions into the *bric a brac* locus generated by P element replacement." Genesis **34**(1-2): 62-65.

Chan, S. W., C. J. Lim, C. Huang, Y. F. Chong, H. J. Gunaratne, K. A. Hogue, W. P. Blackstock, K. F. Harvey and W. Hong (2011). "WW domain-mediated interaction with Wbp2 is important for the oncogenic property of TAZ." Oncogene **30**(5): 600-610.

David, J. R. (1970). "Le nombre d'ovarioles chez *Drosophila melanogaster*: relation avec la fécondité et valeur adaptive." Archives de Zoologie Expérimentale et Générale **111**: 357-370.

Demircan, T. and E. Berezikov (2013). "The Hippo pathway regulates stem cells during homeostasis and regeneration of the flatworm *Macrostomum lignano*." Stem Cells and Development **22**(15): 2174-2185.

Dietzl, G., D. Chen, F. Schnorrer, K. C. Su, Y. Barinova, M. Fellner, B. Gasser, K. Kinsey, S. Oppel, S. Scheiblauer, A. Couto, V. Marra, K. Keleman and B. J. Dickson (2007). "A genome-wide transgenic RNAi library for conditional gene inactivation in *Drosophila*." Nature **448**(7150): 151-156.

Eliazer, S. and M. Buszczak (2011). "Finding a niche: studies from the *Drosophila* ovary." Stem Cell Research and Therapy **2**(6): 45.

Flaherty, M. S., P. Salis, C. J. Evans, L. A. Ekas, A. Marouf, J. Zavadil, U. Banerjee and E. A. Bach (2010). "*chinmo* is a functional effector of the JAK/STAT pathway that regulates eye development, tumor formation, and stem cell self-renewal in *Drosophila*." Developmental Cell **18**(4): 556-568.

Gancz, D. and L. Gilboa (2013). "Insulin and Target of rapamycin signaling orchestrate the development of ovarian niche-stem cell units in *Drosophila*." Development **140**(20): 4145-4154.

Gancz, D., T. Lengil and L. Gilboa (2011). "Coordinated regulation of niche and stem cell precursors by hormonal signaling." PLoS Biology **9**(11): e1001202.

Genevet, A., M. C. Wehr, R. Brain, B. J. Thompson and N. Tapon (2010). "Kibra Is a Regulator of the Salvador/Warts/Hippo Signaling Network." Developmental Cell **18**(2): 300-308.

Gilboa, L. and R. Lehmann (2006). "Soma-germline interactions coordinate homeostasis and growth in the *Drosophila* gonad." Nature **443**(7107): 97-100.

Godt, D. and F. A. Laski (1995). "Mechanisms of cell rearrangement and cell recruitment in *Drosophila* ovary morphogenesis and the requirement of *bric à brac*." Development **121**: 173-187.

Goulev, Y., J. D. Fauny, B. Gonzalez-Marti, D. Flagiello, J. Silber and A. Zider (2008). "SCALLOPED interacts with YORKIE, the nuclear effector of the Hippo tumor-suppressor pathway in *Drosophila*." Current Biology **18**(6): 435-441.

Green II, D. A. and C. G. Extavour (2012). "Convergent Evolution of a Reproductive Trait Through Distinct Developmental Mechanisms in *Drosophila*." Developmental Biology **372**(1): 120-130.

Green II, D. A. and C. G. Extavour (2014). "Insulin Signaling Underlies Both Plasticity and Divergence of a Reproductive Trait in *Drosophila*." Proceedings of the Royal Society of London. Series B: Biological Sciences **281**(1779): 20132673.

Grzeschik, N. A., L. M. Parsons, M. L. Allott, K. F. Harvey and H. E. Richardson (2010). "Lgl, aPKC, and Crumbs regulate the Salvador/Warts/Hippo pathway through two distinct mechanisms." Current Biology **20**(7): 573-581.

Halder, G. and R. L. Johnson (2011). "Hippo signaling: growth control and beyond." Development **138**(1): 9-22.

Hall, C. A., R. Wang, J. Miao, E. Oliva, X. Shen, T. Wheeler, S. G. Hilsenbeck, S. Orsulic and S. Goode (2010). "Hippo pathway effector Yap is an ovarian cancer oncogene." Cancer Research **70**(21): 8517-8525.

Hamaratoglu, F., M. Willecke, M. Kango-Singh, R. Nolo, E. Hyun, C. Tao, H. Jafar-Nejad and G. Halder (2006). "The tumour-suppressor genes NF2/Merlin and Expanded act through Hippo signalling to regulate cell proliferation and apoptosis." Nature Cell Biology **8**(1): 27-36.

Harrison, D. A., P. E. McCoon, R. Binari, M. Gilman and N. Perrimon (1998). "*Drosophila unpaired* encodes a secreted protein that activates the JAK signaling pathway." Genes and Development **12**(20): 3252-3263.

Hayashi, S., K. Ito, Y. Sado, M. Taniguchi, A. Akimoto, H. Takeuchi, T. Aigaki, F. Matsuzaki, H. Nakagoshi, T. Tanimura, R. Ueda, T. Uemura, M. Yoshihara and S. Goto (2002). "GETDB, a database compiling expression patterns and molecular locations of a collection of Gal4 enhancer traps." Genesis **34**(1-2): 58-61.

Heallen, T., M. Zhang, J. Wang, M. Bonilla-Claudio, E. Klysik, R. L. Johnson and J. F. Martin (2011). "Hippo pathway inhibits Wnt signaling to restrain cardiomyocyte proliferation and heart size." Science **332**(6028): 458-461.

Herranz, H., X. Hong and S. M. Cohen (2012). "Mutual repression by Bantam miRNA and Capicua links the EGFR/MAPK and Hippo pathways in growth control." Current Biology **22**(8): 651-657.

Hodin, J. and L. M. Riddiford (1998). "The ecdysone receptor and ultraspiracle regulate the timing and progression of ovarian morphogenesis during *Drosophila* metamorphosis." Development, Genes and Evolution **208**(6): 304-317.

Hodin, J. and L. M. Riddiford (2000). "Different mechanisms underlie phenotypic plasticity and interspeficic variation for a reproductive character in Drosophilds (Insecta: Diptera)." Evolution **5**(54): 1638-1653.

Huang, J., S. Wu, J. Barrera, K. Matthews and D. Pan (2005). "The Hippo signaling pathway coordinately regulates cell proliferation and apoptosis by inactivating Yorkie, the *Drosophila* Homolog of YAP." Cell **122**(3): 421-434.

Huang, J. M., I. Nagatomo, E. Suzuki, T. Mizuno, T. Kumagai, A. Berezov, H. Zhang, B. Karlan, M. I. Greene and Q. Wang (2013). "YAP modifies cancer cell sensitivity to EGFR and survivin inhibitors and is negatively regulated by the non-receptor type protein tyrosine phosphatase 14." Oncogene **32**(17): 2220-2229.

Jia, J., W. Zhang, B. Wang, R. Trinko and J. Jiang (2003). "The *Drosophila* Ste20 family kinase dMST functions as a tumor suppressor by restricting cell proliferation and promoting apoptosis." Genes and Development **17**(20): 2514-2519.

Jukam, D., B. Xie, J. Rister, D. Terrell, M. Charlton-Perkins, D. Pistillo, B. Gebelein, C. Desplan and T. Cook (2013). "Opposite feedbacks in the Hippo pathway for growth control and neural fate." Science **342**(6155): 1238016.

Karpowicz, P., J. Perez and N. Perrimon (2010). "The Hippo tumor suppressor pathway regulates intestinal stem cell regeneration." Development **137**(24): 4135-4145.

King, R. C. (1970). Ovarian Development in *Drosophila melanogaster*. New York, Academic Press.

Li, M. A., J. D. Alls, R. M. Avancini, K. Koo and D. Godt (2003). "The large Maf factor Traffic Jam controls gonad morphogenesis in *Drosophila*." Nature Cell Biology **5**(11): 994-1000.

Lin, A. Y. and B. J. Pearson (2014). "Planarian yorkie/YAP functions to integrate adult stem cell proliferation, organ homeostasis and maintenance of axial patterning." Development **141**(6): 1197-1208.

Lin, T. H., T. H. Yeh, T. W. Wang and J. Y. Yu (2014). "The Hippo Pathway Controls Border Cell Migration Through Distinct Mechanisms in Outer Border Cells and Polar Cells of the Drosophila Ovary." Genetics.

Liu, X., N. Yang, S. A. Figel, K. E. Wilson, C. D. Morrison, I. H. Gelman and J. Zhang (2013). "PTPN14 interacts with and negatively regulates the oncogenic function of YAP." Oncogene **32**(10): 1266-1273.

Matsuoka, S., Y. Hiromi and M. Asaoka (2013). "Egfr signaling controls the size of the stem cell precursor pool in the *Drosophila* ovary." Mechanisms of Development **130**(4-5): 241-253.

Meignin, C., I. Alvarez-Garcia, I. Davis and I. M. Palacios (2007). "The Salvador-Warts-Hippo pathway is required for epithelial proliferation and axis specification in *Drosophila*." Current Biology **17**(21): 1871-1878.

Mummery-Widmer, J. L., M. Yamazaki, T. Stoeger, M. Novatchkova, S. Bhalerao, D. Chen, G. Dietzl, B. J. Dickson and J. A. Knoblich (2009). "Genome-wide analysis of Notch signalling in Drosophila by transgenic RNAi." Nature **458**(7241): 987-992.

Ni, J. Q., L. P. Liu, R. Binari, R. Hardy, H. S. Shim, A. Cavallaro, M. Booker, B. D. Pfeiffer, M. Markstein, H. Wang, C. Villalta, T. R. Laverty, L. A. Perkins and N. Perrimon (2009). "A *Drosophila* resource of transgenic RNAi lines for neurogenetics." Genetics **182**(4): 1089-1100.

Nolo, R., C. M. Morrison, C. Tao, X. Zhang and G. Halder (2006). "The *bantam* microRNA is a target of the Hippo tumor-suppressor pathway." Current Biology **16**(19): 1895-1904.

Oh, H. and K. D. Irvine (2008). "In vivo regulation of Yorkie phosphorylation and localization." Development (Cambridge, England) **135**(6): 1081-1088.

Oh, H., B. V. Reddy and K. D. Irvine (2009). "Phosphorylation-independent repression of Yorkie in Fat-Hippo signaling." Developmental Biology **335**(1): 188-197.

Ohsawa, S., Y. Sato, M. Enomoto, M. Nakamura, A. Betsumiya and T. Igaki (2012). "Mitochondrial defect drives non-autonomous tumour progression through Hippo signalling in *Drosophila*." Nature **490**(7421): 547-551.

Orgogozo, V., K. W. Broman and D. L. Stern (2006). "High-resolution quantitative trait locus mapping reveals sign epistasis controlling ovariole number between two *Drosophila* species." Genetics **173**(1): 197-205.

Polesello, C. and N. Tapon (2007). "Salvador-Warts-Hippo signaling promotes *Drosophila* posterior follicle cell maturation downstream of Notch." Current Biology **17**(21): 1864-1870.

Poon, C. L., X. Zhang, J. I. Lin, S. A. Manning and K. F. Harvey (2012). "Homeodomain-interacting protein kinase regulates Hippo pathway-dependent tissue growth." Current Biology **22**(17): 1587-1594.

Ramos, A. and F. D. Camargo (2012). "The Hippo signaling pathway and stem cell biology." Trends in Cell Biology **22**(7): 339-346.

Reddy, B. V. and K. D. Irvine (2011). "Regulation of *Drosophila* glial cell proliferation by Merlin-Hippo signaling." Development **138**(23): 5201-5212.

Reddy, B. V. and K. D. Irvine (2013). "Regulation of Hippo signaling by EGFR-MAPK signaling through Ajuba family proteins." Developmental Cell **24**(5): 459-471.

Reddy, B. V., C. Rauskolb and K. D. Irvine (2010). "Influence of Fat-Hippo and Notch signaling on the proliferation and differentiation of *Drosophila* optic neuroepithelia." Development **137**(14): 2397-2408.

Ren, F., B. Wang, T. Yue, E.-Y. Yun, Y. T. Ip and J. Jiang (2010). "Hippo signaling regulates *Drosophila* intestine stem cell proliferation through multiple pathways." Proceedings of the National Academy of Sciences of the United States of America **107**(49): 21064-21069.

Robinson, B. S., J. Huang, Y. Hong and K. H. Moberg (2010). "Crumbs regulates Salvador/Warts/Hippo signaling in *Drosophila* via the FERM-domain protein Expanded." Current Biology **20**(7): 582-590.

Sahut-Barnola, I., B. Dastugue and J.-L. Couderc (1996). "Terminal filament cell organization in the larval ovary of *Drosophila melanogaster*: ultrastructural observations and pattern of divisions." Roux's Archives of Developmental Biology **205**: 356-363.

Sarikaya, D. P., A. A. Belay, A. Ahuja, D. A. Green II, A. Dorta and C. G. Extavour (2012). "The roles of cell size and cell number in determining ovariole number in *Drosophila*." Developmental Biology **363**: 279-289

Schlegelmilch, K., M. Mohseni, O. Kirak, J. Pruszak, J. R. Rodriguez, D. Zhou, B. T. Kreger, V. Vasioukhin, J. Avruch, T. R. Brummelkamp and F. D. Camargo (2011). "Yap1 acts downstream of alpha-catenin to control epidermal proliferation." Cell **144**(5): 782-795.

Shaw, R. L., A. Kohlmaier, C. Polesello, C. Veelken, B. A. Edgar and N. Tapon (2010). "The Hippo pathway regulates intestinal stem cell proliferation during *Drosophila* adult midgut regeneration." Development **137**(24): 4147-4158.

Silva, E., Y. Tsatskis, L. Gardano, N. Tapon and H. McNeill (2006). "The tumor-suppressor gene *fat* controls tissue growth upstream of Expanded in the Hippo signaling pathway." Current Biology **16**(21): 2081-2089.

Song, X., G. B. Call, D. Kirilly and T. Xie (2007). "Notch signaling controls germline stem cell niche formation in the *Drosophila* ovary." Development **134**(6): 1071-1080.

Staley, B. K. and K. D. Irvine (2010). "Warts and Yorkie mediate intestinal regeneration by influencing stem cell proliferation." Current Biology **20**(17): 1580-1587.

Stern, C. and C. B. Bridges (1926). "The mutants of the extreme left end of the second chromosome of *Drosophila melanogaster*." Genetics **11**(503-530).

Striedinger, K., S. R. VandenBerg, G. S. Baia, M. W. McDermott, D. H. Gutmann and A. Lal (2008). "The Neurofibromatosis 2 tumor suppressor gene product, Merlin, regulates human meningioma cell growth by signaling through YAP." Neoplasia **10**(11): 1204-1212.

Sun, S., S. Zhao and Z. Wang (2008). "Genes of Hippo signaling network act unconventionally in the control of germline proliferation in *Drosophila*." Developmental Dynamics **237**(1): 270-275.

Sweitzer, S. M., S. Calvo, M. H. Kraus, D. S. Finbloom and A. C. Larner (1995). "Characterization of a Stat-like DNA binding activity in *Drosophila melanogaster*." The Journal of Biological Chemistry **270**(28): 16510-16513.

Tanentzapf, G., D. Devenport, D. Godt and N. H. Brown (2007). "Integrin-dependent anchoring of a stem-cell niche." Nature Cell Biology **9**(12): 1413-1418.

Thompson, B. J. and S. M. Cohen (2006). "The Hippo pathway regulates the bantam microRNA to control cell proliferation and apoptosis in *Drosophila*." Cell **126**(4): 767-774.

Tulina, N. and E. Matunis (2001). "Control of stem cell self-renewal in *Drosophila* spermatogenesis by JAK-STAT signaling." Science **294**(5551): 2546-2549.

Tumaneng, K., R. C. Russell and K.-L. Guan (2012). "Organ size control by Hippo and TOR pathways." Current Biology **22**(9): R368-379.

Udan, R. S., M. Kango-Singh, R. Nolo, C. Tao and G. Halder (2003). "Hippo promotes proliferation arrest and apoptosis in the Salvador/Warts pathway." Nature Cell Biology **5**(10): 914-920.

Willecke, M., F. Hamaratoglu, M. Kango-Singh, R. Udan, C. L. Chen, C. Tao, X. Zhang and G. Halder (2006). "The fat cadherin acts through the Hippo tumor-suppressor pathway to regulate tissue size." Current Biology **16**(21): 2090-2100.

Wu, S., J. Huang, J. Dong and D. Pan (2003). "*hippo* encodes a Ste-20 family protein kinase that restricts cell proliferation and promotes apoptosis in conjunction with *salvador* and *warts*." Cell **114**(4): 445-456.

Wu, S., Y. Liu, Y. Zheng, J. Dong and D. Pan (2008). "The TEAD/TEF family protein Scalloped mediates transcriptional output of the Hippo growth-regulatory pathway." Developmental Cell **14**(3): 388-398.

Yan, R., S. Small, C. Desplan, C. R. Dearolf and J. E. Darnell, Jr. (1996). "Identification of a *Stat* gene that functions in *Drosophila* development." Cell **84**(3): 421-430.

Yu, J., J. Poulton, Y. C. Huang and W. M. Deng (2008). "The Hippo pathway promotes Notch signaling in regulation of cell differentiation, proliferation, and oocyte polarity." PloS ONEs **3**(3): e1761.

Yu, J., Y. Zheng, J. Dong, S. Klusza, W. M. Deng and D. Pan (2010). "Kibra functions as a tumor suppressor protein that regulates Hippo signaling in conjunction with Merlin and Expanded." Developmental cell **18**(2): 288-299.

Zhang, J., J.-Y. Ji, M. Yu, M. Overholtzer, G. A. Smolen, R. Wang, J. S. Brugge, N. J. Dyson and D. A. Haber (2009). "YAP-dependent induction of amphiregulin identifies a non-cell-autonomous component of the Hippo pathway." Nature Cell Biology **11**(12): 1444-1450.

Zhang, L., F. Ren, Q. Zhang, Y. Chen, B. Wang and J. Jiang (2008). "The TEAD/TEF family of transcription factor Scalloped mediates Hippo signaling in organ size control." Developmental Cell **14**(3): 377-387.

Zhang, X., J. George, S. Deb, J. L. Degoutin, E. A. Takano, S. B. Fox, A. S. Group, D. D. L. Bowtell and K. F. Harvey (2011). "The Hippo pathway transcriptional co-activator, YAP, is an ovarian cancer oncogene." Oncogene **30**(25): 2810-2822.

Zhao, B., L. Li, Q. Lei and K.-L. Guan (2010). "The Hippo-YAP pathway in organ size control and tumorigenesis: an updated version." Genes and Development **24**(9): 862-874.

Zhao, B., X. Wei, W. Li, R. S. Udan, Q. Yang, J. Kim, J. Xie, T. Ikenoue, J. Yu, L. Li, P. Zheng, K. Ye, A. Chinnaiyan, G. Halder, Z.-C. Lai and K.-L. Guan (2007). "Inactivation of YAP oncoprotein by the Hippo pathway is involved in cell contact inhibition and tissue growth control." Genes and Development **21**(21): 2747-2761.

Zhou, D., Y. Zhang, H. Wu, E. Barry, Y. Yin, E. Lawrence, D. Dawson, J. E. Willis, S. D. Markowitz, F. D. Camargo and J. Avruch (2011). "Mst1 and Mst2 protein kinases restrain intestinal stem cell proliferation and colonic tumorigenesis by inhibition of Yes-associated protein (Yap) overabundance." Proceedings of the National Academy of Sciences of the United States of America **108**(49): E1312-1320.

Chapter IV:

The effect of ecology and development on ovariole number evolution in Hawaiian *Drosophila*

4. 1 Abstract

Animals evolving on volcanic archipelagos often undergo adaptive radiation, where traits are rapidly diversified in response to the new environments. Hawaiian Drosophila represent a group of close to 1000 species that radiated from a last common ancestor within the last 25 million years, and have evolved to specialize on decaying flowers, leaves, fungi, sap fluxes, and bark of native plants as egg laying substrates. Interestingly, Hawaiian Drosophila have the most extreme range of ovariole number reported in the genus Drosophila, ranging between two to 101 per ovary depending on the species. Previously, it has been suggested that flies that laid eggs on more ephemeral food sources such as flowers and leaves, have fewer ovarioles compared to species that laid eggs on less ephemeral sources such as bark. This chapter describes my ongoing efforts to characterize ovariole number from a diverse range of wild-caught females and conduct phylogenetic comparative analysis of ovariole number and egg laying substrate. In addition, I have reared larvae from 21 species in the laboratory, and identified that ovariole number changes in Hawaiian Drosophila can occur through changes in both TFC number and TFC sorting. My aim is to develop Hawaiian Drosophila as a novel model to investigate how ovariole number evolves in response to ecological niche.

4.2 Introduction

Hawaiian Drosophila phylogeny and ecology

Hawaiian *Drosophila* are one of the most morphologically diverse and species-rich group of species in the genus *Drosophila*. Hawaiian Drosophila species are categorized into five different species groups based on genetic, morphological and ecological similarities: *Scaptomyza*, picture wing, modified mouthpart, Haleakala, and antopocerus-modified tarsus-ciliated tarsus (AMC) groups (Figure 4.1) (O'Grady et al., 2011). *Scaptomyza* species are small species that primarily lay eggs on leaves or flowers (O'Grady and Desalle, 2008). *Scaptomyza* species are the only Hawaiian Drosophilids that have migrated out of Hawaii, and can be found in Asia and North America. Picture wing species are larger species (approximately 2-4x larger than *D. melanogaster*) that have striking pigment patterns on their wings (Edwards et al., 2007). Picture wing species primarily lay eggs on decaying bark or branches of native trees, with some species that specialize on sap fluxes (Magnacca et al., 2008). Modified mouthpart species have male-specific modifications on the mouthparts that are used during mating (Magnacca and O'Grady, 2006), and have the largest range in egg laying substrates, specializing on decaying leaves, fungi, sap or bark (Kambysellis et al., 1995). Haleakala species are dark-colored flies that specifically lay eggs on native fungi. Lastly, AMC species consist of large antopocerus species, as well as medium sized modified or ciliated tarsus species, which have male-specific modifications on the tarsal segments of the front leg. Most AMC species are leaf breeders, though there are a few exceptions in the modified and ciliated tarsus group that appear to have evolved bark-breeding (O'Grady et al., 2011).

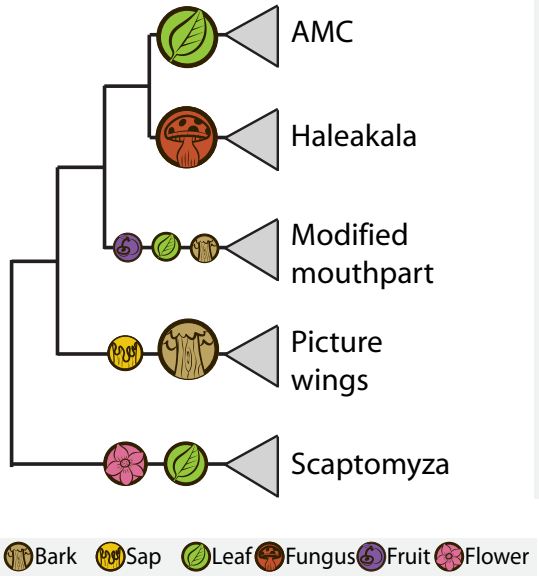

	# Species represented		
Ovariole number	Kambysellis & Heed 1971	2013 Collection	2014 Collection
8-18	8	2	3+
?	0	0	2+
11-25	2	1	3+
24-86	14	10	3
2-8	4	1	4+

Figure 4.1. Simplified phylogeny of Hawaiian Drosophila and egg laying substrates. Tree based on O'Grady et al. (2011) with icons of known egg laying substrates for each species group mapped on the phylogenetic tree. Summarized on the columns are reported ovariole number (per ovary), number of species examined in a previous study (Kambysellis and Heed, 1971), and the number of species for which I collected ovariole number data during my 2013 and 2014 field collections. Numbers with plus signs indicates samples where morphology suggests that these species are represented but DNA bar coding data is needed to validate species identity.

Female reproductive traits in Hawaiian Drosophila

Along with extremely divergent external morphological features, Hawaiian Drosophila also have the most diverse range in ovariole number reported in the genus Drosophila. Kambysellis and Heed (1971) reported measurements of adult phenotypes, including ovariole number, of 24 species of Hawaiian Drosophila, most of which were from the picture wing and AMC group (summarized in Figure 4.1). In this paragraph, I will briefly summarize their findings on ovariole number distributions among the Hawaiian Drosophila species groups. In *Scaptomyza*, flower breeder species had an average of two ovarioles per female, and leaf breeder *Scaptomyza* species had an average of four to eight ovarioles per female. Picture wing species had the most ovarioles and the widest range of ovariole number. A sap flux breeder had an average of 27 ovarioles, while the bark breeders had average of 37-86 ovarioles depending on the species. It should be noted that the highest ovariole number in picture wing species (86) was found in a bark breeder species exhibiting gigantism on Maui island, and that the range of ovarioles within other bark breeder picture wing species was 37-65. They characterized ovariole number from a fruit breeder and a leaf breeder modified mouthpart species, which had an average of 25 and 11 ovarioles respectively. There are no reports of ovariole number from the fungus breeder Haleakala group in the literature to date. Leaf-breeder AMC group species had eight to 18 ovarioles. The highest ovariole number in Hawaiian Drosophila of 101 was reported for *D. primaeva. D. primaeva* often branches as one of the most basal species of Hawaiian Drosophila, and it does not fall into any one of the species groups (O'Grady et al., 2011). For the interest of this chapter, I will focus

on species within the five main species groups, and I have excluded *D. primaeva* from analysis.

Kambysellis and Heed (1971) also characterized egg size of Hawaiian Drosophila species. They noticed an increase in egg size relative to body size in species with low ovariole number, and a difference in egg laying behavior. The flower breeder *Scaptomyza* can retain fertilized eggs and lay eggs shortly before hatching (ovoviviparity). Leaf breeders lay one or two eggs a day, while most bark-breeder picture wing species lay eggs in large clutches of 100+ eggs at a time (although how frequently picture wing species lay these clutches of eggs is unknown). Based on these results, the authors postulated that differences in larval substrate may be driving *r vs k* selection depending on the ephemerality of the food source. Under this hypothesis, in species that lay eggs on ephemeral substrates such as flowers and leaves, the female invests more per offspring by producing larger eggs that are retained during early development, and in species that lay eggs on less ephemeral substrates, females lay many small eggs at a time immediately upon or shortly after fertilization.

To test this hypothesis, the authors built a phylogenetic tree of Hawaiian Drosophilids based on *yolk protein1* (*yp1*) gene, and mapped ovariole number and ecology on to the tree for a subset of species (Kambysellis et al., 1995). In this way, they identified a correlation between switches in egg laying substrates and ovariole number. Specifically, they identified the Antopocerus and modified mouthpart species as most basally branching, with a correlation between leaf breeding and low ovariole number. The picture wing species, which represented 41 out of the 46 species they sampled, were identified as most derived with a correlation of stem breeding with lower ovariole

number compared to bark breeders. However, the sampling of this analysis is heavily biased towards picture wing species, and the phylogenetic analysis is based on analysis of a single nuclear gene, which does not recover the phylogenetic relationships between species shown by a more recent phylogenetic tree based on four mitochondrial genes (O'Grady et al., 2011). Notably, the picture wing species branch furthest from a last common ancestor in the Kambysellis *et al*. (1995) paper, while the phylogenetic tree constructed using mitochondrial genes by O'Grady and colleagues (2011) suggest that the AMC species are most derived. The latter hypothesis is also supported by the observation that most of the AMC species are found on the two youngest islands Maui and Hawaii, but not on the oldest island Kauai.

In addition, Kamybsellis *et al.* (1995) did not take into consideration the striking changes in body size between Hawaiian Drosophila species. The thorax length of Hawaiian Drosophila can range from 0.86 mm to 3mm (Kambysellis and Heed, 1971), representing one of the most diverse body sizes in the genus Drosophila. Though ovariole number can be different in closely related species that have the same body size (Green and Extavour, 2012), it would be worth considering whether some shifts in ovariole number captured in Hawaiian Drosophila are better explained by changes in body size rather than ecology.

Aims

My overall aim for this chapter is to characterize the effect of ecology and development on the evolution of ovariole number in Hawaiian Drosophila, and extend my analysis from Chapter 2 on the terminal filament cells (TFCs) in the larval ovary to

species with a very diverse range of ovariole numbers. To accomplish this, I have two major aims for this chapter:

(1) To test the relationship of adult traits, including body size, egg size and ovariole number, and ecological niche in Hawaiian Drosophila.

(2) To identify developmental mechanisms that are giving rise to the diversity in ovariole number.

Progress to date on both aims is reported in the following sections.

4.3 Material and Methods

Field collections

Field collections of Hawaiian Drosophila species were conducted under the Department of Land and Natural Resources of Hawaii native invertebrate scientific collection permit FHM14-353. Collections were made at the Koke'e State Park and Kui'a NAR on Kauai, West Maui Watershed Reserve, Makawao forest reserve, and Waikamoi Nature Preserve on Maui, and the Volcanoes National Park and Upper Waiakea Forest Reserve on Hawaii island. Flies were collected by aspirating flies from traps or sponges containing fermenting fruit and fungi, or by sweeping leaf litter in forests. Flies were placed in sugar vials provided by Dr. Ken Kaneshiro's laboratory (University of Hawaii, Manoa).

Food recipe for Hawaiian Drosophila

Adult food for females to oviposit was made as follows: 1g Agar and 30mL distilled water were mixed in a flask and microwaved for one minute at 100% power setting. 3 g of powder mix consisting of equal mass wheat germ / Gerber's high-protein baby cereal / Kellogg's Special K (mixed and blended into a dry powder mixture), 24 g Gerber's banana baby food and 15 mL distilled water were mixed together and added to the flask containing the microwaved agar and water mixture. The resulting mixture was microwaved for three minutes at 20% power setting. 45 mL distilled water was then added to the mixture, which was mixed and microwaved for a further five minutes at 60% power setting. The food was mixed using a spoon every minute during this five-minute microwave period. Once the flask had cooled sufficiently so that it was just warm to

touch, 375 uL of Propionic acid and 375 uL of 99% Ethanol was added to the mix, and the mixture was poured into standard *Drosophila* culture vials (approximately 2-3 mL per vial).

Larval food was made as follows and stored in a tupperware at 4 °C for a maximum of one month: 6 g of sgar and 225 mL distilled water were mixed in a large beaker and microwaved for two minutes. 60 g cornmeal, 6.6 g roasted soybean meal and 7.5 g brewer's yeast were mixed, blended and added to the beaker along with an additional 300 mL distilled water, and mixed with a spoon. Lastly, three tablespoons of Karo light corn syrup and one tablespoon of unsulfured molasses was added to the mix, and the mixture was microwaved for three minutes. Food was mixed every minute during microwaving until the mixture started to rise. Once the beaker containing the food had cooled so that it was warm to touch, 3 mL of propionic acid and 3 mL of 99% Ethanol were added, then the food was poured into a tupperware container for storage. The food solidifies at 4 °C. For feeding, the solidified food was mixed with a small quantity of water to soften the consistency before being used to feed larvae.

Laboratory care of Hawaiian Drosophila

Field collected females were placed on adult food vials at 18 °C at 80% humidity. Females were changed into new food vials every 5-7 days. Hawaiian Drosophila food has a tendency to develop fungal or bacterial growth, which can be damaging to the adult. Food vials were changed immediately when fungal or bacterial growth was observed. Decaying egg-laying substrates naturally used by the flies were collected in the field, and first placed in the freezer to prevent mite infestations. A small piece of the appropriate

thawed substrate was placed in vials to help stimulate egg laying in wild caught females. Vials containing larvae were monitored for food consumption, indicated by softening of the food, and extra larval food was added every 2-5 days to keep larvae well fed. One to two teaspoons of softened larval food was added on top of the existing larval food to feed the larvae. The new food was mixed with the old food by tapping the vial against a soft surface. Females that did not lay eggs for over one month after being placed in the lab were dissected for adult analysis. When larvae started to wander out of the food, vials containing these wandering larvae were placed in a glass jar containing 1-2cm of moist sand at the bottom. Placing a piece of cloth or paper towel held in place using a rubber band closed the opening of each jar. Adults that emerged from the sand were aspirated out of the jar into a fresh adult food vial.

Measurement of adult phenotypes

Adult ovaries were dissected in 1X PBS and placed in 2% paraformaldehyde in 1X PBS overnight at 4°C. Ovaries were then stained with the nuclear dye Hoechst 33342 (Sigma, 1:500 of 10mg/ml stock solution) in 1X PBS for two hours at room temperature, then washed with 1X PBS for a total of one hour. Ovaries were mounted on glass slides in Vectashield mounting medium (Vector Labs), and ovarioles were spread apart using tungsten needles for species with high ovariole number. Ovariole number was counted under fluorescence and white light microscopy using a Zeiss AxioImager microscope. Images of eggs were taken from these slides using DIC white light settings. Adult egg volume was estimated by measuring the straight lines across the longest and widest points of the egg, and assuming a prolate spheroid shape following a previously

published protocol (Miles et al., 2011) using ImageJ. Egg dorsal appendage length was measured using ImageJ's segmented line function.

Adult bodies were placed in 99% Ethanol after dissection for DNA extraction and adult size analysis. Lateral view images of the thorax were measured using a Zeiss Lumar Stereomicroscope. The highest point of the anterior tip of the thorax and the posterior-most point of the scutellum in the same image plane were used to measure thorax length. A straight line was drawn between these two points in these images using ImageJ's measure function.

DNA barcoding

A piece of fat tissue from the abdomen of flies after their ovaries were dissected were used for DNA extraction using the Qiagen Blood and Tissue kit to an elution of 50 uL. The DNA of each individual was extracted separately, and samples were not pooled. PCRs were conducted using the following primer sets (from 5' to 3') as published in O'Grady et al. (2011):

COI F	ATT CAA CCA ATC ATA AAG ATA TTG G
COI R	TAA ACT TCT GGA TGT CCA AAA AAT CA
COII F	ATG GCA GAT TAG TGC AAT GG
COII R	GTT TAA GAG ACC AGT ACT TG
16S F	CCG GTT TGA ACT CAG ATC ACG T
16S R	CGC CTG TTT AAC AAA AAC AT

PCRs were conducted using Dynazyme DNA polymerase (Thermo Scientific) as follows: 95 °C 5 minutes, (95 °C 30 seconds, 50 °C (COI and COII) or 54 (16S) °C 30 seconds, 72 °C 30 seconds) x 30, 72 °C 5 minutes. PCR products were cleaned using ExoSAP-IT (Affymetrix) and sequenced by Genewiz (Cambridge, MA). Sequences were analyzed by

4Peaks (Nucleobytes) and closest hits were identified using BLASTn alignment against Nr/Nt collection.

Larval analysis

Wandering larvae or early pupal stage individuals were dissected in 1X PBS + 0.1% Triton-X and fixed in 4% Paraformaldehyde in 1X PBS for 20 minutes at room temperature. Larval ovaries were stained as previously described (Sarikaya et al., 2011) using anti-Engrailed (4D9, Hybridoma, 1:50), FITC-conjugated Phalloidin (1:120), and Hoechst 33342 (Sigma, 1:500 of 10mg/ml stock solution). Samples were post-fixed in 4% Paraformaldehyde in 1X PBS for 15 minutes at room temperature and mounted in Vectashield mounting medium (Vector Labs) for imaging using a Zeiss LSM780 Confocal Microscope at the Harvard Biological Imaging Center. Characterization of TFCs and TFs was conducted as described in Sarikaya et al (2012).

4.4 Results

Field collections and observations

I collected samples primarily from picture wing species during the 2013 field collection, and non-picture wing species during the 2014 field collection (Figure 4.1). I collected a total of 116 female specimens in 2014, but I cannot currently estimate the exact number of species that I have collected as I am currently conducting analysis on identifying species ID through DNA barcoding. However, I anticipate that these data represent at least 30 unique non-picture wing species.

During the two field seasons, I made field observations on the larval food sources. Bark breeder larvae were found by peeling off the bark of decaying endemic *Acadia koa* or *Cheirodendron* trees (Figure 4.2A). The grooves of the decaying bark were often lined with picture wing Drosophila larvae, characterized by their large size and tough cuticle. Picture wing species have also specialized on decaying branches of *Clermontia* trees, especially on Maui island (Figure 4.2B-B'). Sap breeder larvae were found on sap fluxes that appear as black streaks across *Acacia koa* trees (Figure 4.2C). Sap fluxes were prevalent across the forests in Kauai, but were difficult to find on Maui or Hawaii island, potentially due to decline in rainfall in these islands over the past decade. Larvae of leaf breeder species were found in decaying leaf litter in the forest bed, generally two or three layers below the top-most leaves (Figure 4.2D-D'). During the May 2014 collection, Hawaii island was particularly dry, and I observed dried larval cuticles that looked like desiccated Drosophila larvae on leaves (Figure 4.2E). I was not successful in finding larvae of Haleakala species on native fungi, or modified mouthpart species larvae on decaying native fruit, though adult flies of both species groups appeared abundant in the

field sites. I observed *Scaptomyza* adults mating on morning glory flowers on Hawaii island (Figure 4.2F) as well as *Clermontia* flowers on Maui island (Figure 4.2G).

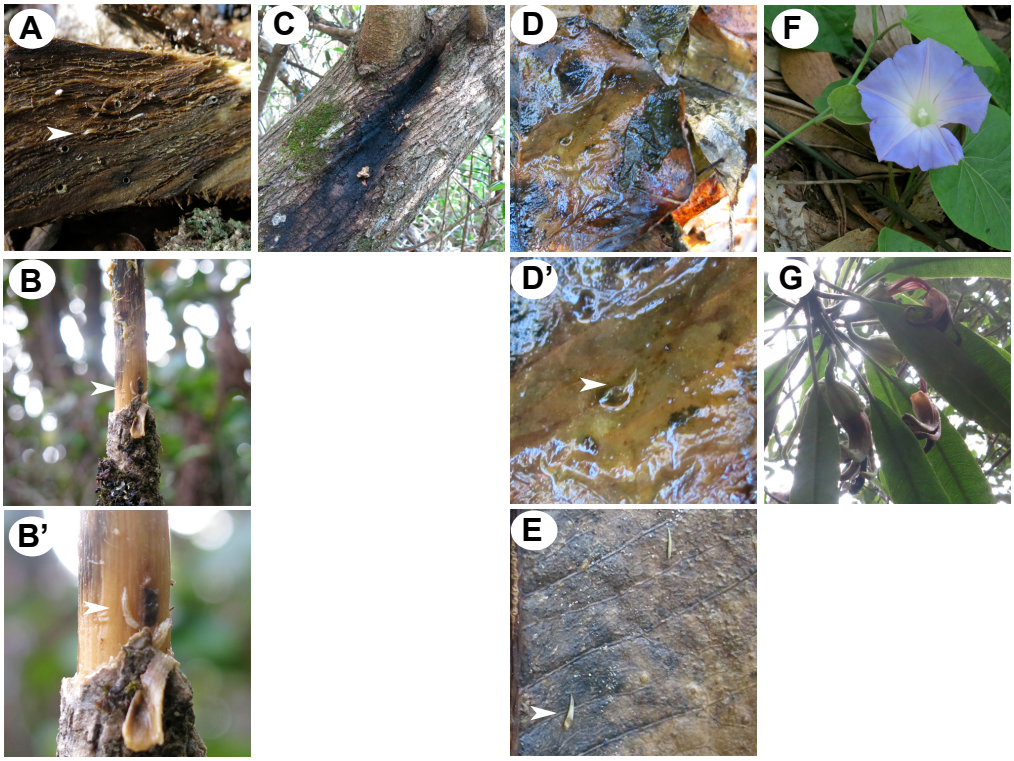

Figure 4.2. Images of egg laying substrates and Drosophila larvae in the field. (A) Decaying *Acacia koa* bark lined with Drosophila larvae (white arrowhead). (B) Decaying *Clermontia arborescens* branches with a Drosophila larva, shown in higher magnification in B'. (C) Black streak of sap flux of *Acacia koa*. (D) Decaying leaves of *Cheirodendron* trees with larva (white arrowhead), shown in higher magnification in D'. (E) Desiccated leaf from a *Cheirodendron* tree during a dry month in Hawaii island with seemingly desiccated Drosophila larvae (white arrowhead). (F) Morning glory flower and (G) *Clermontia arborescens* flowers both used by different *Scaptomyza* species as breeding sites.

DNA barcoding

Hawaiian Drosophila species identification keys are based on the secondary sexual traits of males, and females are often indistinguishable between closely and distantly related species (Magnacca and O'Grady, 2008), which makes studying traits of wild caught females difficult. To overcome this, I tested protocols in conducting DNA barcoding analysis of small amounts of internal tissue collected from dissected females with known species identities (*D. adunca* and *D. mimica*) that were stored in ethanol. BLAST nucleotide alignment sequences of two known species had 99%-100% sequence identity matches to the correct species (Figure 4.3A-B). I am currently expanding this analysis to identify field-collected females at the species level, at least to identify the most closely related known species.

(A) Drosophila adunca voucher 105818 cytochrome c oxidase subunit I (COI) gene, partial cds; mitochondrial

Sequence ID: gb|EU493644.1| **Length:** 1294 **Number of Matches:** 1

Range 1: 1 to 328 GenBank Graphics ▼ Next Match ▲ Previous Match

Score	Expect	Identities	Gaps	Strand
606 bits(328)	7e-170	328/328(100%)	0/328(0%)	Plus/Minus

```
Query  1    TAAAGCTGTAATAACCACTGATCAAACAAATAAAGGTATTCGGTCTAAAGTAATTCCTGA  60
            ||||||||||||||||||||||||||||||||||||||||||||||||||||||||||||
Sbjct  328  TAAAGCTGTAATAACCACTGATCAAACAAATAAAGGTATTCGGTCTAAAGTAATTCCTGA  269

Query  61   TGATCGTATATTAATTACTGTAGTAATAAAATTTACAGCTCCTAAAATTGATGATACTCC  120
            ||||||||||||||||||||||||||||||||||||||||||||||||||||||||||||
Sbjct  268  TGATCGTATATTAATTACTGTAGTAATAAAATTTACAGCTCCTAAAATTGATGATACTCC  209

Query  121  AGCTAAATGAAGAGAGAAAATTGCTAAATCAACTGAAGCACCACCGTGAGCAATTCCAGA  180
            ||||||||||||||||||||||||||||||||||||||||||||||||||||||||||||
Sbjct  208  AGCTAAATGAAGAGAGAAAATTGCTAAATCAACTGAAGCACCACCGTGAGCAATTCCAGA  149

Query  181  AGATAAAGGAGGGTAAACAGTTCAACCTGTACCAGCTCCGTTTTCTACTATTCTACTTAC  240
            ||||||||||||||||||||||||||||||||||||||||||||||||||||||||||||
Sbjct  148  AGATAAAGGAGGGTAAACAGTTCAACCTGTACCAGCTCCGTTTTCTACTATTCTACTTAC  89

Query  241  TAACAAAAGTGTTAAAGCTGGGGGTAATAGTCAAAAACTTATATTATTCATTCGAGGAAA  300
            ||||||||||||||||||||||||||||||||||||||||||||||||||||||||||||
Sbjct  88   TAACAAAAGTGTTAAAGCTGGGGGTAATAGTCAAAAACTTATATTATTCATTCGAGGAAA  29

Query  301  CGCTATATCAGGAGCTCCTAATATTAAA  328
            ||||||||||||||||||||||||||||
Sbjct  28   CGCTATATCAGGAGCTCCTAATATTAAA  1
```

(B) Drosophila mimica voucher 109331 tRNA-Leu gene, partial sequence; cytochrome c oxidase subunit II (COII) gene, ATPase 8 (ATP8) gene, complete cds; and ATPase 6 (ATP6) gene, partial cds; mitochondrial

Sequence ID: gb|EU493793.1| **Length:** 1413 **Number of Matches:** 1

Range 1: 255 to 633 GenBank Graphics ▼ Next Match ▲ Previous Match

Score	Expect	Identities	Gaps	Strand
689 bits(373)	0.0	377/379(99%)	0/379(0%)	Plus/Plus

```
Query  1    ATTATTTTATTATTTATTGCTCTTCCTTCTTTACGTCTTTTATATCTTTTAGATGAAATT  60
            ||||||||||||||||||||||||||||||||||||||||||||||||||||||||||||
Sbjct  255  ATTATTTTATTATTTATTGCTCTTCCTTCTTTACGTCTTTTATATCTTTTAGATGAAATT  314

Query  61   AATGAACCTTCTGTAACTTTAAAGAGAATTGGACACCAATGATATTGAAGTTATGAATAT  120
            ||||||||||||||||||||||||||||||||||||||||||||||||||||||||||||
Sbjct  315  AATGAACCTTCTGTAACTTTAAAGAGAATTGGACACCAATGATATTGAAGTTATGAATAT  374

Query  121  TCAGATTTTAACAATGTAGAATTTGACTCTTATATAATCCCAACAAATGAGTTACCAAAT  180
            ||||||||||||||||||||||||||||||||||||||||||||||||||||||||||||
Sbjct  375  TCAGATTTTAACAATGTAGAATTTGACTCTTATATAATCCCAACAAATGAGTTACCAAAT  434

Query  181  GATGGTTTTCGACTTTTAGACATTGATAACCGAATTATTTTACCTATAAATTCACAAATT  240
            ||||||||||||||||||||| ||||||||||||||||||||||||||||||||||||||
Sbjct  435  GATGGTTTTCGACTTTTAGACGTTGATAACCGAATTATTTTACCTATAAATTCACAAATT  494

Query  241  CGAATTTTATTAACAGCCGCTGATGTAATTCATTCATGAACAATTCCTGCTTTAGGAGTA  300
            ||||||||| ||||||||||||||||||||||||||||||||||||||||||||||||||
Sbjct  495  CGAATTTTAGTAACAGCCGCTGATGTAATTCATTCATGAACAATTCCTGCTTTAGGAGTA  554

Query  301  AAAGTAGATGGTACTCCTGGGCGATTAAATCAAACTAAtttttttATTAACCGACCAGGA  360
            ||||||||||||||||||||||||||||||||||||||||||||||||||||||||||||
Sbjct  555  AAAGTAGATGGTACTCCTGGGCGATTAAATCAAACTAATTTTTTTATTAACCGACCAGGA  614

Query  361  TTATTTTACGGACAATGTT  379
            |||||||||||||||||||
Sbjct  615  TTATTTTACGGACAATGTT  633
```

Figure 4.3 Examples of BLASTn hits of mitochondrial DNA sequences from field specimens. (A) COI sequence from *D. adunca* and (B) COII sequence from *D. mimica* matching the NCBI deposited sequence 100 and 99% respectively.

Common garden experiment

To test the degree to which differences in ovariole number between species that occupy different larval niches is influenced by heritable genetic factors or environmental plasticity, I conducted a common garden experiment by measuring ovariole number in wild-caught females, which had developed in their natural habitats, and their F1 offspring, which were reared in standard laboratory conditions for Hawaiian Drosophila (Figure 4.4A). I observed no significant differences between the ovariole numbers of wild caught females and those of F1 lab-reared females in *D. mimica* (fruit breeder, modified mouthpart; p=0.49), *D. picticornis* (sap breeder, picture wing; p=0.28), *D. silvestris* (bark breeder, picture wing), *Scaptomyza sp.* and AMC *sp.* The latter two species are currently unidentified, as I did not obtain any males from the progeny; I will be conducting DNA barcoding analysis for species identification. The sample size for *D. silvestris, Scaptomyza sp*, and AMC *sp* was one or two individuals per condition, and I could not conduct statistical tests to identify differences. However, the ovariole number from wild females and F1s are very similar (Figure 4.4A). This suggests that ovariole number differences between Hawaiian Drosophila species is likely to be largely genetically determined, and not a result of plastic response to different food sources.

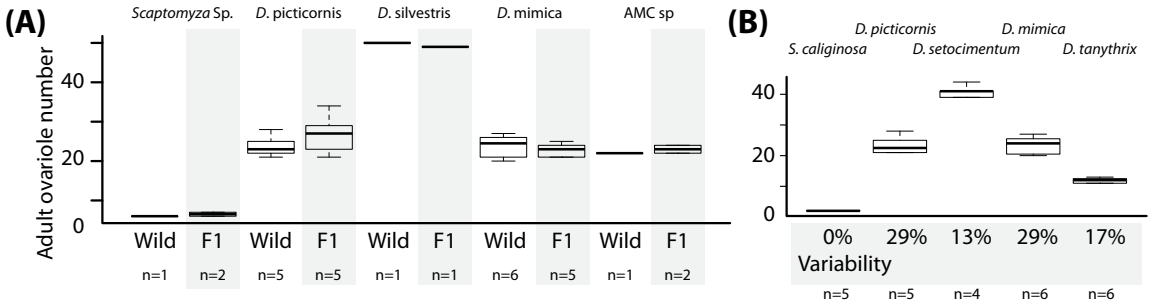

Figure 4.4. Ovariole number variation in Hawaiian Drosophila. (A) Box plot of ovariole number for common garden experiment comparing wild caught females to their F1 offspring reared in the same laboratory condition for each species. Ovariole number is not significantly different between wild females and F1 females for *D. picticornis* and *D. mimica*. (B) Box plot of ovariole number for wild caught females from five species representing flower breeder *Scaptomyza* (*S. caliginosa*), sap flux breeder picture wing (*D. picticornis*), bark breeder picture wing (*D. setocimentum*), fruit feeder modified mouthpart (*D. mimica*), and leaf breeder AMC (*D. tanythrix*) species. Number of specimens for each data point is represented underneath each column.

Allometric ratio of ovariole number to body size varies in Hawaiian Drosophila

The range in thorax length for the Hawaiian Drosophila specimens I collected was between 0.79 mm to 3.21 mm. Most specimens' body size clustered between 1.5 mm to 2 mm (Figure 4.5). Ovariole number ranged from two to 96. The lowest ovariole number and smallest body size belonged to *S. caliginosa*, and the highest ovariole number and body size were those of *D. melanocephala*, consistent with the report of Kambysellis and Heed (1971). Interestingly, there are clear outliers from the general trend (Figure 4.5, highlighted in pink).

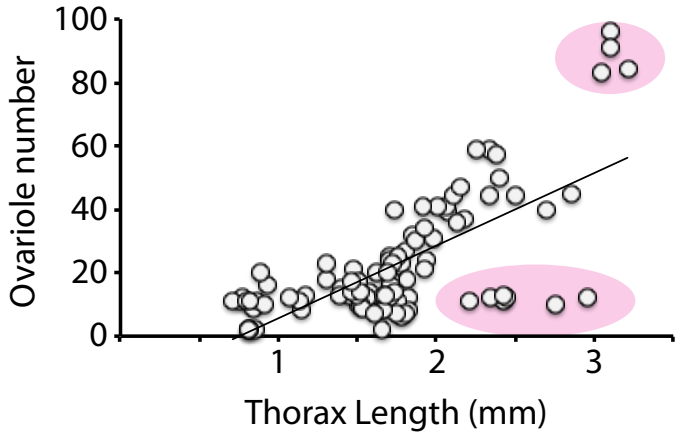

Figure 4.5. Plot of thorax length (mm) and ovariole number of Hawaiian Drosophila. Highlighted in pink are strong outliers from the allometric trend.

Changes in TFC number and TFC sorting

I next analyzed the developmental parameters that I identified in Chapter 2 as influencing ovariole number, in Hawaiian Drosophila. Total TFC number varied between 15 (*S. caliginosa*) to 217 cells (*D. villocipedis*) (Figure 4.6A), and showed a linear relationship to TF number (R^2= 0.97, Figure 4.7A). Average TFC number per TF ranged from 7.5 to 11.5 (Figure 4.6B). While it was common to observe TFC number per TF ranges of 6 to 8 in *melanogaster* subgroup species (Sarikaya et al., 2011), Hawaiian Drosophila appear to have a wider range of TFC number per TF. There was no linear correlation between TFC number per TF and TF number (R^2=0.16, Figure 4.7B). TF number per ovary was similar to adult ovariole number per ovary in all species except in *S. caliginosa* (Table 4.1). *S.caliginosa* adult ovariole number was consistently two per female, yet TF number was two per ovary (Table 4.1), which would be expected to give rise to adults with four ovarioles.

	Sp group	TF number	n	Ovariole number (per ovary)	n	TF:ON Ratio
S. caliginosa	Scaptomyza	2	2	1	4	2.00
D. picticornis	Picture wing	13	2	13.3	10	0.98
D. grimshawi	Picture wing	19.5	4	20.5	12	0.95
D. hawaiiensis	Picture wing	17.6	3	17.58	13	1.00
D. setocimentum	Picture wing	19	2	20.6	8	0.92
D. villocipedis	Picture wing	22	2	18.5	8	1.19
D. mimica	Mod mouthpart	11	2	11	5	1.00
D. tanythrix	AMC	5.75	4	6	12	0.96

Table 4.1. Comparison of TF number per ovary to ovariole number per ovary. Relationship of TF number and ovariole number indicated by dividing TF number by ovariole number. All species except for *S. caliginosa* show close to 1:1 correlation.

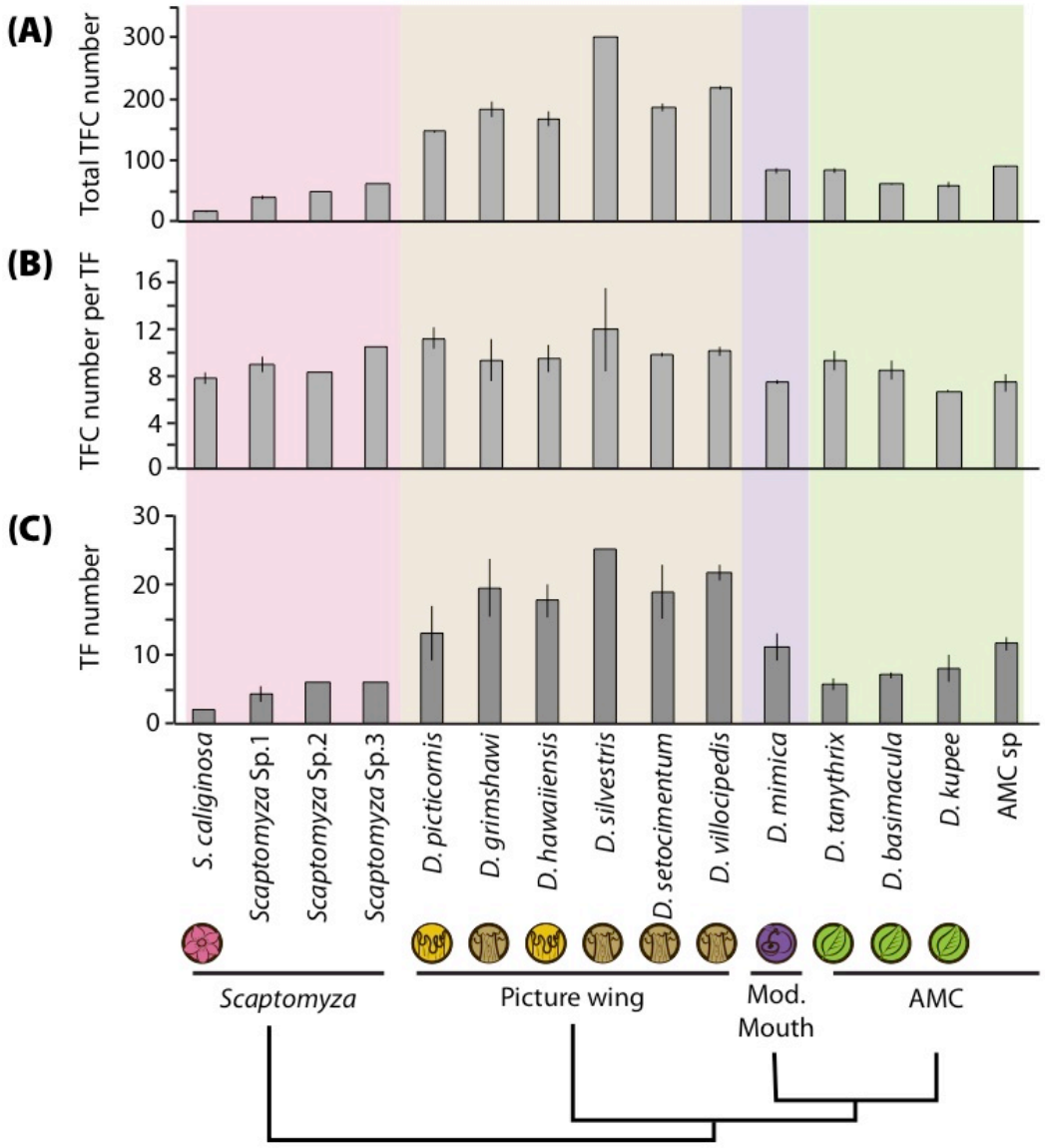

Figure 4.6. Developmental mechanisms underlying ovariole number changes in Hawaiian Drosophila. Total mean TFC number (A), TFC number per TF (B) and TF number (C) differences between 15 Hawaiian Drosophila species representing four species groups. Icons under the species name indicate the egg laying substrate. Unidentified species are labeled as "sp". Error bar indicates standard error. Sample number is as follows: n=1 for *Scaptomyza Sp2* and *Sp3*; n=2 for *S. caliginosa, D. silvestris, D. mimica, D. kupee*, and *AMC sp*; N=3 for *D. hawaiiensis* and *D. setocimentum*; N=4 for *Scaptomyza Sp1* and *D. tanythrix*; N=6 for *D. villocipedis* and *D. basimacula*; n=8 for *D. picticornis* and *D. grimshawi*.

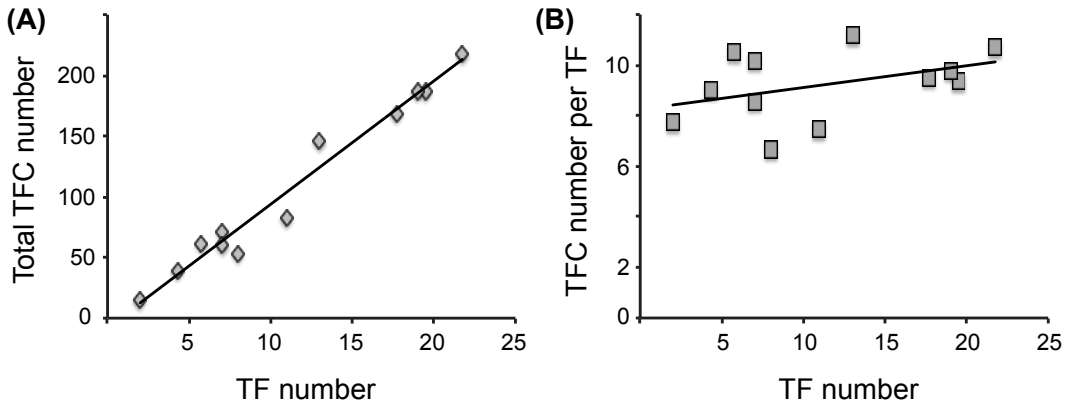

Figure 4.7. Correlation of total TFC number and TFC number per TF with TF number. (A) Graph plotting relationship of TF number and total TFC number in 12 species. R^2=0.96. (B) Graph plotting the relationship between TF number and TFC number per TF. R^2=0.16. Average values for total TFC number, TFC number per TF and TF number are plotted.

4.5 Discussion

The preliminary data obtained in this study provide support for ovariole number as a genetically determined trait in Hawaiian Drosophila. In the five species where I was able to obtain F1 progeny in the laboratory, there were no significant changes in ovariole number compared to wild-caught mothers. In addition, larval TF number from late larval stage ovaries showed similarity to adult ovariole number. The only exception was with the morning glory flower breeder *S. caliginosa*, which had two TFs per ovary (n=2), which is higher than the expected value based on the mean adult ovariole number (two per female). I did not obtain F1 adult females from *S. caliginosa* in the lab, therefore it is not clear whether these individuals would have developed four ovarioles per female, or whether ovarioles are destroyed during pupal development. Terminating development of ovarioles during pupal development is observed in honey bees (Capella and Hartfelder, 1998; Reginato and Da Cruz-Landim, 2002), but has not been reported in *Drosophila*. Alternatively, it may be that the morning glory flowers that *S. caliginosa* feed on as larvae represent one food source that is low in nutritional value, resulting in lower ovariole number than those reared in the lab. However, both wild-caught and lab-reared adult ovariole number from all other species representing leaf, sap, fruit, and bark breeders did not show any significant difference in TF number of lab-reared larvae compared to ovariole number, suggesting that difference in species-specific ovariole number is not due to nutritional plasticity. This is an interesting contrast to *D. melanogaster*, where wild populations can have lower ovariole number and body size than those reared in the laboratory, which suggests that these flies were starved during development in their natural environment (Bouletreau-Merle et al., 1982).

There also appears to be a positive correlation between ovariole number and body size among Hawaiian *Drosophila* species, with some outliers. The current analysis combines data from all species groups. Different species groups of Hawaiian *Drosophila* have notable trends in body size. Picture wing and Antopocerus flies are often 1.5-2.5x larger than modified mouthpart/ Haleakala/ ciliated or modified tarsus species, and 3-4x larger than *Scaptomyza* species. Once I begin the DNA barcoding analysis of the field caught females and obtain a species identity, I will separate the data for each species-group, and test whether there are specific allometric relationships between ovariole number and body size depending on the species group. I predict that while allometry may be important in determining ovariole number within a species group with similar ecological niche, there will be differences in the body size to ovariole relationship between groups of species that lay eggs on different substrate.

The developmental parameters involved in ovariole number diversity in Hawaiian Drosophila appear to be large shifts in TFC number and to some extent, changes in TFC sorting. The largest variation was observed in TFC number, and TFC number shows a close to linear correlation with TF number (Figure 4.7A). TFC number per TF values were much higher than previously observed in *melanogaster* subgroup species, with the highest species averaging around 11.5 cells per TF. It appears that Hawaiian Drosophila use similar developmental mechanisms to *melanogaster* subgroup species to establish ovariole number, but that they alter these mechanism to a larger extent than do *melanogaster* subgroup species, giving rise to the extreme ovariole numbers observed among the Hawaiian species.

Given the different combinations of changes in cell number and sorting, it may be the case that ovariole number variation is also a polygenic trait in Hawaiian *Drosophila* as it is in the *melanogaster* subgroup species. Hawaiian Drosophila nonetheless provide a novel model to investigate the genetics of ovariole number evolution. In particular, focusing on two closely related species with divergent ovariole number and different egg laying substrate can test for genetics of ovariole number evolution and niche-choice. It would be interesting to test whether the genes that regulate ovariole number and ecological niche are linked in Hawaiian Drosophila.

4.6 Acknowledgements

Field collections of Hawaiian Drosophila were assisted by Durrell Kapan, Donald Price, Karl Magnacca, Steve Montgomery, Inanna Carter, and Eva Brill. Laboratory populations of Drosophilids from the laboratories of Ken Kaneshiro and Donald Price were used for analysis. Funding for the fieldwork was supported by NSF Doctoral Dissertation Improvement Grant (DEB-1209570).

4.7 References

Bouletreau-Merle, J., Allemand, R., Cohet, Y., and David, J.R. (1982). Reproductive strategy in Drosophila melanogaster: Significance of a genetic divergence between temperate and tropical populations. Oecologia *53*, 323–329.

Capella, I.C.S., and Hartfelder, K. (1998). Juvenile hormone effect on DNA synthesis and apoptosis in caste-specific differentiation of the larval honey bee (Apis mellifera L.) ovary. J. Insect Physiol. *44*, 385–391.

Edwards, K.A., Doescher, L.T., Kaneshiro, K.Y., and Yamamoto, D. (2007). A database of wing diversity in the Hawaiian Drosophila. PLoS One *2*, e487.

Green, D.A., and Extavour, C.G. (2012). Convergent evolution of a reproductive trait through distinct developmental mechanisms in Drosophila. Dev. Biol. *372*, 120–130.

Kambysellis, M.P., and Heed, W.B. (1971). JSTOR: The American Naturalist, Vol. 105, No. 941 (Jan. - Feb., 1971), pp. 31-49. Am. Nat.

Kambysellis, M.P., Ho, K.F., Craddock, E.M., Piano, F., Parisi, M., and Cohen, J. (1995). Pattern of ecological shifts in the diversification of Hawaiian Drosophila inferred from a molecular phylogeny. Curr Biol *5*, 1129–1139.

Magnacca, K.N., and O'Grady, P.M. (2006). A Subgroup Structure for the Modified Mouthparts Species Group of Hawaiian Drosophila. Proc. Hawaiian Entomol. Soc. *38*, 87–101.

Magnacca, K.N., and O'Grady, P.M. (2008). Revision of the "nudidrosophila" and "ateledrosophila" species groups of Hawaiian Drosophila (Diptera: Drosophilidae), with descriptions of twenty-two new species. Syst. Entomol. *33*, 395–428.

Magnacca, K.N., Foote, D., and O'Grady, P.M. (2008). A review of the endemic Hawaiian Drosophilidae and their host plants. Zootaxa *1728*, 1–58.

Miles, C.M., Lott, S.E., Luengo Hendriks, C.L., Ludwig, M.Z., Manu, Williams, C.L., and Kreitman, M. (2011). Artificial selection on egg size perturbs early pattern formation in Drosophila melanogaster. Evolution (N. Y). *65*, 33–42.

O'Grady, P., and Desalle, R. (2008). Out of Hawaii: the origin and biogeography of the genus Scaptomyza (Diptera: Drosophilidae). Biol. Lett. *4*, 195–199.

O'Grady, P.M., Lapoint, R.T., Bonacum, J., Lasola, J., Owen, E., Wu, Y., and Desalle, R. (2011). Phylogenetic and ecological relationships of the Hawaiian Drosophila inferred by mitochondrial DNA analysis. Mol. Phylogenet. Evol. *58*, 244–256.

Reginato, R.D., and Da Cruz-Landim, C. (2002). Morphological characterization of cell death during the ovary differentiation in worker honey bee. Cell Biol. Int. *26*, 243–251.

Sarikaya, D.P., Belay, A.A., Ahuja, A., Dorta, A., Green, D.A., and Extavour, C.G. (2011). The roles of cell size and cell number in determining ovariole number in Drosophila. Dev. Biol.

Chapter IV:

Discussion

In this thesis, I provided evidence for two different developmental mechanisms affecting ovariole number evolution in African and Hawaiian Drosophila. I also showed that the Hippo pathway regulates cell number in the larval ovary, both autonomously and non-autonomously. The non-autonomous coordination of proliferation between the germ cells and the somatic cells that surround them resulted in proportional growth that required activity of two other growth regulatory pathways. Lastly, I described my ongoing efforts to understand the effect of ecological niche shifts in ovariole number in Hawaiian Drosophila. In this chapter, I will discuss the broader significance of my findings, and future directions that may prove fruitful in advancing our knowledge further.

Genes underlying evolutionary change

Quantitative trait loci (QTL) studies aimed at identifying genes regulating ovariole number within *D. melanogaster* and between two closely related species both suggested that ovariole number difference is regulated by multiple genes (Orgogozo et al., 2006; Telonis-Scott et al., 2005; Wayne and McIntyre, 2002). In this thesis, I demonstrated that ovariole number differences within and between species occur primarily through changes in the number and morphogenesis of one cell type within the larval ovary, terminal filament cells (TFCs). Changes in total TFC number or TFC number per TF were both implicated in plasticity response and species-specific differences in ovariole number. Another graduate student in the laboratory has demonstrated that changes in total TFC number can arise from differences in the number of somatic cells that give rise to the larval ovary or through differences in the number of

anterior cells that are separated to give rise to TFCs and swarm cells (Green and Extavour, 2012). This suggests that not only are there two major changes to TFCs (total number or sorting) that can influence ovariole number, but also that there may be different developmental routes by which similar results can be achieved during development. In Hawaiian Drosophila with very diverse range in ovariole number, I also observed a wide range of total TFC number and TFC sorting. Total TFC number had a linear correlation with TF number, suggesting that it is the primary mechanism that underlies changes in ovariole number in Hawaiian Drosophila. However, there was also a wide range of TFC sorting differences, which could result in more subtle changes between species. It appeared that both mechanisms were being coopted to alter ovariole number.

Similar to the ovary, the sex combs of *Drosophila* also show diverse developmental modes underlying convergent morphologies (Atallah et al., 2009a, 2009b; Tanaka et al., 2009). While some traits show repeated evolution on the same gene which results in very similar changes in development (Jones et al., 2012; Prud'homme et al., 2006), traits like ovariole number and sex combs in Drosophilids may represent a different type of morphological evolution, which display more 'flexibility' during morphogenesis. It would be interesting to test whether repeated selection of the same genes or different set of genes occur different lineages for ovariole number changes.

Of particular interest may be the *bric-à-brac* (*bab*) genes, *bab1* and *bab2*. The *bab* genes are involved in TF morphogenesis and swarm cell migration, and mild loss of function mutants have increased TFC number per TF stack (Bartoletti et al., 2012; Godt and Laski, 1995; Green and Extavour, 2012). In addition, *bab* interacts with a gene that

controls the proliferation of TFCs, *pipsqueak* (Bartoletti et al., 2012). Investigating the evolution of the *bab* locus or *bab1/2* interacting partners in the ovary may also provide new candidate genes for ovariole number evolution. *bab* is regulated by Hox genes in both abdomen and legs of *D. melanogaster* (Baanannou et al., 2013; Williams et al., 2008). If the genetic architecture of *bab* regulation is conserved, Hox genes may also play a role in patterning and evolution of the ovary. *Abdominal-B* determines the identity of the embryonic parasegment 11-12 where the embryonic gonad is located, and may be the interacting partner in the ovary (Scott and O'Farrell, 1986). It should be noted that *abdominal-A* can also be expressed in parasegment 11, and may be involved as well.

Plastic response to the environment is considered by some researchers to provide a source of variation for phenotypic evolution (Moczek et al., 2011). It is interesting to note that the developmental processes contributing to ovariole number that responded to temperature and starvation were not the same (change in TFC sorting versus change in total TFC number) in *D. melanogaster*, and represent two developmental mechanisms that also influence species-specific ovariole number differences. Plastic changes in ovariole number in response to starvation have been well investigated in *D. melanogaster* but remain poorly investigated in other species. Temperature ranges experienced by each species in their native habitat vary dramatically depending on the species. For example, species like *D. melanogaster* and *D. kikkawai* live in habitats with a wide range of temperatures, while other species such as *D. immigrans* live in habitats with less diverse temperature ranges (Parkash et al., 1998; Parsons, 1978). Is ovariole number influenced by rearing temperature in species that do not experience a wide range of temperatures in their natural habitat? Or does plasticity response in ovariole number to temperature

evolve as a response to experiencing diverse temperature ranges? Studying closely related species that experience different ranges of temperatures in the wild may answer these questions.

Other factors that influence fecundity

Though ovariole number positively correlates with the number of eggs laid by a female, egg production rate has also been implicated in difference in fecundity between different species (R' kha et al., 1997). Given that Drosophila oocytes originate from asymmetric division of the germ line stem cells (GSCs), change in fecundity could also be achieved by altering the number of GSCs per ovariole, or GSC division rate. There are 2-3 GSCs per ovariole in *D. melanogaster*, and the GSC division rate is influenced by age and feeding status of the female (Drummond-Barbosa and Spradling, 2004; Hsu and Drummond-Barbosa, 2009; LaFever and Drummond-Barbosa, 2005). R'kha and colleagues (1997) report noticeable individual variation between egg production rate in the three species used in their analysis (*D. simulans, D. mauritiana* and *D. sechellia*). In addition to asynchronous production of eggs in ovaries of species like most *D. melanogaster* strains, some *Drosophila* species produce oocytes synchronously and lay clutches of many eggs at once (Kambysellis and Heed, 1971; Ruiz-Dubreuil et al., 1994; Del Solar, 1968; Takamura and Fuyama, 1980). Aggregate egg laying can be selected for in laboratory conditions using *D. melanogaster*, suggesting that the trait is regulated through heritable genetic differences (Ruiz-Dubreuil et al., 1994). A comparative study of GSCs and supporting niche cells that take into consideration GSC number, division rate,

and synchronicity may provide new insights into how GSC division and oocyte production rates influence fecundity.

Differences in fecundity between species may also be influenced by differences in physiological changes, which could be induced by aging or feeding, and egg-laying behavior traits. Physiological differences may be of particular interest for species that occupy niches that are toxic to other Drosophila species, such as *D. sechellia* or *D. pachea* (Lang et al., 2012; R'Kha et al., 1991). Lower Insulin signaling levels in *D. sechellia* results in different nutritional response during development compared to *D. melanogaster* (Green and Extavour, 2014). Whether the reduced Insulin signaling levels further have an effect during adult life on egg laying patterns in different nutritional environments is not known.

Food source and ovariole number

The correlation of egg laying substrate and ovariole number appears most striking in Hawaiian Drosophila. Given the above-discussed issues of changes in physiology or egg laying behavior, it would be of most interest to identify pairs of species that have differences in ovariole number and ecology. Morphological mimicry of *Heliconius* butterflies to toxic species is regulated by one gene, *doublesex*, called a "supergene" by some authors because it affects multiple phenotypes (Kunte et al., 2014). Evolving to lay eggs on difference larval food sources in Hawaiian Drosophila may also be regulated by one or two loci of strong effect that alter multiple phenotypes at once. Alternatively, there may be multiple loci of small effect that additively determine egg laying substrate and ovariole number.

Considering relative growth of cell types in the ovary

In Chapter I of this thesis, I introduced the work of Huxley and his description of two levels of growth control: the overall size of the animal and the relative size of its parts (Huxley, 1932). I believe the findings in this thesis can be considered in a similar light. I identified developmental mechanisms that can alter the functional size of the ovary (Chapter II), as well as mechanisms that maintain proportionality of different cell types within the ovary (Chapter III). Ovariole number was determined primarily by changes in the number of TFCs. These findings present an interesting paradigm in our understanding of organ size regulation as it appears that the morphogenesis and proliferation of TFCs is independent of the other cell types of the ovary, including germ cells and interstitial cells. Evolution could then in principle act on the proliferation and morphogenesis of TFCs specifically to change the functional size of the organ. The developmental mechanisms that alter ovariole number influence both of the developmental processes that Huxley considered could underlie change in size, namely differentiation and proliferation. Even in the case where the primary difference in ovariole number resulted through changes in total TFC number, there were distinct mechanisms that resulted in difference of TFC number (Green and Extavour, 2012). There may be many different 'routes' that can be taken by evolution to alter TFC number, hence ovariole number.

In Chapter III, I identified changes in relative growth of cell types to one another. Similar to Huxley's deer antlers, which receive hormonal signals from the body to regulate the size of the antlers (Elliott et al., 1992, 1993; Price et al., 1994), germ cells

(GCs) and interstitial cells (ICs) exchange cues to control each others' proliferation and differentiation. Given that hormonal cues are often implicated in such coordination of growth (Emlen et al., 2012; Gancz and Gilboa, 2013; Gancz et al., 2011; Green and Extavour, 2014), it is interesting that the proportional growth of the GCs and ICs are controlled by the Hippo pathway, a genetic pathway that is usually considered to be tissue-intrinsic. I observed an approximately 3:1 ratio of ICs to GCs in the ovary both in the wild type and when Hippo pathway activity was reduced, suggesting that there are cues secreted by the ICs to promote the proliferation of GCs while maintaining a certain proportionality of ICs to GCs. The cues that are secreted by ICs in response to Hippo activity may involve EGFR or JAK/STAT pathway members, as the IC-GC proportionality was no longer maintained in cases when activity of both the Hippo pathway and one of the EGFR or JAK/STAT pathways were altered. More broadly, how or whether cells coordinate their proliferation through creating micro-environments with secreted or physical factors remains an area that needs more study. Another route of investigation may be to study the IC-GC proportions in various *Drosophila* species to identify regulators of IC-GC proportionality, and to determine whether changes in IC-GC proportion have an effect on the number of GSCs that are established during late larval development. We may uncover novel variants of growth pathway genes that modify activity levels to result in different proportions.

Summary

In summary, I have made a modest attempt at understanding how organs change in size during evolution through studying the evolution and development of the

Drosophila larval ovary. I believe the ovary serves as an interesting model for investigating questions in organ size evolution. The developmental mechanisms underlying ovariole number evolution are likely to shed light on the evolution of organs that may take multiple developmental routes to achieve similar morphological outcomes. Another strength of the model is that the trait is easily quantified, which is not trivial for size-related characteristics. Future investigations focusing on the uncovering the developmental modes of change across different closely related species groups, and the genetics underlying ovariole number change will likely be fruitful in furthering our knowledge on how organ size is established and altered during evolution.

4.2 References

Atallah, J., Liu, N.H., Dennis, P., Hon, A., Godt, D., and Larsen, E.W. (2009a). Cell dynamics and developmental bias in the ontogeny of a complex sexually dimorphic trait in Drosophila melanogaster. Evol. Dev. *11*, 191–204.

Atallah, J., Liu, N.H., Dennis, P., Hon, A., and Larsen, E.W. (2009b). Developmental constraints and convergent evolution in Drosophila sex comb formation. Evol. Dev. *11*, 205–218.

Baanannou, A., Mojica-Vazquez, L.H., Darras, G., Couderc, J.L., Cribbs, D.L., Boube, M., and Bourbon, H.M. (2013). Drosophila Distal-less and Rotund Bind a Single Enhancer Ensuring Reliable and Robust bric-a-brac2 Expression in Distinct Limb Morphogenetic Fields. PLoS Genet. *9*.

Bartoletti, M., Rubin, T., Chalvet, F., Netter, S., Dos Santos, N., Poisot, E., Paces-Fessy, M., Cumenal, D., Peronnet, F., Pret, A.-M., et al. (2012). Genetic basis for developmental homeostasis of germline stem cell niche number: a network of Tramtrack-Group nuclear BTB factors. PLoS One *7*, e49958.

Drummond-Barbosa, D., and Spradling, A.C. (2004). α-Endosulfine, a potential regulator of insulin secretion, is required for adult tissue growth control in Drosophila. Dev. Biol. *266*, 310–321.

Elliott, J.L., Oldham, J.M., Ambler, G.R., Bass, J.J., Spencer, G.S.G., Hodgkinson, S.C., Breier, B.H., Gluckman, P.D., and Suttie, J.M. (1992). Presence of insulin-like growth factor-I receptors and absence of growth hormone receptors in the antler tip. Endocrinology *130*, 2513–2520.

Elliott, J.L., Oldham, J.M., Ambler, G.R., Molan, P.C., Spencer, G.S.G., Hodgkinson, S.C., Breier, B.H., Gluckman, P.D., Suttie, J.M., and Bass, J.J. (1993). Receptors for insulin-like growth factor-II in the growing tip of the deer antler. J. Endocrinol. *138*, 233–241.

Emlen, D.J., Warren, I.A., Johns, A., Dworkin, I., and Lavine, L.C. (2012). A mechanism of extreme growth and reliable signaling in sexually selected ornaments and weapons. Science (80-.). *337*, 860–864.

Gancz, D., and Gilboa, L. (2013). Insulin and Target of rapamycin signaling orchestrate the development of ovarian niche-stem cell units in Drosophila. Development *140*, 4145–4154.

Gancz, D., Lengil, T., and Gilboa, L. (2011). Coordinated regulation of niche and stem cell precursors by hormonal signaling. PLoS Biol. *9*, e1001202.

Godt, D., and Laski, F.A. (1995). Mechanisms of cell rearrangement and cell recruitment in Drosophila ovary morphogenesis and the requirement of bric à brac. Development *121*, 173–187.

Green, D.A., and Extavour, C.G. (2012). Convergent evolution of a reproductive trait through distinct developmental mechanisms in Drosophila. Dev. Biol. *372*, 120–130.

Green, D.A., and Extavour, C.G. (2014). Insulin signalling underlies both plasticity and divergence of a reproductive trait in Drosophila. Proc. Biol. Sci. / R. Soc. *281*, 20132673.

Hsu, H.-J., and Drummond-Barbosa, D. (2009). Insulin levels control female germline stem cell maintenance via the niche in Drosophila. Proc. Natl. Acad. Sci. U. S. A. *106*, 1117–1121.

Huxley, J.S. (1932). Problems of Relative Growth (Dover Publications).

Jones, F.C., Grabherr, M.G., Chan, Y.F., Russell, P., Mauceli, E., Johnson, J., Swofford, R., Pirun, M., Zody, M.C., White, S., et al. (2012). The genomic basis of adaptive evolution in threespine sticklebacks. Nature *484*, 55–61.

Kambysellis, M.P., and Heed, W.B. (1971). Studies of oogenesis in natural populations of Drosophilidae. I. Relation of Ovarian development and ecological habitats of the Hawaiian species. Am. Soc. Nat. *105*, 31–49.

Kunte, K., Zhang, W., Tenger-Trolander, A., Palmer, D.H., Martin, A., Reed, R.D., Mullen, S.P., and Kronforst, M.R. (2014). doublesex is a mimicry supergene. Nature *507*, 229–232.

LaFever, L., and Drummond-Barbosa, D. (2005). Direct control of germline stem cell division and cyst growth by neural insulin in Drosophila. Science (80-.). *309*, 1071–1073.

Lang, M., Murat, S., Clark, A.G., Gouppil, G., Blais, C., Matzkin, L.M., Guittard, E., Yoshiyama-Yanagawa, T., Kataoka, H., Niwa, R., et al. (2012). Mutations in the neverland Gene Turned Drosophila pachea into an Obligate Specialist Species. Science (80-.). *337*, 1658–1661.

Moczek, A.P., Sultan, S., Foster, S., Ledón-Rettig, C., Dworkin, I., Nijhout, H.F., Abouheif, E., and Pfennig, D.W. (2011). The role of developmental plasticity in evolutionary innovation. Proc. Biol. Sci. *278*, 2705–2713.

Orgogozo, V., Broman, K.W., and Stern, D.L. (2006). High-resolution quantitative trait locus mapping reveals sign epistasis controlling ovariole number between two Drosophila species. Genetics *173*, 197–205.

Parkash, R., Karan, D., and Munjal, A.K. (1998). Geographical divergence for quantitative traits in colonising populations of Drosophila kikkawai from India. Hereditas *128*, 201–205.

Parsons, P.A. (1978). Habitat selection and evolutionary strategies in Drosophila: an invited address. Behav. Genet. *8*, 511–526.

Price, J.S., Oyajobi, B.O., Oreffo, R.O.C., and Russell, R.G.G. (1994). Cells cultured from the growing tip of red deer antler express alkaline phosphatase and proliferate in response to insulin-like growth factor-I. J. Endocrinol. *143*.

Prud'homme, B., Gompel, N., Rokas, A., Kassner, V.A., Williams, T.M., Yeh, S.-D., True, J.R., and Carroll, S.B. (2006). Repeated morphological evolution through cis-regulatory changes in a pleiotropic gene. Nature *440*, 1050–1053.

R' kha, S., Moreteau, B., Coyne, J.A., and David, J.R. (1997). Evolution of a lesser fitness trait: egg production in the specialist Drosophila sechellia. Genet Res *69*, 17–23.

R'Kha, S., Capy, P., and David, J.R. (1991). Host-plant specialization in the Drosophila melanogaster species complex: a physiological, behavioral, and genetical analysis. Proc Natl Acad Sci USA *88*, 1835–1839.

Ruiz-Dubreuil, G., Burnet, B., and Connolly, K. (1994). Behavioural correlates of selection for oviposition by Drosophila melanogaster females in a patchy environment. Heredity (Edinb). *73 (Pt 1)*, 103–110.

Scott, M.P., and O'Farrell, P.H. (1986). Spatial programming of gene expression in early Drosophila embryogenesis. Annu. Rev. Cell Biol. *2*, 49–80.

Del Solar, E. (1968). Selection for and against gregariousness in the choice of oviposition sites by Drosophila pseudoobscura. Genetics *58*, 275–282.

Takamura, T., and Fuyama, Y. (1980). Behavior genetics of choice of oviposition sites in Drosophila melanogaster. I. Genetic variability and analysis of behavior. Behav. Genet. *10*, 105–120.

Tanaka, K., Barmina, O., and Kopp, A. (2009). Distinct developmental mechanisms underlie the evolutionary diversification of Drosophila sex combs. Proc. Natl. Acad. Sci. U. S. A. *106*, 4764–4769.

Telonis-Scott, M., McIntyre, L.M., and Wayne, M.L. (2005). Genetic architecture of two fitness-related traits in Drosophila melanogaster: ovariole number and thorax length. Genetica *125*, 211–222.

Wayne, M.L., and McIntyre, L.M. (2002). Combining mapping and arraying: An approach to candidate gene identification. Proc Natl Acad Sci USA *99*, 14903–14906.

Williams, T.M., Selegue, J.E., Werner, T., Gompel, N., Kopp, A., and Carroll, S.B. (2008). The regulation and evolution of a genetic switch controlling sexually dimorphic traits in Drosophila. Cell *134*, 610–623.

Appendix A:

Supporting figures for Chapter II

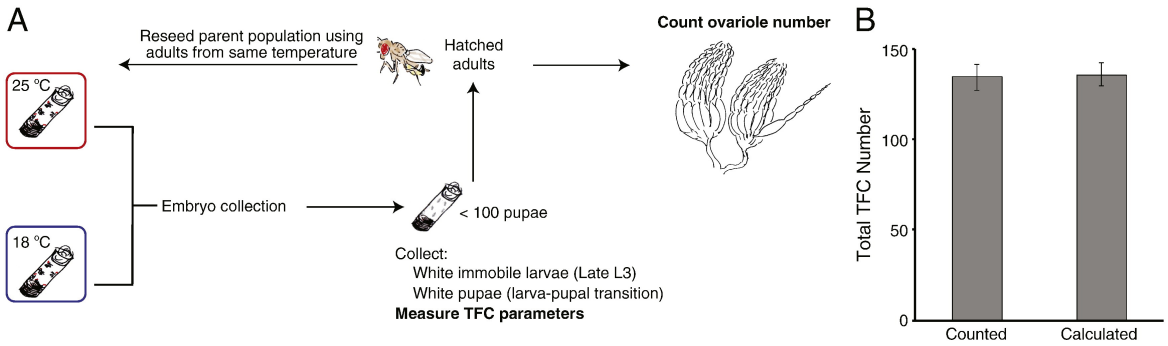

Figure A.1 Experimental design. (A) For temperature controlled experiments, flies were reared at 25 °C or 18 °C at 60% humidity on standard fly media for at least two generations before experiments were conducted. Adults were permitted to lay eggs in vials for two to six hours and then removed from the vial to prevent overcrowding of larvae. Only tubes containing fewer than 100 pupae were used for analysis of larval–pupal ovaries, and for counts of ovariole number in adults. Adults hatched from these tubes were used to create new parent cultures at the same temperature. (B) Comparison of the mean of calculated and manual counts of total TFC number per ovary. To test whether calculated TFC numbers would accurately represent the total TFC number, calculated TFC numbers were obtained by randomly choosing five ovaries where all TFC per TF were counted, and multiplying the average TFC number per TF (obtained from the randomized five data points) by the total number of TFs in the ovary. This was compared to manual counts of total TFC numbers of the same ovaries. Differences between counted and calculated total cell numbers did not exceed ± 4 and were not significantly different ($p = 0.79$). Error bars indicate 95% confidence interval.

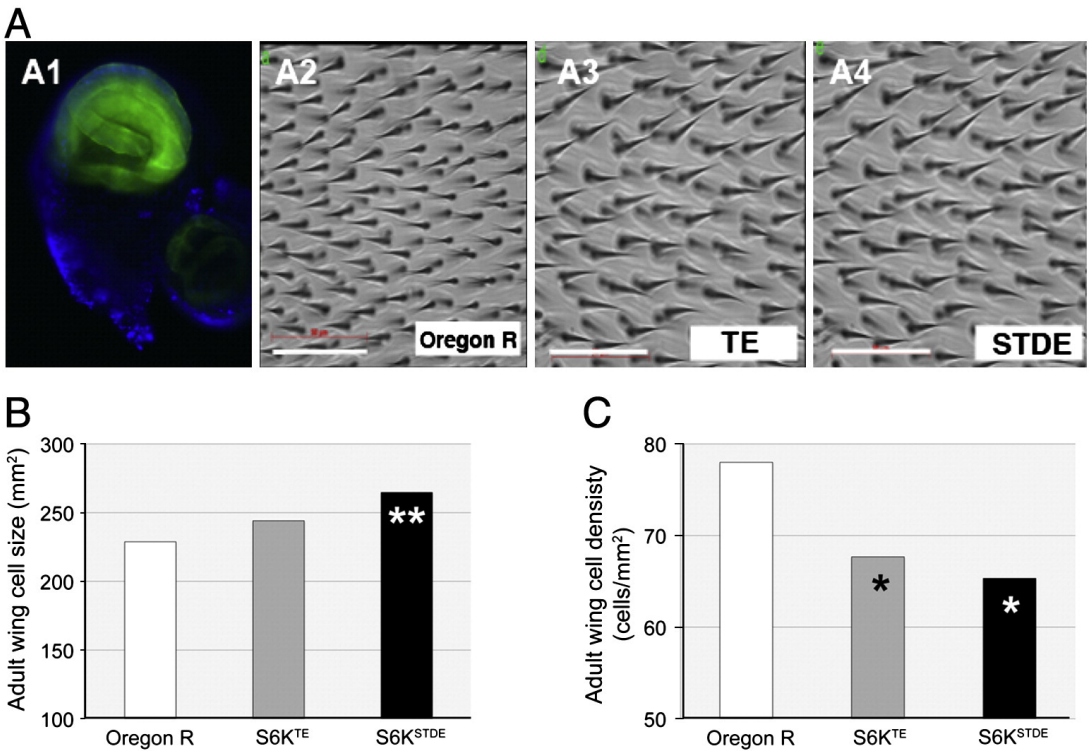

Figure A.2 Constitutively active *S6K* alleles increase wing cell size but do not affect cell number. (A) A *nub:GAL4* driver was used to express constitutively active alleles of *S6K* in the wing pouch. Anterior is up. (A1) The expression domain of the *nub:GAL4* driver revealed by UAS:GFP. Driver expression in the wing imaginal disk is confined to the wing pouch, which gives rise to the wing proper (but not the notum). Green: GFP; blue: Hoechst. (A2) Trichomes in the wing of a wild type adult female, compared with those in the wings of adult females whose wings express $S6K^{TE}$ (A3) or $S6K^{STDE}$ (A4). A2–A4 are at the same magnification; scale bar = 50 μm. (B) Adult wing cell size is larger than controls in wings expressing $S6K^{TE}$, and significantly larger ($p < 0.01$) in wings expressing$S6K^{STDE}$. (C) Consistent with increased cell size, adult wing cell density is significantly smaller than controls in wings expressing either $S6K^{TE}$ or $S6K^{STDE}$ ($p < 0.05$). Total wing cell number is not affected by these mutations.

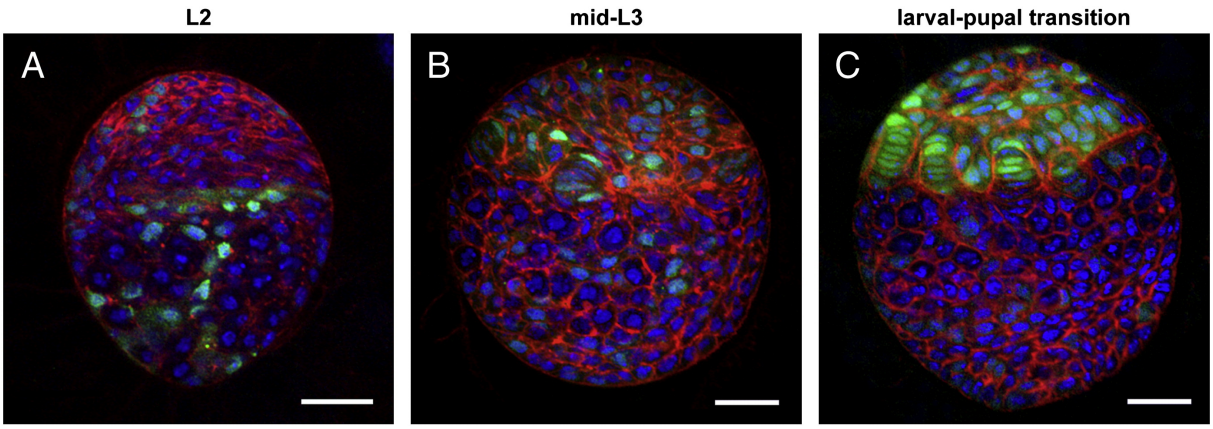

Figure A.3. *bab:GAL4* is expressed in TFCs throughout larval development.
Expression of GFP driven by *bab:GAL4* during larval ovarian development (A) Second larval instar (L2). (B) Mid-third larval instar (L3). (C) Larval–pupal stage. Green: GFP; red: phalloidin; blue: Hoechst. Anterior is up. Scale bar = 20 mm.

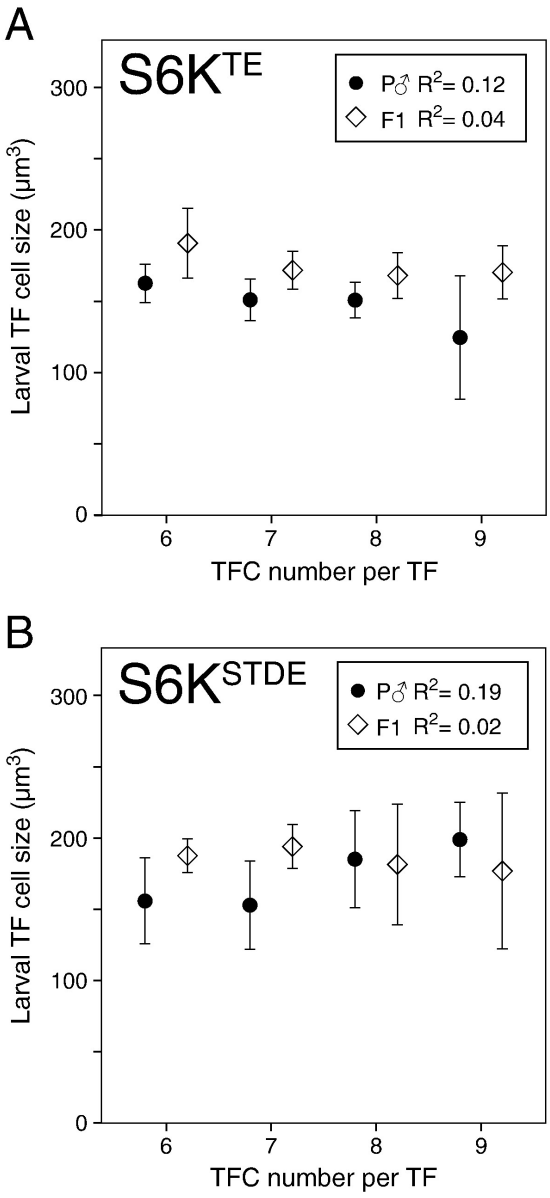

Figure A.4 Number of cells per TF is not correlated with TFC size. Size of TFCs at late L3 larval stages as a function of TFC number per TF, in ovaries overexpressing *S6K*^{TE} (A) or *S6K*^{STDE} (B) compared to parental strains (P♂).Error bars indicate 95% confidence interval.

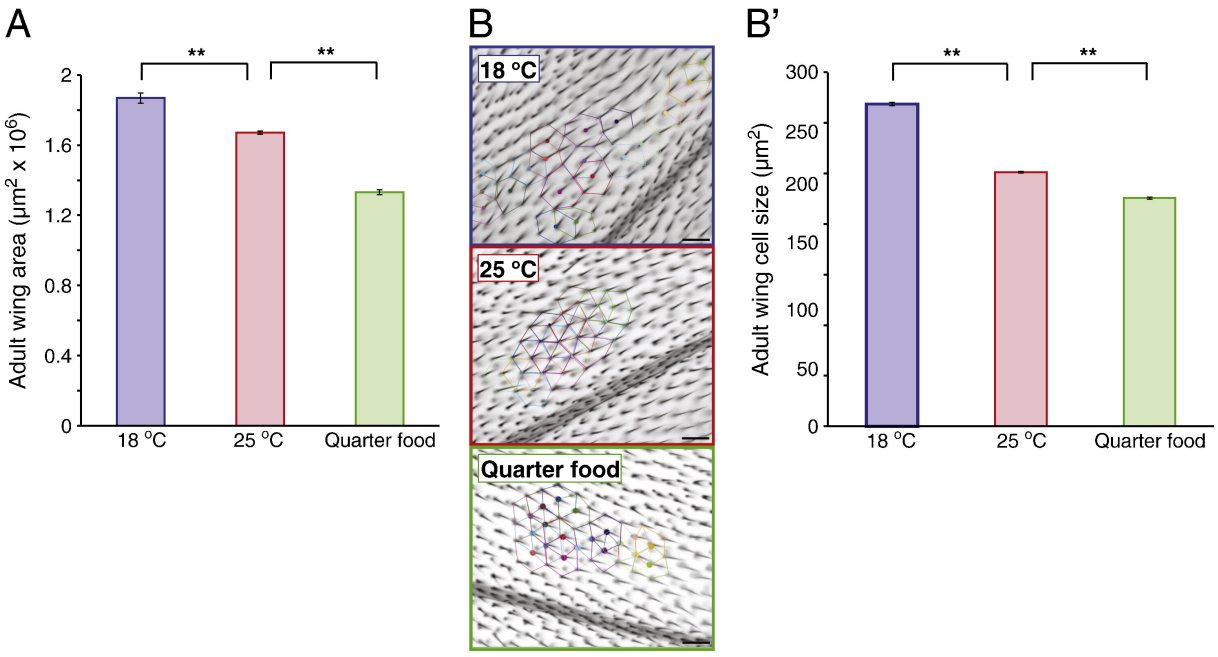

Figure A.5. Effects of temperature and nutrition on wing cell size, wing size, and wing cell number. (A) Measurements of wing surface area of flies reared at 18 °C (blue), 25 °C (red) and on quarter food (green). Measurements were made of the same wings shown in outline in Figure 2.8C. Wings of flies reared at 18 °C are significantly larger than wings of flies reared at 25 °C, and wings of flies reared on quarter food are significantly smaller ($p < 0.001$ for both comparisons). (B) Wing cell size (surface area) was measured by halving the area of the region delimited (colored lines) by the six neighbors of a given microchaete (wing hair), since every wing cell secretes a single microchaete. Scale bar = 20 μm. (B′) Measurements of wing cell size of flies reared at 18 °C and at 25 °C. Wing cells of flies reared at 18 °C are significantly larger than those of flies reared at 25 °C, and wing cells of flies reared on quarter food are significantly smaller ($p < 0.001$ for both comparisons). Error bars indicate 95% confidence interval.

Appendix B:

Comparative developmental analysis of two additional *melanogaster* subgroup species

B.1 Introduction

In Chapter II, I established that changes in TFC number and sorting underlie ovariole number differences in plasticity response to environment in *D. melanogaster*, and TFC number differences underlie species-specific differences *between D. melanogaster* and *D. yakuba* (Sarikaya et al., 2011). We postulated that ovariole number change between species was primarily driven through changes in total TFC number, and that changes in TFC sorting were a temperature-induced plasticity response. The *melanogaster* subgroup species offer an interesting model for investigating ovariole number evolution because there is considerable variation in ovariole number between these species (Figure B.1). There are large changes in mean ovariole number, for example between *D. melanogaster* (43 ovarioles) and *D. sechellia* (18 ovarioles), and finer scale differences between species such as that of *D. yakuba* (28 ovarioles) and *D. teissieri* (26 ovarioles).

Comparative analysis of *D. melanogaster* and *D. sechellia* was conducted by another student in the laboratory (Green and Extavour, 2012, 2014). He identified that differences in total TFC number underlies convergent evolution of lower ovariole number in *D. sechellia* and *D. melanogaster India* strain compared to the *D. melanogaster OregonR* strain. He identified two separate mechanisms that change total TFC number. First, *D. sechellia* has fewer somatic precursor cells at the beginning of larval ovary formation, which leads to fewer cells in the ovary compared to *D. melanogaster*. Second, the *D. melanogaster India* strain has the same number of cells compared to the *OregonR* strain, but during larval ovary morphogenesis, a larger proportion of anterior cells swarm to the posterior, leaving fewer cells in the anterior to form TFCs. This established that

changes in TFC number can be achieved through different developmental mechanisms, and that it may be one of the primary ways in which ovariole number evolves.

To test if the two developmental mechanisms I established previously in Chapter II are relevant for ovariole number evolution between additional species, here I extended my analysis to two new species: *D. mauritiana* and *D. teissieri*.

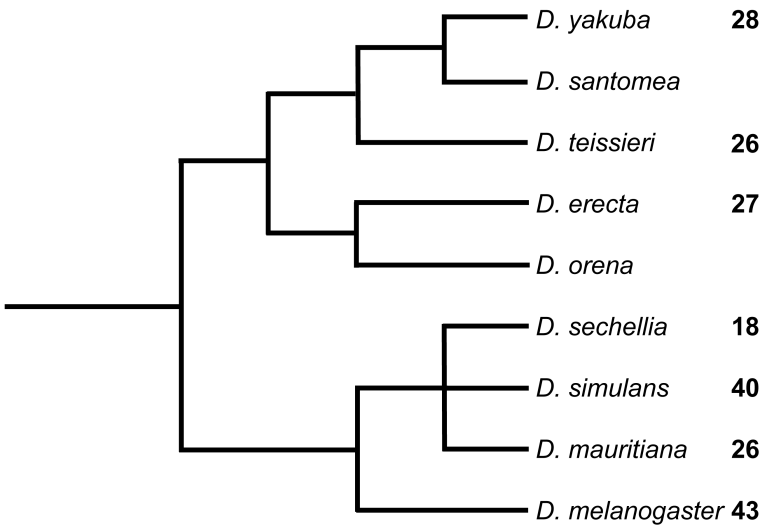

Figure B.1. Phylogenetic relationship of *melanogaster* subgroup species and their average ovariole number. Phylogeny based on (Lachaise and Silvain, 2004), and ovariole number based on (Markow and O'Grady, 2007)

B.2 Material and Methods

Wild-type strains of D. *mauritiana* (14021-0241.05) and *D. teissieri* (14021-0257.01) were obtained from the UCSD Drosophila species stock center and maintained at standard Drosophila laboratory conditions. Larval ovaries were collected, stained and imaged as described in Chapter II (Sarikaya et al., 2012).

B.3 Results

Morphology of the Larval-Pupal stage ovary

There were no major differences in the morphology of the larval-pupal (LP) stage ovary in *D. teissieri* and *D. mauritiana* compared to *D. melanogaster* and *D. yakuba* (Figure B.2). *D. mauritiana* and *D. melanogaster* ovaries appeared to be of similar volume (Figure B.2 A-B). *D. teissieri* LP stage ovaries appeared much smaller than *D. yakuba* (Figure B.2 C-D).

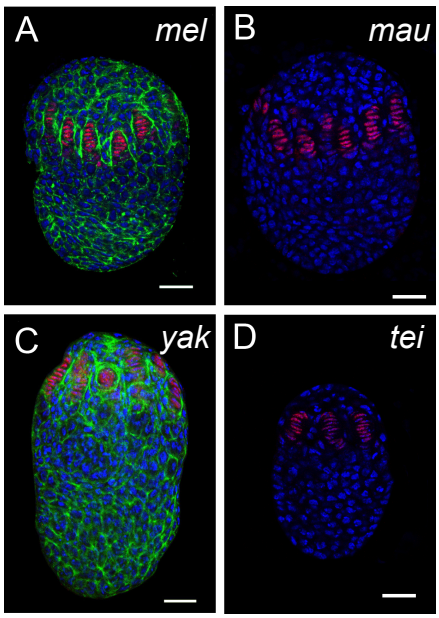

Figure B.2. LP stage morphology of larval ovary in *melanogaster* subgroup species. Panels representing *D. melanogaster* (A), *D. mauritiana* (B), *D. yakuba* (C), and *D. teissieri* (D). Nuclei are labeled in blue, filamentous actin in green, and TFCs in red. White bar in the bottom right corner of image denotes scale bar for 20 um.

TFC number and sorting in two new species

TF number at the LP stage corresponded to the reported adult ovariole number in all four species (Figure B.3A). *D. teissieri* had an average of 12.75 TFs per ovary, which was significantly lower than the other three species. *D. mauritiana* and *D. yakuba* did not differ significantly in TF number. *D. melanogaster* TF number was significantly higher than that of the other three species.

Total TFC number was significantly higher in *D. melanogaster* compared to all other three species (Figure B.3B). TFC number in *D. mauritiana*, *D. yakuba*, and *D. teissieri* were not significantly different from each other. Interestingly, TFC number per TF was higher in *D. teissieri,* with an average of 8.2 TFCs per TF, compared to the other three species, which averaged 7.3 TFCs per TF (Figure B.3C)

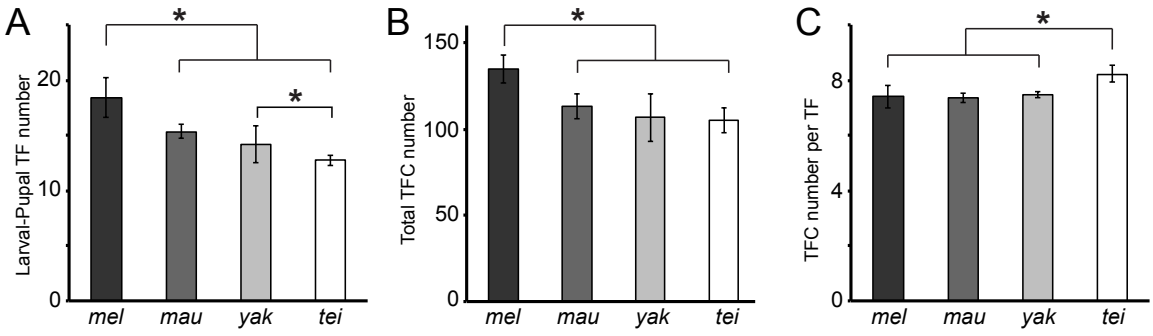

Figure B.3. TFC number and sorting differences between melanogaster subgroup species. Bar graph comparing TF number (A), total TFC number (B), and TFC number per TF (C) between *D. melanogaster (mel*, n=10*), D. mauritiana (mau*, n=3*), D. yakuba (yak*, n=4), and *D. teissieri* (*tei*, n=5). Asterisks indicates statistically significant differences of $p<0.05$. Error bars denote confidence interval.

B.4 Discussion

Comparative studies from Chapter II of this thesis, as well as those of another student in the Extavour lab (Green and Extavour, 2012), suggested that the primary mechanism that drives change in ovariole number between different species of the *melanogaster* subgroup is change in TFC number. I observed that ovariole number differences between *D. melanogaster* and *D. mauritiana* occurred through change in total TFC number. However, in addition to this, I found that *D. teissieri* has lower total TFC number as well as higher number of TFC per TF, compared to other species with a higher average ovariole number. We previously implicated changes in TFC number per TF as a mechanism that regulates ovariole number in response to temperature (Sarikaya et al., 2011). The data presented in this Appendix suggest that it is a mechanism that is relevant for species-specific changes as well.

While multiple genes have been implicated in the evolution and development of TFC number (Gancz and Gilboa, 2013; Gancz et al., 2011; Green and Extavour, 2014; Sarikaya et al., 2011), the primary genes implicated in the sorting process to date are the transcription factor *bric-à-brac1* (*bab1*) and *bab2* (Bartoletti et al., 2012), which regulate TF morphogenesis during development (Godt and Laski, 1995). *bab* genes also regulate the movement of swarm cells, which takes place at the same time as TF morphogenesis in the ovary, and may influence total TFC number by changing the proportion of anterior cells that migrate to the posterior through swarm cell migration versus those that remain in the anterior to give rise to TFCs (Green and Extavour, 2012). The *bab* locus has been implicated in morphological evolution of the abdomen of fruit flies (Gompel and Carroll, 2003; Rogers et al., 2013; Salomone et al., 2013; Williams et al., 2008), and has also

been suggested to play a role in the evolution of leg bristles in Drosophila (Barmina and Kopp, 2007) and horn morphology of beetles (Moczek and Rose, 2009). It would be interesting to test the different effects of the *bab* paralogs *bab1* and *bab2* in ovariole number evolution. The paralogs may be separately employed during evolution to alter total TFC number by changing proportions of anterior cells that undergo swarming, or by altering TFC number per TF during TF morphogenesis.

Another interesting difference between the *melanogaster* subgroup species that I have investigated in this Appendix is the total volume of the ovary. TFC number does not always correlate with total ovary volume, as *D. melanogaster India* strain ovaries have the same volume and same cell number as *OregonR D. melanogaster* strains, but have fewer TFCs due to changes in proportioning of the anterior cell populations (Green and Extavour, 2012). *D. mauritiana* LP stage ovaries appeared similar in size to *D. melanogaster* (Figure B.2 A-B), and were reported to have similar overall cell number at late-L3 stage in a previous study (Hodin and Riddiford, 2000). It would be interesting to test if an increased proportion of anterior somatic cells undergo swarming in the *D. mauritiana* ovaries, similar to the *D. melanogaster India* strain (Green and Extavour, 2012). The volume of *D. yakuba* and *D. teissieri* ovaries at the LP stage appeared very different (Figure B.2 C-D) even though both ovaries did not have significant differences in total TFC number. The larval ovarian cells of *D. teissieri* do not appear significantly smaller than those of *D. yakuba*, therefore it is likely that *D. teissieri* ovaries have fewer total cells in the larval ovary. This may be caused by a reduction of the number of somatic precursor cells that give rise to the larval ovary, or a reduction in the proliferation rate of larval ovarian cells. These findings, combined with thaose of Green and Extavour

(2012), suggest that overall volume or cell count of the LP stage ovary is a poor predictor of ovariole number.

The relationship between plasticity response and species-specific changes in ovariole number has been discussed extensively in Green and Extavour (2014). My experimental results from Chapter II and this Appendix show that similar developmental mechanisms underlie ovariole number evolution between closely related melanogaster subgroup species, and plasticity response to the environment in *D. melanogaster*. The *melanogaster* subgroup species may offer an interesting model to investigate the genetic mechanisms that regulate ovariole number, and its relationship with plasticity response. The availability of genetic tools in the *melanogaster* subgroup of species, and the ease of maintenance in the laboratory offers the potential to investigate the genetics of these mechanisms more readily than other non-model systems.

B.5 References

Barmina, O., and Kopp, A. (2007). Sex-specific expression of a HOX gene associated with rapid morphological evolution. Dev. Biol. *311*, 277–286.

Bartoletti, M., Rubin, T., Chalvet, F., Netter, S., Dos Santos, N., Poisot, E., Paces-Fessy, M., Cumenal, D., Peronnet, F., Pret, A.-M., et al. (2012). Genetic basis for developmental homeostasis of germline stem cell niche number: a network of Tramtrack-Group nuclear BTB factors. PLoS One *7*, e49958.

Gancz, D., and Gilboa, L. (2013). Insulin and Target of rapamycin signaling orchestrate the development of ovarian niche-stem cell units in Drosophila. Development *140*, 4145–4154.

Gancz, D., Lengil, T., and Gilboa, L. (2011). Coordinated regulation of niche and stem cell precursors by hormonal signaling. PLoS Biol. *9*, e1001202.

Godt, D., and Laski, F.A. (1995). Mechanisms of cell rearrangement and cell recruitment in Drosophila ovary morphogenesis and the requirement of bric à brac. Development *121*, 173–187.

Gompel, N., and Carroll, S.B. (2003). Genetic mechanisms and constraints governing the evolution of correlated traits in drosophilid flies. Nature *424*, 931–935.

Green, D.A., and Extavour, C.G. (2012). Convergent evolution of a reproductive trait through distinct developmental mechanisms in Drosophila. Dev. Biol. *372*, 120–130.

Green, D.A., and Extavour, C.G. (2014). Insulin signalling underlies both plasticity and divergence of a reproductive trait in Drosophila. Proc. Biol. Sci. / R. Soc. *281*, 20132673.

Hodin, J., and Riddiford, L.M. (2000). Different mechanisms underlie phenotypic plasticity and interspecific variation for a reproductive character in drosophilids (Insecta: Diptera). Evolution (N. Y). *54*, 1638–1653.

Lachaise, D., and Silvain, J.F. (2004). How two Afrotropical endemics made two cosmopolitan human commensals: The Drosophila melanogaster-D. simulans palaeogeographic riddle. In Genetica, pp. 17–39.

Markow, T.A., and O'Grady, P.M. (2007). Drosophila biology in the genomic age. Genetics *177*, 1269–1276.

Moczek, A.P., and Rose, D.J. (2009). Differential recruitment of limb patterning genes during development and diversification of beetle horns. Proc. Natl. Acad. Sci. U. S. A. *106*, 8992–8997.

Rogers, W.A., Salomone, J.R., Tacy, D.J., Camino, E.M., Davis, K.A., Rebeiz, M., and Williams, T.M. (2013). Recurrent Modification of a Conserved Cis-Regulatory Element Underlies Fruit Fly Pigmentation Diversity. PLoS Genet. *9*.

Salomone, J.R., Rogers, W.A., Rebeiz, M., and Williams, T.M. (2013). The evolution of Bab paralog expression and abdominal pigmentation among Sophophora fruit fly species. Evol. Dev. *15*, 442–457.

Sarikaya, D.P., Belay, A.A., Ahuja, A., Dorta, A., Green, D.A., and Extavour, C.G. (2011). The roles of cell size and cell number in determining ovariole number in Drosophila. Dev. Biol.

Williams, T.M., Selegue, J.E., Werner, T., Gompel, N., Kopp, A., and Carroll, S.B. (2008). The Regulation and Evolution of a Genetic Switch Controlling Sexually Dimorphic Traits in Drosophila. Cell *134*, 610–623.

Appendix C:

Supporting figures for Chapter III

Sarikaya and Extavour Figure S1

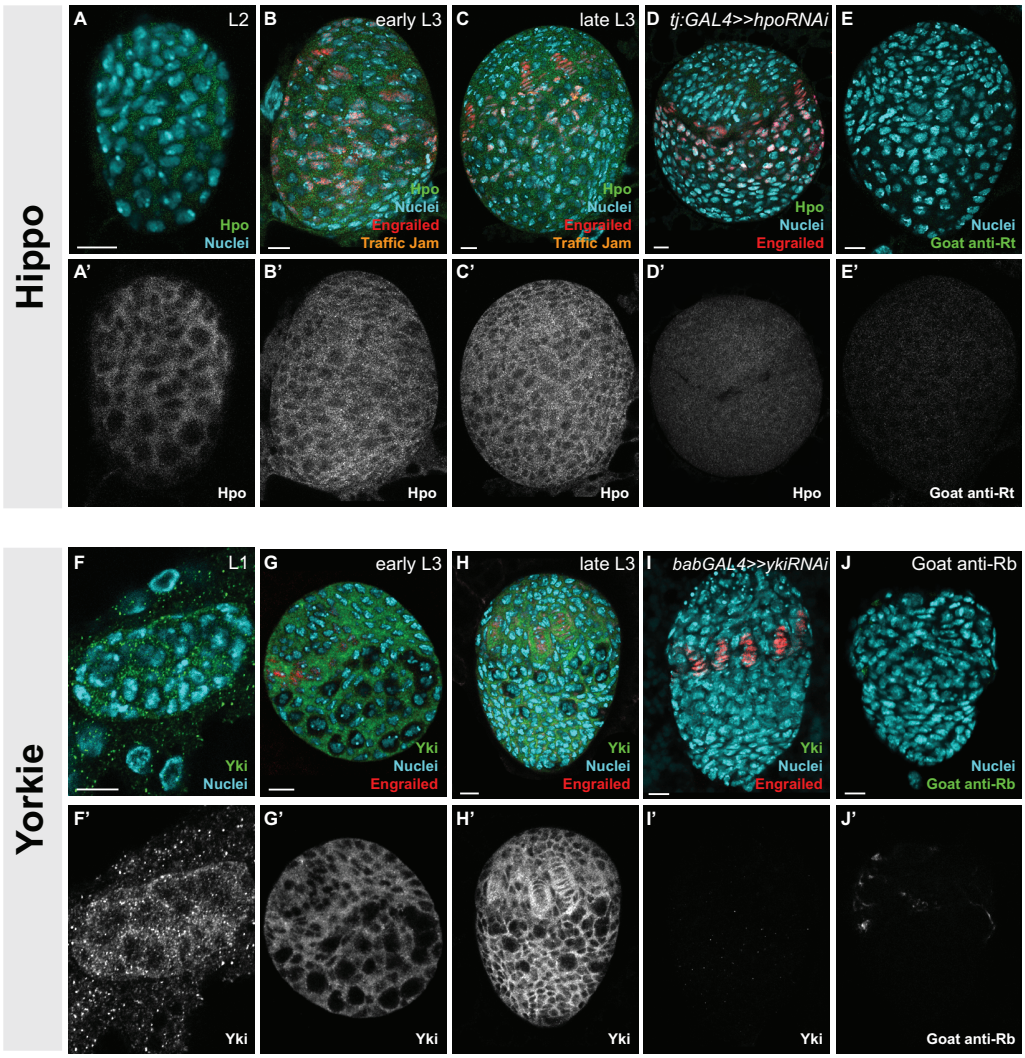

Figure C.1. Hippo pathway core components are expressed in the larval ovary. (A-C) Hippo protein is expressed ubiquitously in the larval ovary throughout development. (D) Hippo expression is strongly reduced in ovaries expressing RNAi against *hpo* under the somatic driver *tj:GAL4*, confirming specificity of the anti-Hpo antibody used in A-C and validating the RNAi line used. The decrease in Hpo protein levels observed throughout the ovary is likely due to the fact that the *tj:GAL4* driver is initially expressed in all somatic cells of the ovary. (E) Secondary only control for Hippo antibody staining. Panels (B-E) were imaged at the same laser confocal settings. (F-H) Yorkie is detected in all somatic cells during larval ovarian development. (I) Yorkie expression is undetectable in ovaries expressing RNAi against *yki* using the somatic driver *bab:GAL4*, confirming specificity of the anti-Yki antibody used in F-H and validating the RNAi line used. The decrease in Yki protein levels observed throughout the ovary is likely due to the fact that the *bab:GAL4* driver is initially expressed in all somatic cells of the ovary, as previously reported. (J) Secondary only control for Yki antibody. Panels in (H-J) were taken at the same laser confocal settings. Green: Hippo or Yorkie; cyan: nuclei; red: Engrailed; orange: Traffic Jam. Scale bar = 10 μm.

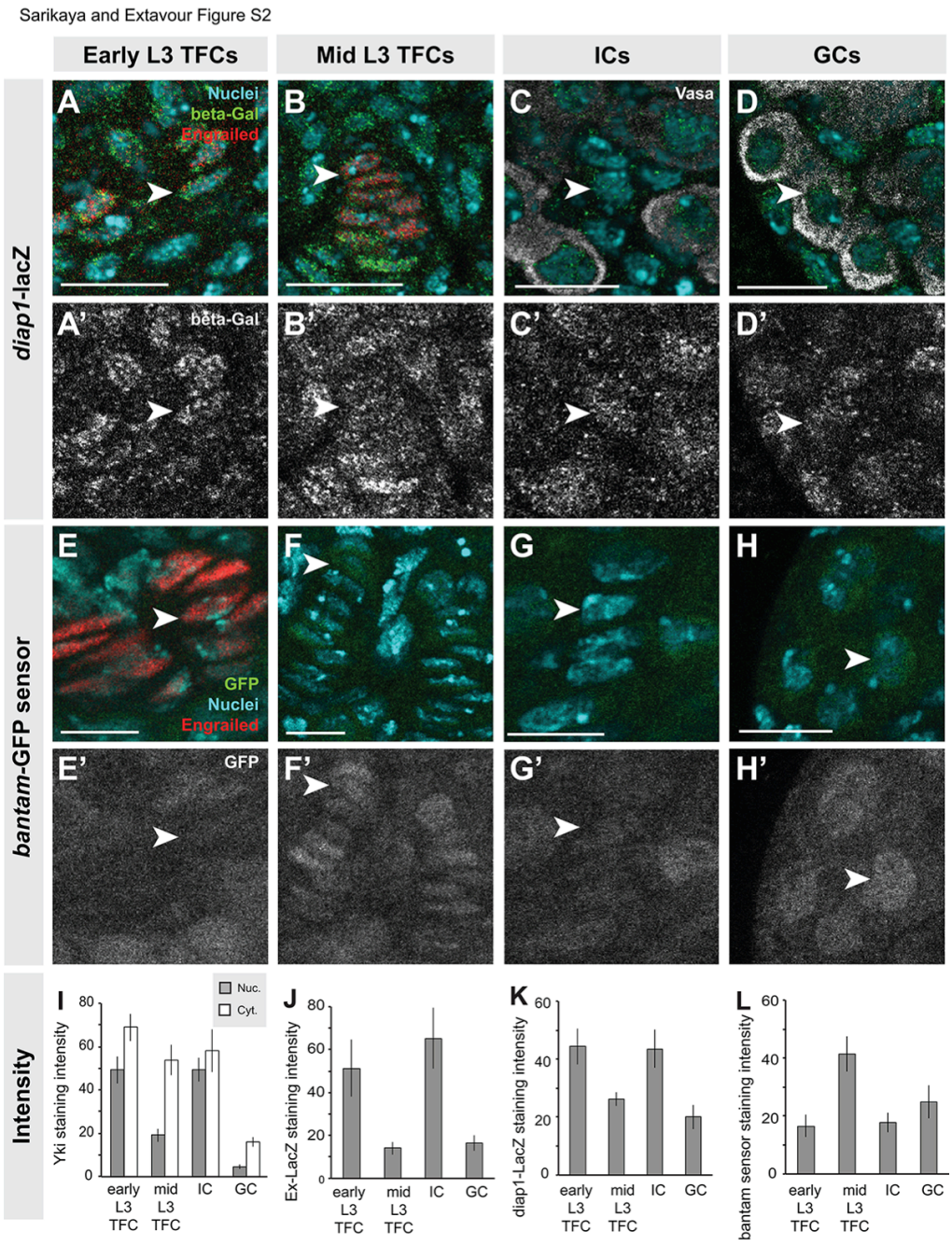

Figure C.2. Expression pattern of Hippo pathway activity reporter lines in larval ovarian cell types. Expression of (A-D, K) *diap1-LacZ* and (E-H, L) *bantam*-GFP reporters in larval ovarian cell types. (A) Engrailed-positive cells beginning to differentiate into disc-shaped TFCs express *diap1-LacZ*. (B) TFCs within a TF stack in mid-late L3 do not have strong *diap1* expression. (C-D) ICs and GCs express *diap1*. (E-H) Expression of the *bantam-GFP* sensor line in larval ovarian cell types. The reporter line contains a GFP construct with three *bantam* miRNA target sites, so that GFP mRNA is degraded when *bantam* is expressed; GFP expression therefore indicates to little or no *bantam* expression. (E) Early TFCs express *bantam* (GFP expression is not detected). (F) TFCs in a mature TF express little to no detectable *bantam* (GFP

(Continued)
expression is detected). (G) Low levels of GFP are detected in ICs, suggesting that *bantam* is expressed. (H) GCs express little or no detectable *bantam* (GFP expression is detected). Arrowheads point to an example of the specific cell types in each column. Green: β-gal (A-B) or GFP (E-H); cyan: nuclei; red: Engrailed; white: Vasa (C-D). Scale bar = 10 μm. (I-L) Quantification of relative intensity of (I) Yki, (J) *expanded*-LacZ, (K) *diap1*-LacZ, and (L) the bantam-GFP sensor in early and mid L3 TFCs, ICs, and GCs. Error bars denote confidence intervals. n=5 per measurement.

Sarikaya and Extavour Figure S3

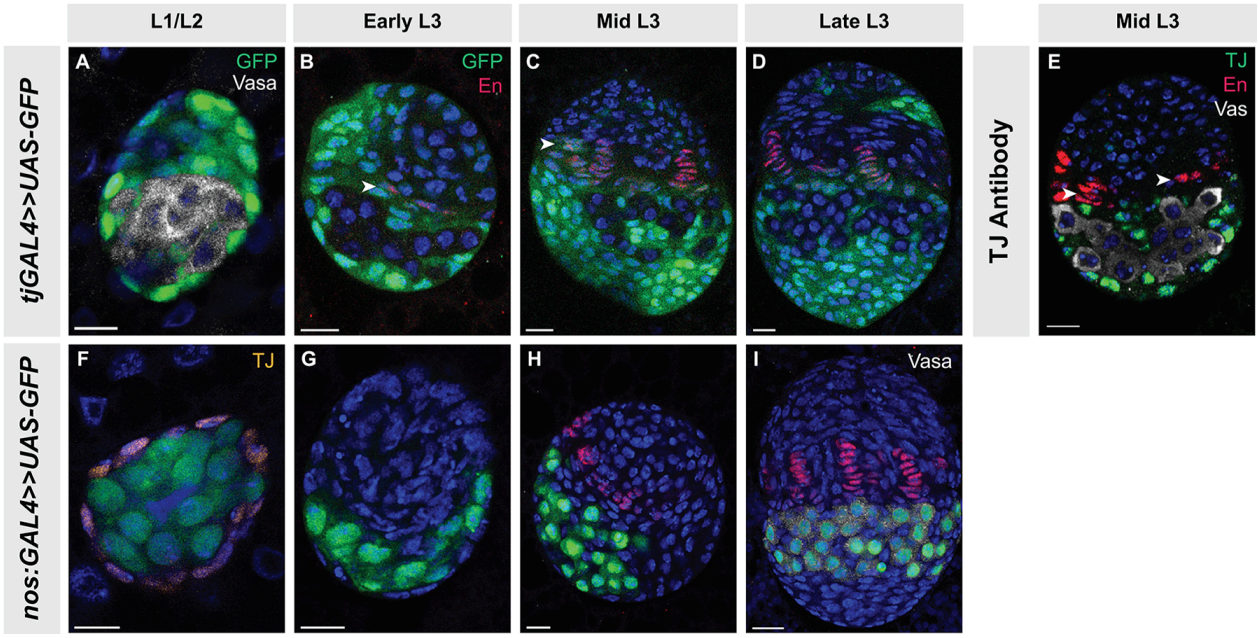

Figure C.3. GFP expression driven by *traffic-jam* and *nanos* GAL4 during larval ovarian development. (A-D) *tj:GAL4* is expressed in most somatic cells in early larval development. Expression becomes confined to posterior cells in L3, persisting in a few TFCs and anterior patches of somatic cells. Expression in TFCs is strongest while TF stacking is occurring (arrowheads). GCs do not express *tj:GAL4*. (E) An anti-Traffic Jam antibody (green) detects a subset of the cells that express the *tj:GAL4* driver. (F-H) *nos:GAL4* is specific to GCs throughout larval ovarian development. . Green: GFP in A-D, F-I; Traffic Jam in E; blue: nuclei in all panels; red: Engrailed in all panels; orange: Traffic Jam in F; white: Vasa in A, E and I. Scale bar = 10 μm.

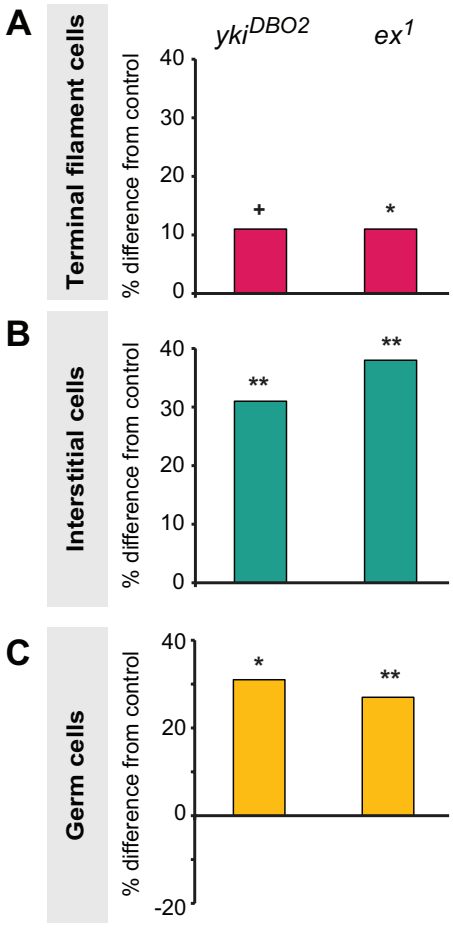

Figure C.4. Homozygous mutants of Hippo pathway components significantly influence TFC, IC, and GC number. Percent difference of (A) TFCs, (B) ICs, and (C) GCs of ex^{1} and yki^{DBO2} homozygous mutants compared to w^{1118} control line. + p=0.06, * p<0.05, ** p<0.01. n=10 for ex^{1} and w^{1118}, and n=6 for yki^{DBO2}. Numerical values can be found in Table S2.

Sarikaya and Extavour Figure S5

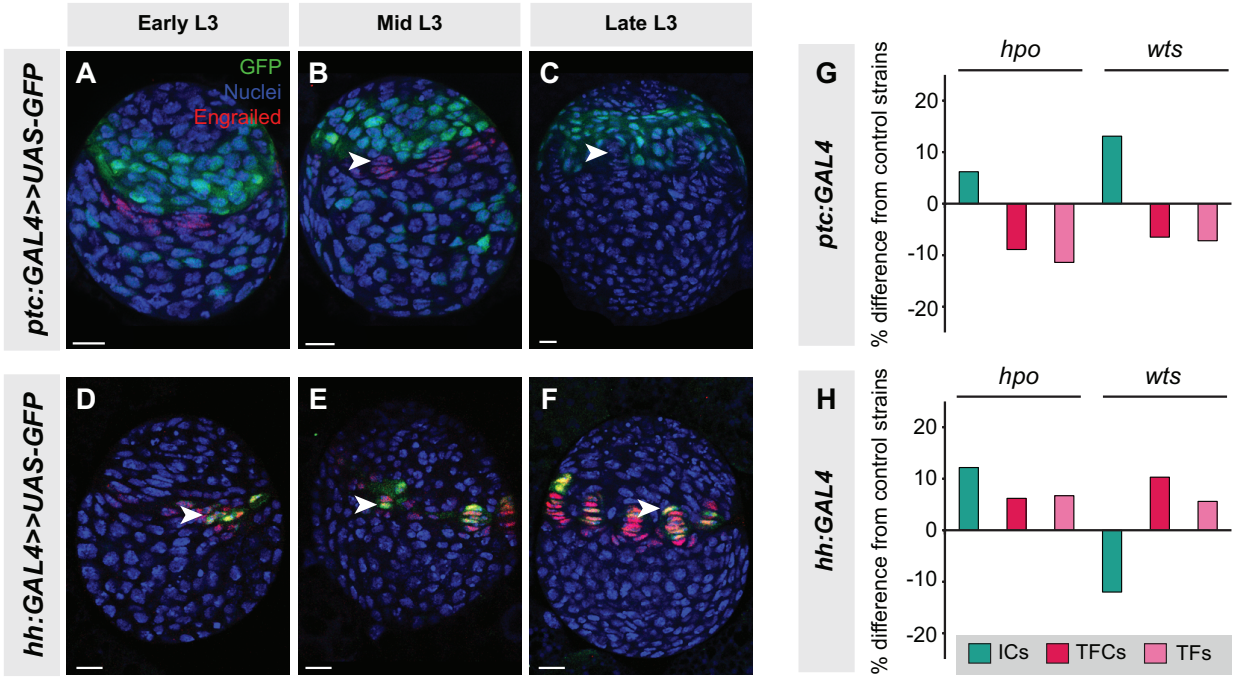

Figure C.5. RNAi against Hippo pathway members driven by *ptc:*GAL4 or *hh:*GAL4 drivers does not significantly influence proliferation of larval ovarian cell types non-autonomously. (A-C) Expression domain of *ptc:GAL4* in L3 larval ovaries. (A) *ptc:GAL4* is expressed weakly in ICs and strongly in anterior somatic cells, but is not detected in TFCs (arrowheads in B and C). (D-F) Expression domain of *hh:GAL4* in L3 larval ovaries. *hh:GAL4* is expressed in a mosaic pattern in TFCs (arrowheads) with some expression in early and later stages of TF stacking, but not before TFC intercalation begins. (G-H) No significant difference in IC, TFC or TF number is observed when hpo^{RNAi} or wts^{RNAi} are expressed under (G) *ptc:GAL4* or (H) *hh:GAL4* drivers. Green bars: ICs; red bars: TFCs; pink bars: TFs.

Sarikaya and Extavour Figure S6

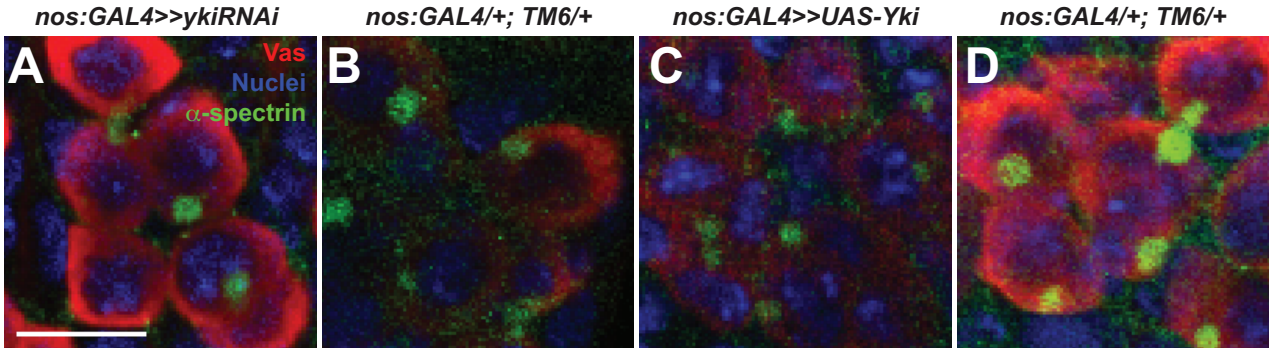

Figure S6. Spectrosome morphology does not change when *yki* activity is altered in GCs. Alpha-spectrin staining (green) in LP stage GCs of (A) *nos:GAL4>>yki*^{RNAi} and (C) *nos:GAL4>>UAS-yki* larvae and their siblings (controls: B and D). Round spectrosomes (green), indicating germ cells (red) that have not initiated oogenesis, are found in most GCs at this stage in all four genotypes. Scale bar = 10 μm.

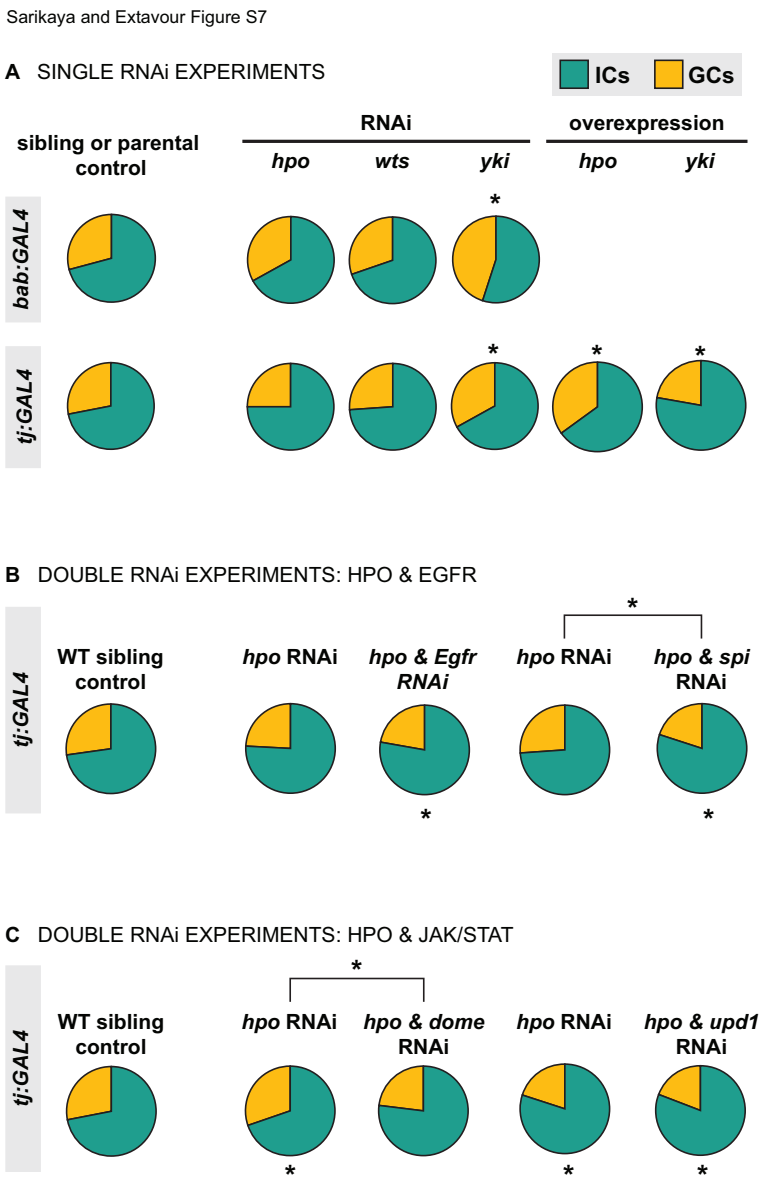

Figure S7. ICs and GCs generally maintain homeostatic growth when Hippo pathway activity is reduced in the soma. Pie charts show proportion of ICs (green) and GCs (yellow) when we knocked down (A) Hippo pathway members alone, or in combination with (B) EGFR signaling pathway components or (C) JAK/STAT signaling pathway components using *bab:GAL4* and *tj:GAL4*. * denotes $p<0.05$, and ** denotes $p<0.01$. See Table S6 for numerical values.

Sarikaya and Extavour Figure S8

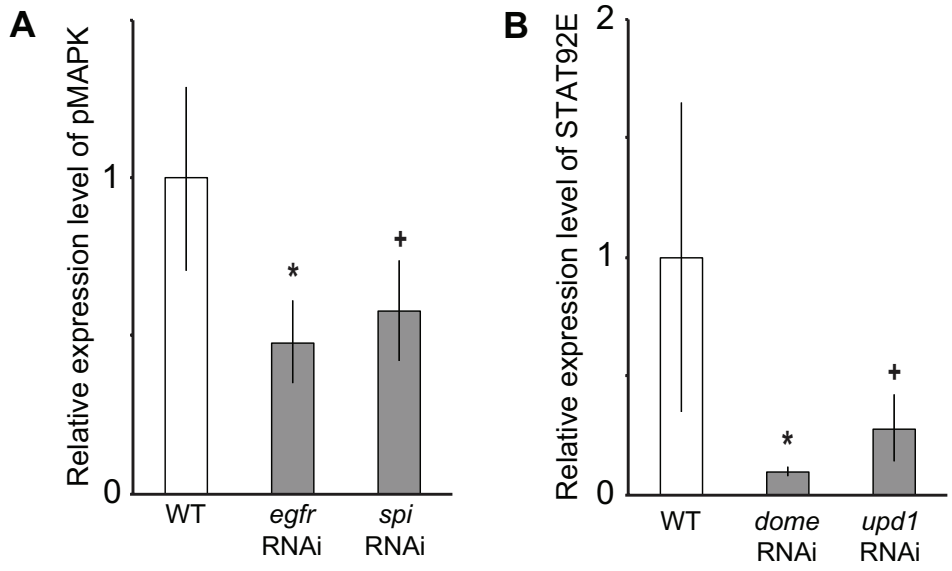

Figure C.8. RNAi against EGFR and JAK/STAT pathway components reduce respective pathway activity in the larval ovary. Relative intensity of (A) anti-pMAPK fluorescence in WT compared to *egfr* or *spi* RNAi expressed under *tj:GAL4* (n=5), and (B) anti-Stat92E fluorescence in WT compared to *dome* or *upd1* RNAi expressed under *tj:GAL4* (n=5) in L3 larval ovaries. + p=0.06, * p<0.05.

Tables

Genotype	TFC Number TFC#	SD	vs RNAi	vs GAL4	vs Sib	TF Number TF #	SD	vs RNAi	vs GAL4	vs Sib	n
Controls											
bab:GAL4 (bab)	143.6	23.0				19.1	2.9				10
tj:GAL4 (tj)	148.0	16.8				19.5	2.6				10
nos:GAL4 (nos)	156.8	22.4				22.5	2.6				10
UAS-hpo^{RNAi}	169.9	13.5				22.2	1.9				10
UAS-wts^{RNAi}	157.1	15.1				20.9	2.0				10
UAS-yki^{RNAi}	153.5	14.8				21.3	2.2				10
Experimental											
bab>>hpo^{RNAi}	201.8	21.9	<0.01	<0.01		25.8	2.2	<0.01	<0.01		10
bab>>wts^{RNAi}	188.6	15.8	<0.01	<0.01		24.9	1.9	<0.01	<0.01		10
bab>>yki^{RNAi}	124.2	11.8	<0.01	0.02		18.3	1.3			0.01	10
tj>>hpo^{RNAi}	186.7	15.3	0.02	<0.01		25.5	2.0	<0.01	<0.01		10
tj>>wts^{RNAi}	188.3	31.6	0.01	<0.01		23.6	3.7	0.04	0.01		10
tj>>yki^{RNAi}	126.5	24.3	<0.01	0.03		17.1	3.0	<0.01	0.07		10
tj>>UAS-yki	183.0	28.2			0.04	26.0	4.4			<0.01	10
tj>>UAS-yki Sib	156.5	24.5				20.1	3.7				10
tj>>UAS-hpo	123.4	16.4			0.02	15.3	2.1			0.04	10
tj>>UAS-hpo Sib	144.3	20.2				17.5	2.2				10
nos>>hpo^{RNAi}	154.1	17.7	0.04	0.77		21.1	2.1	0.20	0.24		10
nos>>wts^{RNAi}	169.8	33.5	0.29	0.32		22.6	4.3	0.21	0.95		10
nos>>yki^{RNAi} (VDRC)	160.6	18.9	0.69	0.36		22.1	2.6	0.73	0.47		10
nos>>yki^{RNAi} (TRiP)	152.6	24.5			0.65	20.9	3.2			0.19	10
nos>>yki^{RNAi} Sib	156.5	18.9				22.3	2.6				10
nos>>UAS-yki	148.9	17.1			0.37	21.2	2.4			0.02	10
nos>>UAS-yki Sib	142.3	14.9				18.7	1.9				10
nos>>UAS-hpo	149.0	16.4			0.07	20.2	2.1			<0.01	10
nos>>UAS-hpo Sib	134.0	17.0				17.4	1.9				10

Table C1. Summary of mean TFC and TF number in LP stage ovaries of genotypes used in RNAi analysis. Abbreviated names for GAL4 drivers are indicated in parentheses in leftmost column of first three rows. SD = standard deviation. Two-tailed t-tests were conducted for analysis and *p*-values are reported in columns compared to the UAS-RNAi parental strain (vs RNAi), GAL4 parental strain (vs GAL4), or the sibling (Sib) carrying balancers (vs Sib). Red shading indicates significant differences $p \leq 0.01$ (indicated by ** in Figure 2); yellow shading indicates significant differences $0.01 < p \leq 0.05$ (indicated by * in Figure 2); orange shading indicates near-significant differences $0.05 < p \leq 0.1$ (indicated by + in Figure 2). VDRC indicates line 104523 from the Vienna Drosophila RNAi Center; TRiP indicates Transgenic RNAi Project line 34067 from the Bloomington Stock Center.

	Ovariole Number			TFC Number			IC Number			GC Number			
Genotype	ON	SD	vs Control	TFC#	SD	vs Control	IC #	SD	vs Control	GC #	SD	vs Control	n
Control													
Oregon R	17.6	2.4											10
w^{1118}				137.8	14.6		358.2	49.3		147.5	14		10
Mutants													
yki^{DBO2}				155.1	19	0.06	515.5	75.8	<0.01	212.3	97.3	0.05	6
ex^{1}	21.3	5.4	<0.01	185.4	18.9	<0.01	577.1	112	<0.01	200.8	56	<0.01	10

Table C2. Summary of mean ovariole, TFC, IC and GC number in ovaries of genotypes used in mutant analysis. SD = standard deviation. Two-tailed t-tests were conducted for analysis and *p*-values are reported in columns compared to the OregonR for ovariole number, and compared to w^{1118} for TFC, IC and GC number. Red shading indicates significant differences $p \leq 0.01$; yellow shading indicates significant differences $0.01 < p \leq 0.05$; orange shading indicates near-significant differences $0.05 < p \leq 0.1$.

	IC Number					GC Number					
Genotype	IC #	SD	vs RNAi	vs GAL4	vs Sib	GC #	SD	vs RNAi	vs GAL4	vs Sib	n
Controls											
bab:GAL4 (bab)	528.8	63.2				223.4	59.0				10
tj:GAL4 (tj)	466.7	124.9				140.7	23.7				10
nos:GAL4 (nos)	526.7	120.8				167.2	32.8				10
UAS-hpo^{RNAi}	477.2	123.4				218.8	40.7				10
UAS-wts^{RNAi}	543.6	79.0				187.9	43.8				10
UAS-yki^{RNAi} (VDRC)	470.0	49.6				226.1	67.1				10
UAS-ex^{RNAi}	n/a					188.2	23.2				10
UAS-hipk^{RNAi}	n/a					228.3	26.7				10
UAS-sd^{RNAi}	n/a					216.4	46.2				9
Experimental											
bab x hpo^{RNAi}	625.2	157.5	0.03	0.09		298.4	44.3	<0.01	<0.01		10
bab x wts^{RNAi}	638.4	119.8	0.02	0.05		265.8	49.8	<0.01	0.09		10
bab x yki^{RNAi} (VDRC)	266.8	74.9			<0.01	211.5	38.4			0.76	10
bab x yki^{RNAi} Sib	462.7	41.0				207.5	17.7				10
tj x hpo^{RNAi}	818.2	124.5	<0.01	<0.01		267.2	24.3	<0.01	<0.01		10
tj x wts^{RNAi}	796.1	168.0	<0.01	<0.01		271.5	57.9	<0.01	<0.01		10
tj x yki^{RNAi} (VDRC)	322.5	83.6	<0.01	<0.01		157.7	43.2	<0.01	0.28		10
tj x UAS-yki	1186.9	382.7			<0.01	329.5	23.7			0.047	10
tj x UAS-yki Sib	477.7	111.2				275.1	77.4				10
tj x UAS-hpo	301.6	40.8			<0.01	166.6	35.3			0.04	10
tj x UAS-hpo Sib	505.7	125.7				219.4	65.3				10
nos x hpo^{RNAi}	609.7	95.5	0.01	0.11		193.9	39.4	0.18	0.11		10
nos x wts^{RNAi}	573.4	123.1	0.53	0.40		202.8	36.8	0.42	0.03		10
nos x yki^{RNAi} (VDRC)	477.6	86.1	0.81	0.31		136.5	33.3	<0.01	0.05		10
nos x yki^{RNAi} (TRiP)	424.0	108.0			0.47	120.5	15.0			<0.01	10
nos x UAS-yki	495.0	108.5			<0.01	315.7	97.7			<0.01	10
nos x UAS-yki Sib	353.6	86.5				167.0	34.9				10
nos x UAS-hpo	492.5	94.4			0.53	97.9	14.2			<0.01	10
nos x UAS-hpo Sib	517.6	81.1				206.5	31.0				10
Nos x UAS-YkiS168A						/239,1	91.6	n/a	0.03		8
nos x ex^{RNAi}	n/a					176.1	29.8	0.32	0.53		10
nos x hipk^{RNAi}	n/a					181.9	37.8	<0.01			10
nos x sd^{RNAi}	n/a					132.1	18.8	<0.01	<0.01		10
nos x hpo/wts/ex^{RNAi}	n/a					237.1	41.6				10
nos x hpo/wts/ex^{RNAi} Sib	n/a					239.2	33.0				9

Table C3. Summary of mean IC and GC number in LP stage ovaries of genotypes used in RNAi analysis. Abbreviated names for GAL4 drivers are indicated in parentheses in leftmost column of first three rows. SD = standard deviation. Two-tailed t-tests were conducted for analysis and *p*-values are reported in columns compared to the UAS-RNAi parental strain (vs RNAi), GAL4 parental strain (vs GAL4), or the sibling (Sib) carrying balancers (vs Sibs). Red shading indicates significant differences $p \leq 0.01$ (indicated by ** in Figures 3 and 4); yellow shading indicates significant differences $0.01 < p \leq 0.05$ (indicated by * in Figure 3); orange shading indicates near-significant differences $0.05 < p \leq 0.1$ (indicated by + in Figure 3). VDRC indicates line 104523 from the Vienna Drosophila RNAi Center; TRiP indicates Transgenic RNAi Project line 34067 from the Bloomington Stock Center.

Genotype	TFC Number				IC Number				GC Number				
	TFC#	SD	vs WT	vs *hpo* sib	IC #	SD	vs WT	vs *hpo* sib	GC #	SD	vs WT	vs *hpo* sib	n
EGF pathway													
WT control: *spi*^{RNAi}/+; *hpo*^{RNAi}/+	127.9	16.9			432.4	100.3			164.5	23.2			10
tjGAL4/+;hpo^{RNAi}/+ [*egfr*^{RNAi} cross]	151.0	15.0	<0.01		709.8	144.6	<0.01		237.5	92.1	0.03		10
tjGAL4/egfr^{RNAi};*hpo*^{RNAi}/+	153.3	12.1	<0.01	0.72	577.7	87.8	<0.01	0.03	161.6	30.8	0.82	0.03	9
tjGAL4/egfr^{RNAi};+	131.9	11.4	0.54	<0.01	396.5	70.1	0.36	<0.01	205.8	55.8	0.04	0.36	10
tjGAL4/+;hpo^{RNAi}/+ [*spi*^{RNAi} cross]	165.4	21.8	<0.01		688.1	91.1	<0.01		245.0	32.7	<0.01		9
tjGAL4/spi^{RNAi};*hpo*^{RNAi}/+	171.3	16.9	<0.01	0.50	632.3	103.0	<0.01	0.24	185.6	79.6	0.43	0.05	9
tjGAL4/spi^{RNAi};+	137.2	9.2	0.14	<0.01	447.1	76.6	0.72	<0.01	185.2	29.9	0.10	<0.01	10
JAK/STAT pathway													
WT control: *upd1*^{RNAi}/+; *hpo*^{RNAi}/+	134.9	13.8			418.9	87.4			163.9	22.3			9
tjGAL4/+;hpo^{RNAi}/+ [*dome*^{RNAi} cross]	162.5	26.3	<0.01		680.1	110.4	<0.01		293.9	55.9	<0.01		9
tjGAL4/dome^{RNAi};*hpo*^{RNAi}/+	138.4	19.6	0.64	0.04	516.3	111.1	0.05	<0.01	154.7	36.6	0.52	<0.01	10
tjGAL4/dome^{RNAi};+	114.4	12.1	<0.01	<0.01	363.0	31.9	0.07	<0.01	157.6	30.9	0.85	<0.01	10
tjGAL4/+; hpo^{RNAi}/+ [*upd1*^{RNAi} cross]	155.2	24.4	<0.01		783.9	174.3	0.03		200.6	42.4	<0.01		9
tjGAL4/upd1^{RNAi}; *hpo*^{RNAi}/+	163.6	31.7	<0.01	0.51	613.1	33.2	<0.01	<0.01	146.8	32.1	0.20	<0.01	9
tjGAL4/upd1^{RNAi}; +	136.4	16.1	0.82	0.07	396.6	105.1	0.63	<0.01	171.2	23.9	0.51	0.09	9

Table C4. Summary of mean TFC, IC and GC number in LP stage ovaries of genotypes used in double RNAi analysis. SD = standard deviation. Two-tailed t-tests were conducted for analysis and *p*-values are reported in columns compared to the wild type control (vs WT) and the *hpo* RNAi control (vs *hpo* sib). Red shading indicates significant differences $p \leq 0.01$ (indicated by ** in Figures 5 and 6); yellow shading indicates significant differences $0.01 < p \leq 0.05$ (indicated by * in Figures 5 and 6); orange shading indicates near-significant differences $0.05 < p \leq 0.1$.

Genotype	TFC Number				TF Number				IC Number				n
	TFC#	SD	vs RNAi	vs GAL4	TF #	SD	vs RNAi	vs GAL4	IC #	SD	vs RNAi	vs GAL4	
Controls													
ptc:GAL4	145.8	18.9			19.5	2.1			624.0	67.6			10
hh:GAL4	137.5	20.8			18.1	2.3			568.6	95.8			10
UAS-hpo^{RNAi}	169.9	13.5			22.2	1.9			477.2	123.4			10
UAS-wts^{RNAi}	158.7	17.1			20.7	1.9			543.6	79.0			10
Experimental													
ptc x hpo^{RNAi}	145	10.0	<0.01	0.90	18.6	1.1	<0.01	0.24	586.8	83.8	0.30	0.03	10
ptc x wts^{RNAi}	142.9	18.4	0.06	0.76	18.7	2.7	0.07	0.49	667.1	75.5	0.20	<0.01	10
hh x hpo^{RNAi}	166.2	19.3	0.01	0.63	21.9	3.1	0.01	0.80	577.5	122.7	0.08	0.87	10
hh x wts^{RNAi}	165.56	12.9	<0.01	0.37	20.7	1.9	0.02	1.00	486.1	123.7	0.17	0.23	10

Table C5. Summary of TFC and IC number in *ptc:GAL4* and *hh:GAL4* analysis. SD = standard deviation. Two-tailed t-tests were conducted for analysis and *p*-values are reported in columns compared to the UAS-RNAi parental strain (vs RNAi) or the GAL4 parental strain (vs GAL4). Red shading indicates significant differences $p \leq 0.01$; yellow shading indicates significant differences $0.01 < p \leq 0.05$; orange shading indicates near-significant differences $0.05 < p \leq 0.1$.

Single RNAi Genotype	GC-IC Proportion GC	IC	vs RNAi	vs GAL4	vs Sib
Controls					
bab:GAL4 (bab)	29%	71%			
tj:GAL4 (tj)	23%	77%			
nos:GAL4 (nos)					
UAS-hpo^{RNAi}	30%	70%			
UAS-wts^{RNAi}	25%	75%			
UAS-yki^{RNAi} (VDRC)	30%	70%			
Experimental					
bab x hpo^{RNAi}	32%	68%	0.59	0.12	
bab x wts^{RNAi}	29%	70%	0.09	0.86	
bab x yki^{RNAi} (VDRC)	45%	55%			<0.01
bab x yki^{RNAi} Sib	31%	69%			
tj x hpo^{RNAi}	25%	75%	0.03	0.37	
tj x wts^{RNAi}	25%	75%	0.74	0.22	
tj x yki^{RNAi} (VDRC)	33%	67%	0.02	<0.01	
tj x UAS-yki	22%	78%			<0.01
tj x UAS-yki Sib	35%	65%			
tj x UAS-hpo	35%	65%			<0.01
tj x UAS-hpo Sib	30%	70%			

Double RNAi Genotype	GC-IC Proportion GC	IC	vs WT	vs hpo Sib
EGF pathway				
WT control: spi^{RNAi}/+; hpo^{RNAi}/+	27%	73%		
tjGAL4/+;hpo^{RNAi}/+ [egfr cross]	24%	76%	0.10	
tjGAL4/egfr^{RNAi};hpo^{RNAi}/+	22%	78%	<0.01	0.18
tjGAL4/egfr^{RNAi};+	33%	67%	<0.01	<0.01
tjGAL4/+;hpo^{RNAi}/+ [spi cross]	26%	74%	0.51	
tjGAL4/spi^{RNAi};hpo^{RNAi}	20%	80%	<0.01	<0.01
tjGAL4/spi^{RNAi};+	29%	71%	0.49	0.13
JAK/STAT pathway				
WT control: upd1^{RNAi}/+; hpo^{RNAi}/+	28%	72%		
tjGAL4/+;hpo^{RNAi}/+ [dome cross]	30%	70%	0.48	
tjGAL4/dome^{RNAi};hpo^{RNAi}/+	23%	77%	<0.01	<0.01
tjGAL4/dome^{RNAi};+	30%	70%	0.16	0.81
tjGAL4/+; hpo^{RNAi}/+ [upd1 cross]	21%	79%	<0.01	
tjGAL4/upd1^{RNAi}; hpo^{RNAi}/+	19%	81%	<0.01	0.12
tjGAL4/upd1^{RNAi}; +	30%	70%	0.32	<0.01

Table C6. Summary of GC-IC proportion for single and double RNAi experiments influencing IC and/or GC number. Two-tailed t-tests were conducted for analysis and *p*-values are reported in columns compared to the RNAi parental control (vs RNAi), the GAL4 parental control (vs GAL4) or and the *hpo* RNAi control (vs *hpo* sib). Red shading indicates significant differences $p \leq 0.01$; yellow shading indicates significant differences $0.01 < p \leq 0.05$ (indicated by * in Figures 7 and S6); orange shading indicates near-significant differences $0.05 < p \leq 0.1$.

Appendix D:

FACS sorting of larval ovary cells

D.1 Introduction

The larval ovary has three major cell types, the terminal filament cells (TFCs), interstitial cells (ICs) and germ cells (GCs). The interaction of these cell types with each other or with similar growth regulatory pathways is critical for proper development (Gancz and Gilboa, 2013; Gancz et al., 2011; Gilboa and Lehmann, 2006). In Chapter III, I described interesting differences between TFCs and ICs with respect to how these two cell types respond differently to the Hippo pathway. I also found non-autonomous influence of ICs to GCs, which suggests that ICs secrete signals to regulate the proliferation of GCs. A technique that would allow for the separation of each cell type to conduct gene expression or protein level analysis would yield new insights into how the larval ovary develops. In this Appendix, I will describe a protocol for fine-dissecting larval ovaries and using FACS sorting to separate somatic cells versus GCs using third instar larval ovaries.

D.2 Material and Methods

Fly strains

Flies were reared in standard conditions as described in Chapter III. *w*; P{vas.EGFP.HA}* (Kyoto stock center K109-171) were used for all experiments.

Isolation of late L3 larval ovaries for RNA extraction or FACS sort

All surfaces used for dissection, including forceps, tungsten needles, petri dishes and glass slides were first cleaned using RNaseZap (Life Technologies). Well-fed wandering L3 female larvae were placed in a petri dish containing freshly made ice-cold 1X PBS made with DEPC-treated water, and the fat body of 3-5 individuals were dissected. Fatbodies of well-fed larvae will sink to the bottom of the liquid. Fat bodies that floated to the top of the 1xPBS solution were not used.

The fat body was transferred to a plain glass slide containing a drop of approximately 100 uL ice-cold 1X PBS made with DEPC-treated water. Larval ovaries were identified by morphology, then verified by *vasa-EGFP* expression. Larval ovaries appear as a transparent dot within the fat body at lower magnifications, and depending on the larval stage, will either be located on top of the fat body, or embedded between two pieces of the fat body. The larval ovary was teased apart from the fat body using tungsten needles. The most effective method was to slide one tungsten needle between the ovary and the fat body, and using the other needle to tease apart the rest of the fat body. Separated ovaries were transferred into a 1.5 mL eppendorf tube containing 100uL of 1x PBS in DEPC-water using a P10 pipettor. A minimum of 10 ovaries were pooled per

tube. The tube was kept on ice at all times. Dissections were done so that they were conducted within a one-hour time frame.

Preparation of dissected larval ovaries for FACS sorting

To the tube containing larval ovaries, 500 uL of 1x PBS DEPC water containing 0.25% Trypsin and Hoeschst (1:500 dilution of 10 mg/ml) was added, and the tube was agitated by hand for 5 minutes. 500 uL of FBS was added to each tube to terminate the trypsin reaction, and cells were collected by centrifuging at 800x g for 7 minutes. The supernatant was removed and cells were resuspended in 500 uL 1xPBS made in DEPC water.

FACS sorting was conducted by Harvard University's Bauer Core Facility using MoFlo Astrios (Beckman Coulter). GFP positive particles and non-GFP positive particles were separated into separate eppendorf tubes containing 500 uL 1xPBS made with DEPC-water.

Preparation of larval fat bodies containing ovaries for FACS sorting

Female late L3 larval fat bodies were dissected in ice-cold 1x PBS made with DEPC-water. Fat bodies from 20 individuals were pooled in one 1.5 mL Eppendorf tube, then rinsed in calcium-free 1X PBS in DEPC-water for three times. Samples were incubated in 0.25% Trypsin for five minutes and were agitated by hand. Samples were then passed through a 40 um mesh using a pipettor 3-4 times. The resulting sample was mixed with 100 uL of FBS to terminate the Trypsin reaction. Cells were collected by centrifugation at 800x g for 7 minutes. The pellet was resuspended in 1% PFA in 1x PBS

with Hoeschst (1:500 dilution of 10mg/ml) and placed on the nutator for five minutes, then collected by centrifugation at 800x g for 7 minutes. Cells were then suspended in 1x PBS and subjected to FACS sorting.

RNA extraction and cDNA synthesis

RNA extraction for experiments in this Appendix was conducted using Trizol's reduced volume (0.8 mL) protocol for small numbers of cells. To assist precipitation of RNA, linear polyacrylamide was added during the precipitation stage of the extraction as per Trizol's protocol's recommendation for small quantity of RNA. The extracted RNA was either treated with Turbo DNase (Ambion) or Turbo DNase DNA-free kit (Ambion). The concentration of RNA was measured using a NanoDrop. 2-10 ug of RNA was used to generate cDNA using the Superscript III cDNA synthesis kit (Invitrogen).

D.3 Results and Discussion

D.3.1 RNA extraction from dissected larval ovaries

To test whether sufficient RNA can be collected to do gene expression analysis from late third instar larval ovaries, I first dissected ten ovaries per RNA extraction from wild type L3 larvae. This RNA extraction initially yielded 12.8 ng of product. However, when the product was treated with DNase and re-exacted using phenol-chloroform, the RNA yield was 0.4 ng. In an alternative attempt, RNA extraction from ten ovaries followed by Turbo DNase DNA-free kit resulted in 2.8 ug of RNA, which appeared to improve RNA yield. The DNA-free kit bypasses the phenol-chloroform extraction step needed in other DNase kits by using a proprietary DNase inactivation ingredient, which may lead to the increased yield. Expression of a control (housekeeping) gene RD39 was detected using RT-PCR from cDNA generated from the Turbo DNase treatment.

D.3.2 FACS sorting of ovarian cells using fat bodies

Past studies have conducted mass isolation of larval imaginal discs from fat body tissue by agitating the fat body to separate various imaginal discs (Fristrom and Mitchell, 1965). While such protocols exist for the wing and genital discs (Fristrom and Mitchell, 1965), there are no such protocols for ovarian primordia. Given that dissecting larval ovaries can be time consuming and technically challenging, I first tested whether it is possible to treat the fat body still containing the ovary to collect ovarian cells for FACS analysis. To have a visible marker for the gonad and to separate GCs from somatic cells, I used a line carrying a *vasa-EGFP* transgene, which marks the GCs. Female larval fat bodies were dissected, treated with trypsin, then passed through a 40um mesh several

times. Fat body cells are much larger than the larval ovary cells, and this method aims to separate them using the mesh. However, when I observed the supernatant under a fluorescent microscope, I did not observe any GFP expressing cells. Similarly, the FACS sorter did not detect any GFP expressing cells, and I did not continue pursuing this method. While this was not the aim of this study, I noticed that slightly agitating the fat body was a very reliable way of separating out the testis primordium.

D.3.3 FACS sorting of dissected L3 ovaries

Given that the previous method of trying to isolate ovarian cells from ovaries still embedded within the fat body did not yield positive results, I dissected larval ovaries free from the fat body, disaggregated cells using Trypsin, and conducted FACS sorting. FACs sorting of larval ovarian cells from a strain carrying *vasa-EGFP* revealed a distinct population of cells expressing GFP (Figure D.1B-C, green versus purple). These are expected to be the GCs. The same GFP expressing population also had higher level of nuclear dye staining levels (Figure D.1A).

While GFP-positive cells aggregated in a cluster that displayed similar scatter patterns, the GFP-negative population showed a wide scatter more similar to cellular debris. Nevertheless, these particles were collected along with the GFP-positive particles for RNA extraction and gene expression analysis. Over six trials, I recovered an average of 1312 GFP-expressing particles, which yielded an average of 199 ng of RNA (measured from 3/6 trials), and 40,167 GFP-negative particles, which yielded 254 ng of RNA (measured from 2/6 trials). There is an average of 300 GCs in mid-late L3 larval ovaries(Green and Extavour, 2012; Sarikaya and Extavour, 2015), therefore the recovery

rate for GCs was about ~40%. There area bout 2000 somatic cells per ovary at this stage, and I would have expected maximum of 20,000 cells to be recovered for the GFP-negative FACS sort. Given that the number was almost twice the expected, it appears that the GFP-negative sort is recovering a high amount of debris. In trial RT-PCRs conducted from cDNA synthesized from RNA extracted from FACS sorted cells, I detected control genen RD39 expression in the GFP-positive samples 2/4 trials, but not in the GFP-negative samples. I did not, however, detect expression of *vasa*, a gene specifically expressed in germ cells, in either GFP positive and negative samples. This may be due to the quality of the RNA, or PCR conditions.

While there were more particles registered as GFP-negative, the RNA quality and quantity was much lower than the GFP-positive particles. Combined with the scatter plot and the poor quality of RNA, it is likely that the GFP-negative collection primarily consists of cellular debris. The results from the GFP-positive cells seemed promising as it yielded relatively better quality of RNA that could detect expression of the control gene in RT-PCR conditions. These results suggest that FACS sorting of larval ovarian cells marked with a specific and robust fluorescent tag is possible, and could be used for gene expression analysis.

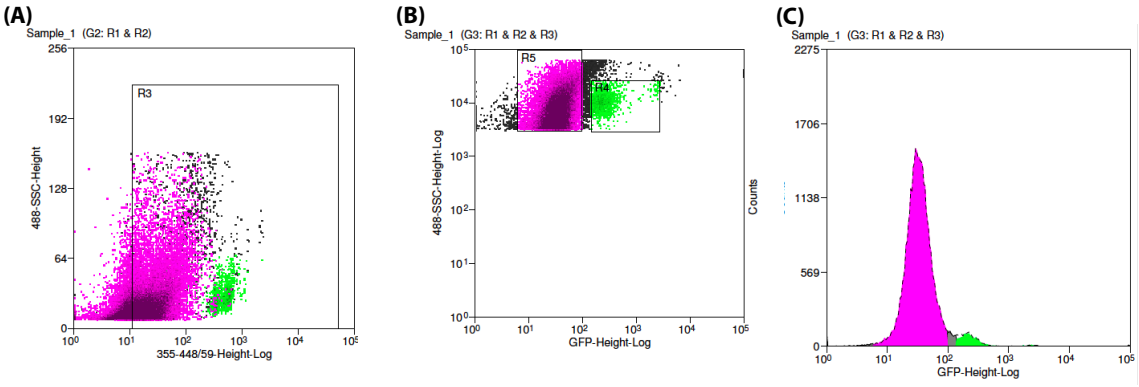

Figure D.1. FACS sort results from the larval ovary. Green dots label particles that were sorted as positive for GFP expression, and purple dots label particles that were presumed to be somatic cells (GFP-negative particles). (A) Plot of the nuclear stain levels on x-axis. (B) Plot of GFP levels on the x-axis. (C) Histogram of particles that were sorted along an axis of GFP expression on the x-axis.

	GFP+			GFP-		
	# particles	Total RNA	RD39	# particles	Total RNA	RD39
Sort 1 (Feb 26, 13)	1700	213.6	+	75000	poor quality	N/A
Sort 2 (Mar 13, 13)	170	N/A	+	20000	poor quality	N/A
Sort 3 (Mar 20, 13)	1000	182	-	10000	208	-
Sort 4 (Mar 21, 13)	2200	201.6	-	51,000	300.3	-
Sort 5 (Mar 25, 13)	1300	N/A	N/A	60000	N/A	N/A
Sort 6 (Mar 26, 13)	1500	N/A	N/A	25,000	N/A	N/A
Average	1,312	199.0666667	2/4 trials	40,167	254.15	0/2 trials

Table D.1. Summary of FACS sort trials. FACS sort experiment with date and the results for number of particles, total RNA yield, and detection of *RD39* control gene expression in RT-PCR reaction.

D.4 Acknowledgements

FACS sorting at the Bauer Core facility of Harvard University was done with the help of Patricia Rogers.

D.5 References

Fristrom, J.W., and Mitchell, H.K. (1965). The preparative isolation of imaginal discs from larvae of Drosophila melanogaster. J. Cell Biol. *27*, 445–448.

Gancz, D., and Gilboa, L. (2013). Insulin and Target of rapamycin signaling orchestrate the development of ovarian niche-stem cell units in Drosophila. Development *140*, 4145–4154.

Gancz, D., Lengil, T., and Gilboa, L. (2011). Coordinated regulation of niche and stem cell precursors by hormonal signaling. PLoS Biol. *9*, e1001202.

Gilboa, L., and Lehmann, R. (2006). Soma-germline interactions coordinate homeostasis and growth in the Drosophila gonad. Nature *443*, 97–100.

Green, D.A., and Extavour, C.G. (2012). Convergent evolution of a reproductive trait through distinct developmental mechanisms in Drosophila. Dev. Biol. *372*, 120–130.

Sarikaya, D.P., and Extavour, C.G. (2015). The hippo pathway regulates homeostatic growth of stem cell niche precursors in the Drosophila ovary. PLoS Genet. *11*, e1004962.